

**EXPERIMENTAL STUDY OF THE EFFECTS OF  
COMBUSTION PARAMETERS ON  
PERFORMANCE AND EMISSION  
CHARACTERISTICS OF A DUAL FUEL ENGINE  
UTILIZING BIOGAS AND DIESEL**

**ARNOLD TAREMWA**

**MASTER OF SCIENCE**

**(Mechanical Engineering)**

**JOMO KENYATTA UNIVERSITY OF  
AGRICULTURE AND TECHNOLOGY**

**2016**

**Experimental Study of the Effects of Combustion Parameters on  
the Performance and Emission Characteristics of a Dual Fuel  
Engine Utilizing Biogas and Diesel**

**Arnold Taremwa**

**A Thesis Submitted in Fulfillment for the Degree of Master of  
Science in Mechanical Engineering in the Jomo Kenyatta  
University of Agriculture and Technology**

**2016**

## **DECLARATION**

This thesis is my original work and has not been presented for a degree in any other university.

Signature..... Date.....

**Arnold Taremwa**

This thesis has been submitted for examination with our approval as the University Supervisors:

Signature..... Date.....

**Dr. Robert Kiplimo**

**JKUAT, Kenya**

Signature..... Date.....

**Dr. Stephen Wanjii**

**JKUAT, Kenya**

## **DEDICATION**

With Love, I dedicate this work to my loving and caring mum, Miss. Kellen Busingye Rwantengye. It has been your unconditional love, unending support and relentless sacrifice that has brought me to achieve this. May God bless you so much. I love you mum.

## **ACKNOWLEDGEMENT**

This thesis would not have been possible without the support of many people. First and foremost I would like to thank God for giving me this life, the opportunity and the wisdom to do this research. For constructive and scholarly advice and guidance and tremendous support, deep gratitude goes to my supervisors Dr. Robert Kiplimo and Dr. Stephen Wanji. I would like to acknowledge the support from Mobility to Enhance Training of Engineering Graduates in Africa (METEGA) in this research. I would also like to appreciate Regional Universities Forum for Capacity Building in Agriculture (RUFORUM) for funding this research, Japan International Corporation Agency (JICA) for providing biogas and Jomo Kenyatta University of Agriculture and Technology (JKUAT) for providing the diesel engine that was used during the research. I would like to acknowledge the support and advice of Dr. Eng. Hiram Ndiritu. I would like to appreciate my colleagues Kakande Lawrence, Hawi Meshack, Okure Deo, Andwanirira Paul, Quarty Gideon, Sam Ching, Robert Ofuso and Yin Edward for their support, encouragements and help in formatting and organising this thesis. I would also like to appreciate Mr. Eric Waiyaki and Mr. Joseph Muigai for their technical advice during the experiments. My sincere gratitude goes to my family my family; mum, my brothers, my sisters, Sharon, Sheila and all the relatives who loved me, prayed for me and encouraged me to have the strength to carry on until the end. I would like to say that thank you so much and may God bless you abundantly.

## **TABLE OF CONTENTS**

<b>COVER PAGE . . . . .</b>	<b>i</b>
<b>DECLARATION . . . . .</b>	<b>ii</b>
<b>DEDICATION . . . . .</b>	<b>iii</b>
<b>ACKNOWLEDGEMENT . . . . .</b>	<b>iv</b>
<b>TABLE OF CONTENTS . . . . .</b>	<b>v</b>
<b>LIST OF FIGURES . . . . .</b>	<b>xii</b>
<b>LIST OF TABLES . . . . .</b>	<b>xv</b>
<b>LIST OF APPENDICES . . . . .</b>	<b>xvi</b>
<b>LIST OF ABBREVIATIONS . . . . .</b>	<b>xvii</b>
<b>LIST OF SYMBOLS . . . . .</b>	<b>xix</b>
<b>ABSTRACT . . . . .</b>	<b>xxi</b>
<b>CHAPTER ONE . . . . .</b>	<b>1</b>
<b>1.0 INTRODUCTION . . . . .</b>	<b>1</b>
1.1 Background . . . . .	1
1.2 Problem statement . . . . .	5

1.3	Objectives . . . . .	6
1.3.1	General objective . . . . .	6
1.3.2	Specific objectives . . . . .	6
1.4	Organisation of the Thesis . . . . .	7
<b>CHAPTER TWO</b>		<b>8</b>
<b>2.0</b>	<b>LITERATURE REVIEW . . . . .</b>	<b>8</b>
2.1	Introduction . . . . .	8
2.2	Dual Fuel Engines . . . . .	9
2.2.1	Gaseous Fuel System . . . . .	9
2.2.2	Pilot Fuel Injection . . . . .	11
2.2.3	Performance of Dual-Fuel Engines . . . . .	12
2.3	Production and Application of Biogas . . . . .	13
2.3.1	Production of Biogas . . . . .	13
2.3.2	Application of Biogas . . . . .	15
2.4	Parameters that Affect the Performance of Dual-Fuel Engine . . . . .	17
2.4.1	Effect of Injection Timing on Dual-Fuel Engine . . . . .	17
2.4.2	Effect of Compression Ratio on Dual-Fuel Engine . . . . .	19
2.4.3	Effect of Exhaust Gas Recirculation (EGR) on Dual Fuel Engine	20
2.5	Other Fuels used in Dual-Fuel Engines . . . . .	22
2.5.1	Hydrogen . . . . .	22
2.5.2	Natural gas . . . . .	23

2.5.3	Biodiesel . . . . .	24
2.5.4	Ethanol . . . . .	24
2.6	Justification . . . . .	25
<b>CHAPTER THREE . . . . .</b>		<b>28</b>
<b>3.0</b>	<b>EXPERIMENTAL METHODOLOGY . . . . .</b>	<b>28</b>
3.1	Introduction . . . . .	28
3.2	Experimental Design . . . . .	28
3.2.1	Research Diesel Engine Setup . . . . .	29
3.2.2	Components of the Research Engine . . . . .	30
3.2.2.1	Dynamometer . . . . .	30
3.2.2.2	Engine Control Panel . . . . .	32
3.2.2.3	Fuel Tank . . . . .	32
3.2.2.4	Air Box . . . . .	33
3.3	Engine Modification . . . . .	33
3.3.1	Biogas Supply . . . . .	34
3.3.1.1	Dehydrator . . . . .	35
3.3.1.2	Desulphuriser . . . . .	36
3.3.1.3	Biogas Pressure Pump . . . . .	37
3.4	Fuel-Air Mixing Unit . . . . .	39
3.4.1	Design of the mixing chamber . . . . .	40
3.4.2	Design of Biogas Inlet Pipe . . . . .	41



3.4.3	Exhaust Gas Recirculation Unit . . . . .	43
3.5	Measurement Devices and Parameters . . . . .	44
3.5.1	Engine Brake Power . . . . .	45
3.5.2	Indicated Power . . . . .	46
3.5.3	Fuel Consumption . . . . .	46
3.5.3.1	Biogas Fuel Consumption . . . . .	47
3.5.3.2	Diesel Fuel Consumption . . . . .	48
3.5.4	Thermal Efficiency . . . . .	50
3.5.4.1	Brake Thermal Efficiency . . . . .	50
3.5.4.2	Indicated Thermal Efficiency . . . . .	51
3.5.5	Measurement of Emissions . . . . .	51
3.5.5.1	Emission Measuring Procedure . . . . .	52
3.6	Experimental Procedure . . . . .	53
3.6.1	Varying the Compression Ratio . . . . .	53
3.6.1.1	Procedure . . . . .	54
3.6.2	Varying the Injection Timing . . . . .	54
3.6.2.1	Procedure . . . . .	55
3.6.3	Variation in Biogas and EGR Flow Rates . . . . .	56
<b>CHAPTER FOUR</b>	<b>. . . . .</b>	<b>57</b>
<b>4.0 RESULTS AND DISCUSSION</b>	<b>. . . . .</b>	<b>57</b>
4.1	Introduction . . . . .	57

4.2	Simulation of the Gas Mixing Unit . . . . .	57
4.3	Effect of Compression Ratio on Combustion, Performance and Emission	57
4.3.1	Combustion Characteristics Analysis . . . . .	58
4.3.1.1	Cylinder Pressure . . . . .	58
4.3.1.2	Net Heat Release . . . . .	60
4.3.2	Performance Characteristics Analysis . . . . .	60
4.3.2.1	Brake Thermal Efficiency . . . . .	60
4.3.2.2	Brake Specific Fuel Consumption (BSFC) . . . . .	62
4.3.2.3	Mechanical Efficiency . . . . .	63
4.3.3	Emission Analysis . . . . .	64
4.3.3.1	Carbon-dioxide Emission . . . . .	64
4.3.3.2	NO <sub>x</sub> Emission . . . . .	65
4.3.3.3	Carbon monoxide Emission . . . . .	66
4.3.3.4	Unburnt Hydrocarbons . . . . .	67
4.4	Effect of Injection Timing on Combustion, Performance and Emission	67
4.4.1	Combustion Characteristics Analysis . . . . .	68
4.4.1.1	Cylinder Pressure . . . . .	68
4.4.1.2	Net Heat Release . . . . .	70
4.4.2	Performance Characteristics Analysis . . . . .	71
4.4.2.1	Brake Thermal Efficiency . . . . .	71
4.4.2.2	Brake Specific Fuel Consumption . . . . .	72
4.4.2.3	Mechanical Efficiency . . . . .	73

4.4.3	Emission Analysis . . . . .	75
4.4.3.1	Unburned Hydrocarbons . . . . .	75
4.4.3.2	Carbon monoxide Emission . . . . .	75
4.4.3.3	NO <sub>x</sub> Emission . . . . .	76
4.4.3.4	Carbon-dioxide Emission . . . . .	78
4.5	Effect of EGR on the Performance and Emission . . . . .	78
4.5.1	Performance Characteristics Analysis . . . . .	79
4.5.1.1	Brake Thermal Efficiency . . . . .	79
4.5.1.2	Brake Specific Fuel Consumption . . . . .	80
4.5.2	Emission Analysis . . . . .	81
4.5.2.1	NO <sub>x</sub> Emission . . . . .	81
4.5.2.2	HC Emission . . . . .	82
4.5.2.3	CO Emission . . . . .	82
4.5.2.4	CO <sub>2</sub> Emission . . . . .	84
4.6	Effect of Biogas Ratio on Performance and Emission . . . . .	85
4.6.1	Performance Characteristics Analysis . . . . .	85
4.6.1.1	Brake Thermal Efficiency . . . . .	85
4.6.1.2	Brake Specific Fuel Consumption . . . . .	85
4.6.2	Emission Characteristics Analysis . . . . .	87
4.6.2.1	NO <sub>x</sub> Emission . . . . .	87
4.6.2.2	HC Emission . . . . .	88
4.6.2.3	CO Emission . . . . .	89

4.6.2.4	CO <sub>2</sub> Emission . . . . .	90
<b>CHAPTER FIVE</b>	. . . . .	<b>91</b>
<b>5.0</b>	<b>CONCLUSIONS AND RECOMMENDATIONS . . . . .</b>	<b>91</b>
5.1	Concluding Remarks . . . . .	91
5.2	Recommendations . . . . .	93
<b>REFERENCES</b>	. . . . .	<b>95</b>
<b>Air-Gas Mixing Unit</b>	. . . . .	<b>110</b>
A.1	Types of Air-Gas Mixers . . . . .	110
A.2	Considered Designs for the Mixer . . . . .	110
<b>APPENDICES</b>	. . . . .	<b>110</b>

## LIST OF FIGURES

<b>Figure 1.1</b>	2013 Global CO <sub>2</sub> emissions from fuel combustion . . . . .	3
<b>Figure 2.1</b>	Schematic illustration of biogas production system . . . . .	14
<b>Figure 2.2</b>	Production and storage of biogas . . . . .	15
<b>Figure 3.1</b>	The Experimental Pictorial View . . . . .	29
<b>Figure 3.2</b>	The schematic experimental setup . . . . .	30
<b>Figure 3.3</b>	The research engine used in this experiment . . . . .	32
<b>Figure 3.4</b>	Eddy current dynamometer . . . . .	33
<b>Figure 3.5</b>	Engine Control Panel . . . . .	34
<b>Figure 3.6</b>	Dehydrator . . . . .	36
<b>Figure 3.7</b>	Desulphuriser . . . . .	37
<b>Figure 3.8</b>	Biogas Pressure Pump . . . . .	38
<b>Figure 3.9</b>	Air, Biogas and EGR Mixing Unit . . . . .	39
<b>Figure 3.10</b>	Mixing Unit . . . . .	40
<b>Figure 3.11</b>	EGR connection from the exhaust pipe to the mixer . . . . .	43
<b>Figure 3.12</b>	Rotary encoder fitted on the engine shaft . . . . .	46
<b>Figure 3.13</b>	Biogas Flow Meter . . . . .	47
<b>Figure 3.14</b>	Glass Burette for Measuring Diesel Flow . . . . .	49
<b>Figure 3.15</b>	Testo 350-S Gas Analyser . . . . .	52
<b>Figure 3.16</b>	Compression Ratio Adjustment Mechanism . . . . .	54

<b>Figure 3.17</b>	Injection Point Adjustment System . . . . .	55
<b>Figure 4.1</b>	Velocity distribution in the gas mixer . . . . .	58
<b>Figure 4.2</b>	Temperature distribution in the mixer . . . . .	59
<b>Figure 4.3</b>	Variation of cylinder pressure with crank angle at different CR	59
<b>Figure 4.4</b>	Variation of net heat release with crank angle at different CR	61
<b>Figure 4.5</b>	Brake thermal efficiency variation with engine load at different CR . . . . .	62
<b>Figure 4.6</b>	Variation in brake specific fuel consumption with load at different CR . . . . .	63
<b>Figure 4.7</b>	Variation in mechanical efficiency with load at different CR .	64
<b>Figure 4.8</b>	Variation in CO <sub>2</sub> emission with load at different CR . . . . .	65
<b>Figure 4.9</b>	Variation in NO <sub>x</sub> emission with load at different CR . . . . .	65
<b>Figure 4.10</b>	Variation in CO with load at different CR . . . . .	67
<b>Figure 4.11</b>	Variation in HC with load at different CR . . . . .	68
<b>Figure 4.12</b>	Variation in cylinder pressure with crank angle at different IT	69
<b>Figure 4.13</b>	Variation of NHR with crank angle at different IT . . . . .	71
<b>Figure 4.14</b>	Variation in brake thermal efficiency with load at different IT	72
<b>Figure 4.15</b>	Variation of injection timing with load at different IT . . . . .	73
<b>Figure 4.16</b>	Variation of mechanical efficiency with load at different IT .	74
<b>Figure 4.17</b>	Variation in HC with load at different IT . . . . .	76
<b>Figure 4.18</b>	Variation of CO with load at different IT . . . . .	77

<b>Figure 4.19</b>	Variation of $\text{NO}_x$ with load at different IT . . . . .	77
<b>Figure 4.20</b>	Variation of $\text{CO}_2$ emission with load at different IT . . . . .	79
<b>Figure 4.21</b>	Variation of BTE with load . . . . .	80
<b>Figure 4.22</b>	Varation of BSFC with load . . . . .	81
<b>Figure 4.23</b>	Variation in $\text{NO}_x$ with load . . . . .	82
<b>Figure 4.24</b>	Variation of HC with load . . . . .	83
<b>Figure 4.25</b>	Variation of CO emission with load . . . . .	83
<b>Figure 4.26</b>	Variation of $\text{CO}_2$ with load . . . . .	84
<b>Figure 4.27</b>	Variation of BTE with load at different biogas ratios . . . . .	86
<b>Figure 4.28</b>	Variation of BSFC with load at different biogas ratios . . . . .	86
<b>Figure 4.29</b>	Variation in $\text{NO}_x$ emission with load at different ratios . . . . .	87
<b>Figure 4.30</b>	Variation of HC with load at different biogas ratios . . . . .	88
<b>Figure 4.31</b>	Variation of CO with load at different biogas ratios . . . . .	89
<b>Figure 4.32</b>	Variation of $\text{CO}_2$ with load at different biogas ratios . . . . .	90
<b>Figure A.1</b>	First mixer design . . . . .	111
<b>Figure A.2</b>	First mixer design . . . . .	112
<b>Figure A.3</b>	Second design of the gas mixer . . . . .	113
<b>Figure A.4</b>	Velocity distribution in the gas mixer . . . . .	113
<b>Figure A.5</b>	Temperature distribution in the mixer . . . . .	114
<b>Figure A.6</b>	Velocity distribution before EGR . . . . .	114

## LIST OF TABLES

<b>Table 3.1</b>	Research Engine Specification . . . . .	31
<b>Table 3.2</b>	Composition of Biogas . . . . .	35



## **LIST OF APPENDICES**

<b>Appendix A</b>	Dimensions of the Crusher Assembly .....	<b>??</b>
<b>Appendix B</b>	Exploded View of the Jaw Crusher Assembly .....	<b>??</b>

## LIST OF ABBREVIATIONS

<b>aTDC</b>	After Top Dead Centre
<b>A/F</b>	Air-Fuel
<b>BTE</b>	Brake Thermal Efficiency
<b>BSFC</b>	Brake Specific Fuel Consumption
<b>BMEP</b>	Brake Mean Effective Pressure
<b>BDC</b>	Bottom Dead Centre
<b>bTDC</b>	Before Top Dead Centre
<b>CA</b>	Crank Angle
<b>CO</b>	Carbon monoxide
<b>CFD</b>	Computational Fluid Dynamics
<b>CR</b>	Compression ratio
<b>CNG</b>	Compressed Natural Gas
<b>CV</b>	Calorific value
<b>CI</b>	Compression Ignition
<b>deg</b>	Degree
<b>DICI</b>	Direct Injection Compression Ignition
<b>EGR</b>	Exhaust Gas Recirculation
<b>HCCI</b>	Homogeneous Charge Compression Ignition
<b>HC</b>	Hydrocarbons
<b>HHV</b>	Higher heating value

<b>IC</b>	Internal Combustion
<b>IT</b>	Injection timing
<b>LPG</b>	Liquified Petroleum Gas
<b>LHV</b>	Lower heating value
<b>NO<sub>x</sub></b>	Oxides of nitrogen
<b>ON</b>	Octane Number
<b>PM</b>	Particulate Matter
<b>ppm</b>	Parts per million
<b>SI</b>	Spark Ignition
<b>TDC</b>	Top Dead Centre

## LIST OF SYMBOLS

$\rho$	Density
$\dot{W}$	Power
$\dot{m}$	Mass flow rate
$\eta$	Efficiency
$r$	Radius
$d$	Diameter
$A$	Area
$V$	Volume
$N$	Revolutions per minute
$L$	Length
$C$	Velocity
$Q$	Heat Release
$P$	Cylinder Pressure
$\theta$	Crank Angle
$\gamma$	Specific Heat Ratio

## LIST OF SUBSCRIPTS

$a$	air
$b$	biogas
$bt$	brake thermal

bc	biogas fuel consumption
c	combustion chamber
d	diesel
egr	exhaust gas recirculation
f	fuel
in	intake
it	indicated thermal
m	mass
ther	thermal
vol	volume

## ABSTRACT

The use fossil fuels in internal combustion engines has contributed highly to the emission of greenhouse gases. For this reason, stringent regulations are being set to minimise their emission to the environment. Researchers have conceived a concept of dual fuel engines that use alternative fuels to replace a percentage of fossil fuels in internal combustion engines. Biogas as one of the renewable source of energy has advantages in dual fuel application because of its ability to mix with air, high flammability and the ability to reduce  $\text{NO}_x$  emission and particulate matter to the environment.

In this study, a variable compression ratio CI engine was modified to operate as a dual fuel engine using biogas. The modification included designing of an air-gas mixer to introduce biogas into the combustion chamber as air-biogas mixture charge and an exhaust gas recirculation (EGR) system to recirculate exhaust gas back into the combustion chamber. Operating the engine at a constant speed of 1500 rpm and varying engine load, combustion, performance and emission characteristics of the dual fuel engine were studied under different engine parameters.

Experiments were carried out to study the effects of compression ratio, injection timing and emission characteristics of a dual fuel engine. The effect of EGR on the  $\text{NO}_x$  emission of a dual fuel engine fueled with biogas and diesel was also conducted. Investigation of compression ratio was done with the engine running with the injection

timing of  $23^\circ$  before top dead center (bTDC) while varying the compression ratios. The study for injection timing was done with the engine compression set to 18:1 and the experiments to study the effect of biogas flow rate were done with the engine compression ratio set at 18:1 and injection timing of  $29.5^\circ$  bTDC.

Increasing the compression ratio and advancing fuel injection timing increased the thermal efficiency, in-cylinder pressure and net heat release rate. The highest brake thermal efficiency, in-cylinder pressure, net heat release and mechanical efficiency of 25.7%, 49 bar, 60 J/deg and 49.9% respectively were found to be at compression ratio of 18:1 and injection timing of  $29.5^\circ$  bTDC. Increasing the compression ratio from 14 to 18 improved the brake specific fuel consumption of the engine by 26%. It was found that  $\text{NO}_x$  and  $\text{CO}_2$  emission increased with the increase in compression ratio and was highest at compression ratio of 18:1. HC and CO emissions reduced with increase in compression ratio and were highest at the compression ratio of 14:1. This study found out that at compression ratio of 18:1, injection timing of  $29.5^\circ$  bTDC, EGR ratio of 20%, 40% biogas and 60% diesel, load of 12kg and engine speed of 1500 rpm, the dual fuel engine had superior performance and emission characteristics.

## CHAPTER ONE

### 1.0 INTRODUCTION

#### 1.1 Background

With the current trend in industrialization and mechanization, world energy demand is greatly increasing and various sources of energy are currently being exploited. Fossil fuels contribute more than 80% of the world total energy [1, 2]. In automotive sector alone, fossil fuel powered internal combustion engines are the main power source for transportation. They provide power for off-road machinery, ships, and many other applications despite that some other alternative power sources are being developed. These internal combustion engine derive their power from combustion of fossil fuels (petroleum products) that are currently faced with stringent emission regulations due to their contribution to global warming [3, 4].

Fossil fuels are the major sources of greenhouse gas and other emissions such as PM and  $SO_x$ . Reports suggested that by 2010, fossil fuels contributed over 64% of the world greenhouse gas emission [5]. Fossil fuels such as petroleum products are the main source of energy in transport sector which in turn is a big contributor to the emission of greenhouse gases in the world. This is due to the fact that most automobiles operate on internal combustion engines that burn fossil fuels to generate energy. In 2013, the transport sector contributed 23% of world  $CO_2$  emissions from fuel combustion as shown in Fig.1.1 with the road sector largely dominating [6]. The emissions



from the transport sector can be reduced by the use of alternative fuels to replace fossil fuels.

Petroleum products are non-renewable sources of energy and because of that, they are being depleted due to over exploitation and utilisation by the continuously growing industrialization. Utilisation of these petroleum products poses a world wide threat to the environment due to pollution by the emission of greenhouse gases from burning of conventional fuels as energy sources. Therefore, there is need to utilise alternative energy sources to substitute or reduce the use of fossil fuels. Different countries across the globe have put up policies to facilitate the rapid development and utilization of renewable energy as one way of reducing the environmental challenges caused by fossil fuels [7].

For many years, different researchers have focused on the use of gaseous fuels as alternative for fossil fuels in internal combustion engines [8, 9]. Gaseous fuels are considered to be good for internal combustion engines because of their good mixing characteristics with air. They have wide flammability limits and high self-ignition temperatures. This enables them to operate with lean mixtures and higher compression ratios, resulting in an improvement in the thermal efficiency and reduction in emissions mostly HC, CO<sub>2</sub>, NO<sub>x</sub>, SO<sub>x</sub> and particulate matter. Gaseous fuels include produce gas, natural gas or (compressed natural gas), hydrogen and biogas that can be used in internal combustion engines [10–13]. As one of the alternatives for the fossil fuels, bio-

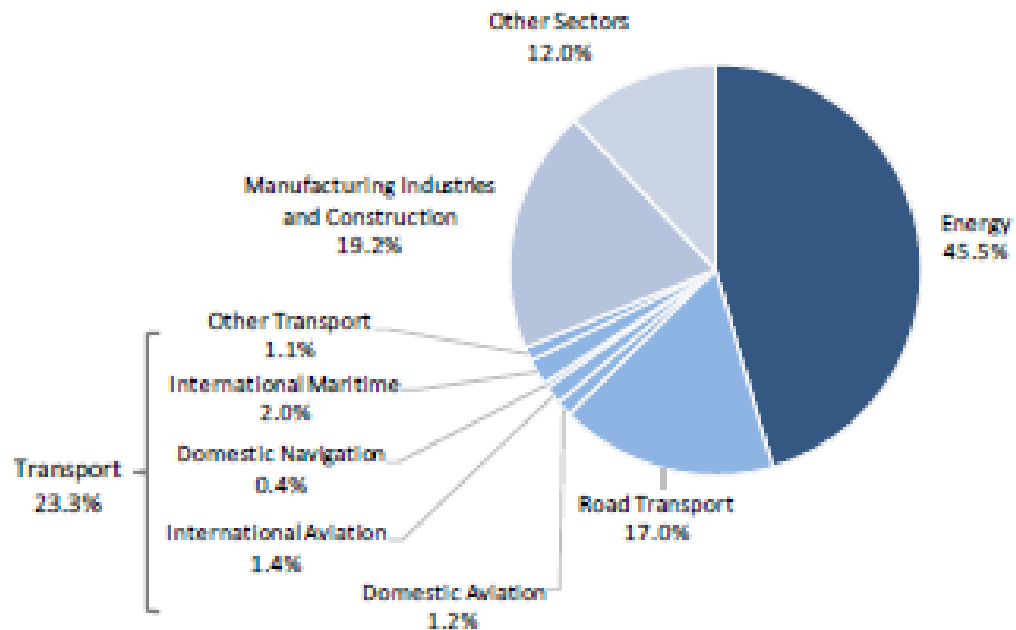


Figure 1.1: 2013 Global CO<sub>2</sub> emissions from fuel combustion

gas is a potential renewable energy source which if properly prepared can be adapted for use in transport vehicles. Research has been carried out on various ways of using biogas as a gaseous source of energy in internal combustion engines (ICE) [8, 14–19].

Biogas is a renewable source of energy produced from raw materials such as agricultural waste, manure, municipal waste, plant material, sewage or food waste [20, 21]. Every country on the globe is putting effort to regulate climate change; biogas utilization in automobile engines can be a great step to curb the contribution of fossil fuels to the global climate change on top of its ability to improve fuel economy. There is a very great potential for biogas fuel production in most developing countries like Kenya [22, 23]. The primary contents of a typical biogas are methane and carbon-dioxide, other gases are in smaller quantities: methane – CH<sub>4</sub> (50- 75%), carbon dioxide – CO<sub>2</sub> (25-50%), nitrogen – N<sub>2</sub> (0-10%), hydrogen – H<sub>2</sub> (0-1%), hydrogen

sulphide –  $\text{H}_2\text{S}$  (0-3%) and oxygen –  $\text{O}_2$  (0-2%) [24]. The methane concentration in biogas determines its calorific value, for-example, biogas containing 40% methane has a calorific value of  $14.35 \text{ MJ/m}^3$ , whereas a biogas with a 70% methane concentration has a calorific value of  $25.13 \text{ MJ/m}^3$  thus a higher combustion value [25]. Biogas being a gaseous fuel, is considered to be good for internal combustion engines on account of its high flammability and ability to readily form a mixture with air.

Dual-fuel engine operation combines the use of liquid fossil fuel and gaseous fuel which improves fuel economy and minimises the emissions especially of  $\text{NO}_x$  and particulate matter (PM) thereby curbing the challenges posed by the use of fossil fuels in conventional internal combustion engines. Different researchers have focused on this particular area [8, 17, 26]. Most researchers have considered the performance characteristics such as brake thermal efficiency, brake power, brake specific fuel consumption and emission parameters of the engine for-example  $\text{CO}$ ,  $\text{HC}$ ,  $\text{NO}_x$ ,  $\text{CO}_2$ . However, there is need to optimize combustion parameters such as compression ratio and injection timing in comparison with the performance and emission characteristics of biogas- diesel fueled engine operation.

M. Hawi *et al.*, [27] investigated the performance and emission characteristics of a dual fuel engine using biogas and diesel in a dual fuel operation but the results of the investigation show low performance of a dual fuel engine and require improvement. The experiment only focused on the effect of biogas on dual fuel engine brake power,

brake thermal efficiency, brake specific fuel consumption and emissions of HC, CO, CO<sub>2</sub>. This requires a critical study of the combustion characteristics; cylinder peak pressure, injection timing, compression ratio, combustion duration and ignition delay period and how to optimize them to improve the performance and emission characteristics of the dual fuel engine using biogas and diesel.

This research was therefore focused on investigating how to optimize the combustion parameters to improve the performance and emission characteristics of a biogas-diesel dual fuel engine.

## **1.2 Problem statement**

Internal combustion engines are the common sources of energy in automobiles in the world. This kind of application means that the rate of fossil fuel utilisation is high and so is the rate at which petroleum reserves are getting depleted. This increased demand has raised the prices of these petroleum fuels. Furthermore, the use of fossil fuels has presented a very significant contribution to the production of greenhouse gases and global climate change in general. Burning of fossil fuels produces pollutants such as carbon dioxide (CO<sub>2</sub>), nitrogen oxides NO<sub>x</sub>, carbon monoxide (CO), unburned hydrocarbons and other oxides of sulphur that pollute the environment [28]. These challenges have therefore led to a need for alternative source of fuel for automobiles, which has motivated many researchers to focus on biogas as one candidate to curb the challenges caused by use of petroleum fuels.

A lot of research has been carried out for the last decade about dual fuel engines using diesel and biogas but most work has been focused on the performance and emission characteristics [29,30]. The results of the previous work have not given very conclusive results of how to optimize the use of dual-fuel engine . Most research work shows that there is a reduction in engine performance characteristics such as thermal efficiency and a reduction in engine emissions such as  $\text{NO}_x$  while using biogas in a dual fuel engine operation but no optimum operating parameters have been suggested [27,31–35]. This research was therefore focused on investigating combustion parameters; compression ratio, injection timing and rate of heat release in order to improve the performance characteristics and emission characteristics to come up with the optimum parameters for the dual-fuel engine operation.

### **1.3 Objectives**

#### **1.3.1 General objective**

The main objective of this research was to investigate the effect of combustion parameters on the combustion, performance and emission characteristics of a dual fuel engine operating on biogas as the primary fuel and diesel as the pilot fuel.

#### **1.3.2 Specific objectives**

The main objective of this research was achieved through the following specific objectives.

- To determine the effect of compression ratio on combustion, performance and

emission characteristics of the dual fuel engine

- To determine the effect of injection timing on combustion, performance and emission characteristics of the dual fuel engine
- To investigate the effect of EGR on  $\text{NO}_x$  emission of the dual fuel engine
- To investigate the effect of flow rate of biogas on combustion, performance and emission characteristics of dual fuel engine

#### **1.4 Organisation of the Thesis**

This thesis is composed of five chapters. The first chapter is the introduction which explains the problem the research was aimed at solving and suggests the procedure through which the solution of the problem was to be achieved. The second chapter is the literature review which highlights the existing literature about the same problem. It explains the research that has been done about the use of alternative fuels and points out the gaps that need to be tackled.

Chapter three is the methodology. This contains the experimental setup, the procedure of carrying out the experiments in varying the engine compression ratio, injection timing, biogas flow rate and the EGR rates. In chapter four, the results from the experiments are presented and their variations and trends discussed. In chapter five, conclusions are drawn from results and then recommendations for further work also presented.

## **CHAPTER TWO**

### **2.0 LITERATURE REVIEW**

#### **2.1 Introduction**

More stringent engine emission regulations have been set to reduce the greenhouse gas emission from internal combustion engines. However internal combustion engines will continue to be the main power source in the foreseeable future for transportation, off-road machinery, ships and many other applications. In order to meet these emission regulations, various concepts have been considered. One majorly promising concept being considered by various researchers is the concept of dual fuel engines.

Different researchers have put much emphasis on the use gaseous fuels to be used in internal combustion engines under dual fuel operation. Gaseous fuels are a cheaper source of energy for internal combustion engines and also have the ability to reduce  $\text{NO}_x$ , particulate matter and other greenhouse gas emissions that are produced by the use of petroleum fuels. Research is being carried out to optimize these fuels in order to substitute or minimise the use of petroleum fuels where possible. This chapter therefore reviews the research work that has been carried out on the use of gaseous fuels mainly focusing on biogas with diesel fuel in a dual fuel engine operation so as to identify the gaps to be addressed.

## **2.2 Dual Fuel Engines**

A dual fuel engine is one in which more than one fuel is used simultaneously. It is a technology that is being developed to minimise the challenges of over dependence on petroleum products that are faced with depletion, price fluctuations and cause environmental pollution [36]. In a dual fuel engine, the gaseous fuel (primary fuel) is mixed with air to form the charge and compressed in the combustion chamber but does not self-ignite so a spray of diesel (pilot fuel) is induced into the combustion chamber which ignites the charge.

In dual fuel engine operation, intake of gaseous fuel and injection of pilot fuel are very important in both fuel-air mixing and combustion. Different researchers have studied different alternatives of gaseous fuel system and pilot fuel injection into the dual fuel engine to improve the performance of the engine.

### **2.2.1 Gaseous Fuel System**

A dual fuel engine works on the diesel engine cycle (compression ignition) but in this case, a mixture of gaseous fuel (primary fuel) and fresh air is supplied to the cylinder. This mixture is known as the charge and is introduced into the combustion chamber and then compressed before the pilot fuel is injected to ignite the compressed charge.

Different researchers have considered various gaseous fuels for dual fuel operation. Gaseous fuels such as natural gas, hydrogen gas and biogas have been studied for ap-



plication in dual fuel engine. Madhujit *et al.*, [37] investigated the effect of hydrogen-diesel combustion on the dual fuel engine performance and emission and concluded that hydrogen improves thermal efficiency in the dual fuel engines. Research done by Hosmath *et al.*, [38] about the effect of compression ratio, compressed natural gas (CNG) flow rate and injection timing on the performance of dual fuel engine observed that there was an increase in thermal efficiency, low  $\text{NO}_x$  and HC with advanced injection timing in the dual fuel engine.

A mixing chamber for the fresh air and gaseous fuel is required for homogeneous mixing of charge before being introduced into the combustion chamber. In the mixing chamber (device), an appropriate amount of air is mixed with an appropriate amount of gaseous fuel for efficient combustion. The mixture is then induced into the combustion chamber for compression and combustion.

N. Banapurmath *et al.*, [10] studied two gas mixers, Y-shaped and parallel gas entry mixer. The results showed that a parallel entry mixer gave better mixing of the gas and the air. A. Supee *et al.*, [39] used venturi mechanism with four injectors to introduce gaseous fuel into the air intake system of the engine and concluded that there was a homogeneous CNG-air mixing. Gurneesh *et al.*, [40] compared premixed and manifold injection modes of gaseous fuel induction where fuel was introduced directly into the air manifold without prior mixing. In this experiment, the premixed mode showed lower volumetric efficiency as the air-fuel mixture was throttled. M. Hawi *et al.*, [27]

used a T-shaped gas mixer for the biogas mixing with air in the air intake system of a dual fuel engine. However all these researches did not give the most efficient gas-air mixer for homogeneous mixture.

### **2.2.2 Pilot Fuel Injection**

In a dual-fuel engine, the primary fuel and air mixture (charge) does not auto ignite due to a high octane number. Biogas octane number is higher than that of diesel allowing it to withstand high compression ratios. Octane number is defined as the standard measure of the performance of an engine fuel and the higher the octane number, the more compression the fuel can withstand before it self-ignites. Therefore, a small amount of diesel is sprayed into the combustion chamber at the end of the compression stroke to ignite the highly compressed charge. This diesel fuel is called the pilot fuel and due to its auto-ignition property, it acts as the source of ignition for the compressed charge. The amount of diesel fuel needed for sufficient ignition is between 10-20% of the amount needed for operation on diesel alone at normal working loads [33].

Self-ignition of the pilot fuel in dual fuel engine is a very important characteristic and it is required that the pilot fuel should have high cetane number. Cetane number (diesel fuel) and octane number (biogas) both measure the tendency of the fuel to ignite spontaneously. In the cetane number scale, high values represent fuels that ignite readily while in the octane number scale, high values represent fuels that resist spontaneous ignition. Cetane number is an important factor in determining the quality of

diesel fuel. It is the inverse function of a fuel's ignition delay so the higher the cetane number, the more easily the fuel will burn in a combustion chamber.

Most of the research conducted on dual fuel engines has been done on a conventional direct injection (DI) engine [26, 41, 42]. In direct injection, pilot fuel is pressurized and injected through a common rail line directly into the combustion chamber of each cylinder. Therefore there is a need to study the effects of fuel injection on combustion efficiency and ignition delay in dual fuel engine.

### **2.2.3 Performance of Dual-Fuel Engines**

The performance of the dual fuel engine highly depends on the quality of the primary fuel for example the calorific value of the fuel, the mixing ability of the fuel with air, the carbon-dioxide percentage in the fuel etc. Such factors affect flame propagation, emissions and general performance characteristics. A number of researchers have put an effort to determine ways to get optimum results from the application of dual fuel operation. Debabrata *et al.*, [43] modified a stationary, single cylinder, 4 stroke direct injection engine into a biogas-diesel dual fuel engine. The modification involved adding a biogas inlet and the mixing chamber for the air-biogas mixing and exhaust gas recirculation unit (EGR).

Iván Darío Bedoya *et al.*, [44] studied the effects of mixing system and pilot fuel quality on the engine performance in a diesel-dual fuel engine and suggested that bet-

ter mixing of biogas and air improved the thermal efficiency of the dual fuel engine. Thermal efficiency ( $\eta_{ther}$ ) of an engine is a dimensionless performance measure that indicates the extent to which the energy added by heat is converted to net work output. Park *et al.*, [17] studied the performance and emission characteristics of a SI engine fueled by low calorific biogas blended with hydrogen. This research found out that hydrogen addition in appropriate amount of hydrogen to biogas can be beneficial to thermal efficiency, combustion characteristics and HC emissions. However, emission of  $\text{NO}_x$  was found to increase with increase in hydrogen percentage.

Braga *et al.*, [12] carried out a study on the performance and gaseous emissions characteristics of a natural gas and diesel dual fuel turbocharged engine. This research suggested that, at lower loads, specific fuel consumption of a dual fuel engine was higher compared to diesel fuel operation.  $\text{NO}_x$  emission in a dual fuel engine were significantly lower than in diesel engine. However, the study reported high levels of CO and HC in dual fuel engine. All these studies mainly focus on the performance and emission characteristics and do not analyze the combustion characteristics and their effect on the performance and emission of the dual fuel engine.

## **2.3 Production and Application of Biogas**

### **2.3.1 Production of Biogas**

Biogas is produced by anaerobic digestion of various organic substances such as food waste, agricultural waste, animal waste such as cow dung, municipal solid waste and

other sources. Anaerobic digestion is a biochemical degradation process, in which biodegradable organic matters are decomposed by bacteria in the absence of oxygen forming biogas as a gaseous byproduct. Anaerobic digestion is a very long process commonly divided into four stages; hydrolysis, acidogenesis, acetogenesis or dehydrogenation, and methanation. These processes include the breakdown of polymers and monomers into acetate, hydrogen, and volatile fatty acids for production of acetogenic bacteria and methanogens; the bacteria that is necessary for the production of methane gas, the main constituent of biogas [20,43]. Biogas production plant describing the anaerobic digestion process using cattle dung is shown in Fig.2.1.

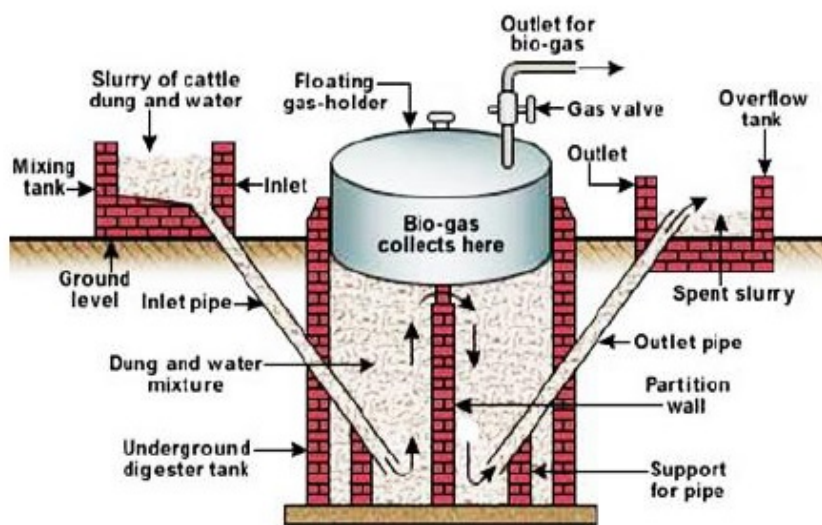


Figure 2.1: Schematic illustration of biogas production system

Biogas production is always away from the point of its application, therefore there is always need for storage for either transportation to the point of use or future utilization. Biogas has a density which approximates to  $1.2 \text{ kg/m}^3$  at ambient conditions, therefore

it requires a larger volume for its storage instead of storing it in a compressed form. Biogas can be compressed in order to reduce the volume of space required for its storage during application. Fig.2.2 shows an example of the biogas digester and the gas storage bag used to store biogas after production.

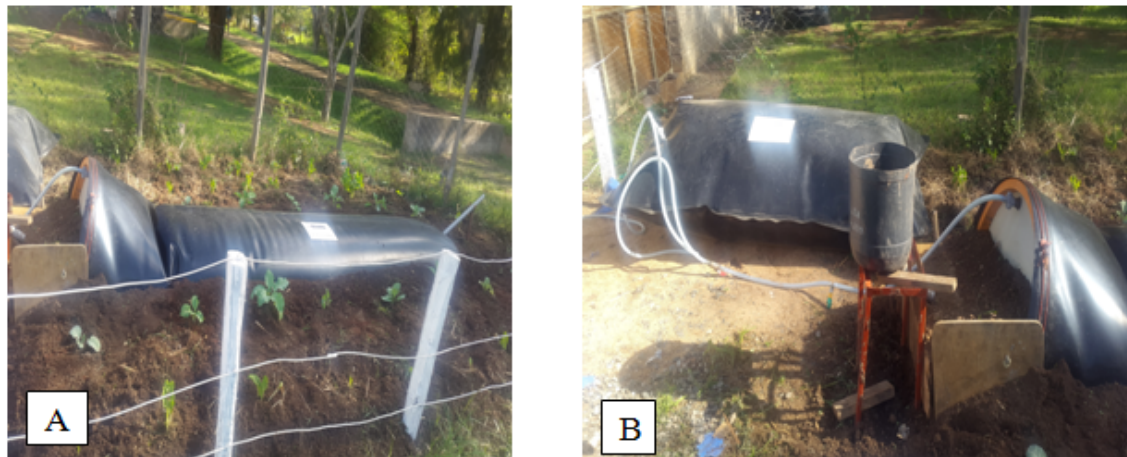


Figure 2.2: Production and storage of biogas

### 2.3.2 Application of Biogas

The primary contents of a typical biogas are methane and carbon-dioxide and other gases are in smaller quantities with a methane content ranging between (50 - 75%) per volume on average [8,24]. With this high percentage of methane, biogas is highly flammable and has high potential to produce energy.

Biogas has been used by rural households as a source of fuel for cooking, in farms normally for heat, shaft power and electricity generation in irrigation systems [45]. Biogas has a high octane number, this makes it suitable for engines with a relatively high compression ratio to maximize thermal efficiency and may be applied to conventional compression ignition engines with minor modifications.

Phan Minh *et al.*, [9] carried out a study on biogas premixed charge diesel dual fueled engine with the main aspects of concern being engine performance, diesel substitution, energy consumption and the effect of long term use. During the study, a small single cylinder indirect injection CI engine Kubota RT120 with rated power output of 7.73 kW at 2400 rpm was used. The air intake manifold of the engine was modified to add the air and gas mixer and as the means to introduce biogas into the engine. The engine was coupled to an alternator to form a system loaded by variable resistances. Parameters including brake torque, brake power, specific diesel consumption, specific total energy consumption, brake total energy conversion efficiency and volumetric efficiency were studied under full and part engine load. The study showed slightly higher energy conversion efficiencies than in diesel engine at full loads, lower exhaust temperatures, increased diesel fuel substitution, soot reduction, high unburnt hydrocarbons at part loads.

The results of the study showed improvement in the performance characteristics of the dual fuel engine, however the study did not consider the effect of biogas flow rate to the engine, the test were only carried out for high speeds, between 1500 rpm and 2400 rpm. The research did not consider designing a proper gas mixer with a gas compressor/pump to improve the volumetric efficiency.

## **2.4 Parameters that Affect the Performance of Dual-Fuel Engine**

Combustion, performance and emission characteristics of a dual-fuel engine operating on biogas-diesel fuel are affected by different factors. In the quest to improve the performance, combustion and emission characteristics of a dual-fuel engine using biogas and diesel fuel, various researchers have embarked on studies of different factors such as injection timing, carbon dioxide percentage in biogas, compression ratio, oxygen content in biogas and others.

### **2.4.1 Effect of Injection Timing on Dual-Fuel Engine**

Injection timing is a process of admitting fuel into an internal combustion engine at a particular time. The timing of the induction (injection timing) of the diesel fuel is so important and affects the combustion and exhaust emissions. Injection timing mainly defines the state at which the charge is in when introducing the pilot fuel into the combustion chamber. It determines whether the pilot fuel is introduced into the combustion early before that charge is compressed or after compression thus varying the ignition delay, maximum temperature in the combustion chamber, performance and exhaust emission characteristics. In a dual-fuel engine operating on gaseous fuel and diesel, the operation is that the gaseous fuel (primary fuel) is mixed with air to form the charge and then the charge is compressed in the combustion chamber. Towards the end of compression stroke, a spray of a pilot fuel (in this case diesel fuel) is inducted to ignite the charge.



Violeta Makareviciene *et al.*, [8] experimentally found out that the thermal efficiency depends on the start of injection timing. The thermal efficiency of the engine was enhanced by increasing the biogas (methane) quantity and advancing the start of injection timing. Advancing the injection timing means that the pilot fuel is injected early into the combustion chamber and combustion starts earlier. This increases the peak cylinder pressure because more fuel is burnt before the top dead center [32].

The effect of advancing the injection timing on the exhaust gases is that  $\text{NO}_x$  tend to increase but carbon monoxide and unburnt hydrocarbons reduce. This is due to the fact that advancing the injection timing increases the peak cylinder pressure which leads to increased temperature thus increased  $\text{NO}_x$  but also leads to complete combustion in the combustion chamber leading to a great reduction in the unburnt hydrocarbon gases in the exhaust. Reduction in carbon monoxide is due to overall lean mixture in combustion chamber [29]. The results of this research show great performance and emission characteristics however, the research does not consider conditions of various loads to investigate the effect of advanced injection timing at different loads and engine speeds.

Nwafor [46] carried out an experiment to study the effect of advanced injection timing on the performance of natural gas in diesel engines operating in a dual fuel engine mode. The experiments were done on an air-cooled, high speed, indirect injection four-stroke Petter model AC1 single cylinder diesel engine. The results of this research showed increased brake thermal efficiency; brake thermal efficiency is the ratio

of brake power to the heat supplied. The experiment also showed that the exhaust gas temperatures were high and lower carbon monoxide and carbon dioxide emissions with advanced injection timing. However, the study did not show the effect injection timing on  $\text{NO}_x$  emission. Bo Yang *et al.*, [47] investigated the effect of pilot injection timing on combustion noise and particle emission of a diesel/natural gas dual-fuel engine at low load. The study concluded that by appropriately advancing the injection timing, higher brake thermal efficiency, lower CO and HC emissions are achieved but did not suggest ways to minimise the  $\text{NO}_x$  emission.

#### **2.4.2 Effect of Compression Ratio on Dual-Fuel Engine**

Compression ratio in piston engine is the ratio between the volume of the cylinder and combustion chamber when the piston is at the bottom of its stroke (BDC), to the volume of the combustion chamber when the piston is at the top of its stroke (TDC). With high self-ignition temperature, biogas can achieve high compression ratios without causing engine knocks that in turn leads to improved thermal efficiency. Mathur *et al.*, [30] carried out an experiment to optimize compression ratio of diesel fuel engine and concluded that at the maximum brake thermal efficiency, brake specific fuel consumption and optimum emission were obtained at the compression ratio of 17 which was a medium compression ratio tested between 19 and 15.

E. Porpatham *et al.*, [18] carried out a study about effect of compression ratio on the performance and combustion of a biogas fueled engine and found that as the compres-

sion ratio increases the thermal efficiency increases following the improvement in the peak power. The results show improvement in the performance characteristics, however, high compression ratios lead to high level of  $\text{NO}_x$  emission and the research did not consider investigating the effect of exhaust gas recirculation as a way to reduce the  $\text{NO}_x$  emission. In their research [48] to study the influence of compression ratio on performance of CI engine, Hariram *et al.* found out that thermal efficiency, rate of heat release and peak pressure are obtained at high compression ratio of 18. The research however does not show what effect the high compression ratio had on the emission mostly of  $\text{NO}_x$ .

#### **2.4.3 Effect of Exhaust Gas Recirculation (EGR) on Dual Fuel Engine**

The exhaust gases from the combustion process contain products such as water vapor ( $\text{H}_2\text{O}$ ), carbon dioxide ( $\text{CO}_2$ ), nitrogen oxides ( $\text{NO}_x$ ), particulate matter (PM), hydrocarbons (HC) and carbon monoxide (CO) that apart from water vapor are harmful to the environment. These combustion exhaust products should be regulated to reduce their impact on the environment [49]. Exhaust gas recirculation is one way employed to reduce the exhaust products of combustion.

Exhaust gas recirculation is a system that uses the exhaust gas to improve the performance of the dual fuel engine by returning it to the combustion chamber. The substitution of burnt gas (which takes no further part in combustion) for oxygen rich air reduces the proportion of the cylinder contents available for combustion. This causes

a correspondingly lower heat release and peak cylinder temperature, and reduces the formation of  $\text{NO}_x$ . Applying EGR on the biogas-diesel dual fuel engine reduces the  $\text{NO}_x$  in the exhaust gas but increases carbon dioxide, unburnt hydrocarbons, carbon monoxide in the exhaust gases [50–53].

Meshack. H *et al.*, [54] carried out an experiment to study the effect of exhaust gas recirculation on performance and emission characteristics of a diesel-piloted biogas engine. The results showed that exhaust gas recirculation introduced extra carbon-dioxide into the combustion chamber which led to the reduction in combustion temperature that caused poor flame propagation resulting into increased unburnt hydrocarbons and increased carbon monoxide emissions. However, the effect of EGR on  $\text{NO}_x$  emission from a dual fuel engine using biogas was not determined in this research.

A. Paykani *et al.*, [55] in an experiment carried out to investigate the effects of exhaust gas recirculation and intake preheating on performance and emission characteristics of dual fuel engines at part loads found out that introducing exhaust gas improved the combustion thus reducing the HC and CO emissions. While C. Jun *et al.*, [52] found out that EGR increases CO. Therefore, the effect of EGR on the emission of HC and CO remains inconclusive since different researches give different results.

## **2.5 Other Fuels used in Dual-Fuel Engines**

The environmental pollution, depletion and political instability from major petroleum producing economies that has led to petroleum fuels price fluctuations are the major factors that have led to the need for alternative fuel to minimise the use of petroleum fuels. The contribution of the transportation sector to the emission of greenhouse gases is proportionally high which has led researchers to study different forms of fuel to reduce the effects of petroleum products in internal combustion engines.

### **2.5.1 Hydrogen**

Currently, most of the research on fuels is focused on ways to reduce the contribution of transport sector towards the emission of greenhouse gases and some work has been done on the use of hydrogen in internal combustion dual fuel engines. Hydrogen is a highly flammable fuel that can be used in internal engines. Hydrogen is a gaseous fuel that is easy and economical to produce by various methods such as electrolysis of water and coal gasification.

R. Senthil Kumar *et al.*, [56] investigated the performance, emission and combustion characteristics of dual fuel engine fueled with diesel and hydrogen and experimentally found out that using hydrogen in a dual fuel engine operation increases the thermal efficiency and reduces the fuel consumption. This is mainly attributed to the steady combustion of hydrogen. However, use of hydrogen showed a very big rise in  $\text{NO}_x$  emission. This is mainly due to its high in-cylinder temperature during combus-

tion [37].

Duraïd. F *et al.* [57] in an experiment to investigate the performance and emissions of a multi-cylinder diesel engine fueled with hydrogen-diesel blends showed that varying the loads and hydrogen flow rates gave optimum loads and flow rates that reduced the emission of  $\text{NO}_x$ . The research however did not consider the use of EGR as the known method to reduce  $\text{NO}_x$  emissions.

### **2.5.2 Natural gas**

Natural gas is a fossil fuel formed when layers of buried plants and gases are exposed to intense heat and pressure over thousands of years. A typical natural gas is a hydrocarbon gas mixture consisting primarily of about 92.69% methane, carbon dioxide 0.52%, ethane 3.43% and other small quantities of nitrogen and hydrogen sulfide.

A. Supee *et al.* [39] carried out a research to study the performance of dual fuel engine using compressed natural gas. They concluded that during the study, there was higher power output because of better combustion, low carbon dioxide emissions due to a higher hydrogen-to-carbon ratio than diesel, low carbon monoxide gas emissions due to high combustion quality of natural gas, low unburnt hydrocarbons due to homogeneous fuel-air mixture but high  $\text{NO}_x$  due to high temperatures [36]. The experiment however does not indicate the particular flow rate of compressed natural gas (CNG), engine load and speed that produces reduced emissions of  $\text{NO}_x$ .

### 2.5.3 Biodiesel

Biodiesel refers to a vegetable oil - or animal fat-based diesel fuel consisting of long-chain alkyl (methyl, ethyl, or propyl) esters. Ni Zhang *et al.* [58] studied the combustion and emission characteristics of a turbo-charged common rail diesel engine fueled with diesel-biodiesel engine and experimentally found that use of biodiesel increased the brake specific fuel consumption at a particular brake mean effective pressure. This is mainly because of the low heating value thus more fuel has to undergo combustion to produce the same brake mean effective pressure.

Biodiesel enhances combustion thus increases peak cylinder temperature due to oxygenated fuel that contributes to increase in  $\text{NO}_x$ . Particulate matter reduces due to the presence of oxygen that suppresses formation of soot. Unburnt hydrocarbons and carbon monoxide emissions are also reduced due to complete burning of the charge in the combustion chamber. Regardless of the increase in the  $\text{NO}_x$ , this research showed positive attributes in performance and emission characteristics using biodiesel. However, the research did not investigate the combustion characteristics of biodiesel in the dual fuel engine.

### 2.5.4 Ethanol

Ethanol is a highly flammable type of alcohol based fuel produced by the fermentation of sugars by yeasts commonly from sugarcane. N. Vinayagam *et al.* [59] in an experimental investigation concluded that use of ethanol in a dual fuel engine leads

to reduced  $\text{NO}_x$  at low loads compared to conventional compression ignition engines but  $\text{NO}_x$  emissions increase remarkably at high loads. Complete and early combustion produced by the use of ethanol also leads to reduction in unburnt hydrocarbons and carbon monoxide emissions. There is less diesel fuel consumed as part of the fuel is replaced by ethanol. [60]. These results show a positive trend in the application of ethanol in dual fuel engine operation. However, the experiment was run at constant speed. The results do not show the variation in performance and emission characteristics with varying engine speeds and loads.

## **2.6 Justification**

Recently the petroleum sector has been faced with price instabilities and depletion due to over exploitation and utilisation. The expanding world demand for energy from fossil fuels has played a major role in the production of emissions that are mainly the greenhouse gases that have contributed to the global climate change and environmental degradation.

Reports estimate that in 2012, global carbon dioxide  $\text{CO}_2$  emission was 31.7 gigatonnes ( $\text{GtCO}_2$ ) which shows how greatly the emission increases each year [4]. The increase of these emissions largely depends on the increasing combustion of fossil fuels in automobiles and industries. The European Union (EU) in an effort to minimize the causes of global climate change has set objectives for 2020 that is 20% reduction in greenhouse gas emissions compared with 1990, 20% of total energy consumption



from renewable energy and 20% increase in energy efficiency [61].

Gaseous fuels have presented a very good alternative source of energy to reduce the use of petroleum based fuels in automobile industry because of their ability to mix thoroughly with air to form a more homogeneous charge that burns more readily and also because of their low emissions compared to petroleum fuels. The ability of biogas to be used as fuel in internal combustion engines and its easy and economic way of production has caused it to be highly considered as the solution to the problems faced in the petroleum industry as the source of energy for automobiles. Biogas can be produced by anaerobic digestion, a very economical process of obtaining energy from waste organic matter for example farm waste, agricultural waste, municipal waste and animal waste [20]. This gas contains a high percentage of methane and can be used as fuel in internal combustion engines such as the dual fuel engine operation with diesel.

In the world of transport, biogas can play a very big role towards alleviating the problems associated with the use of petroleum products when used as the source of energy in internal combustion engine. This can be achieved in a dual fuel engine operation where biogas replaces a percentage of petroleum fuel because of its flammability due to its high methane content.

With the availability of biogas potential in kenya, research about its application in dual fuel engine is very important. Research has been done [9, 44, 54] on the use of

biogas and diesel in a dual fuel operation to come up with the best way to substitute a percentage of diesel fuel in the engine with the biogas that will reduce the challenges caused by petroleum fuels.

## **CHAPTER THREE**

### **3.0 EXPERIMENTAL METHODOLOGY**

#### **3.1 Introduction**

The main objective of this experimental study was to investigate the effects of combustion parameters on the performance and emission characteristics of a dual fuel engine operating on diesel as the pilot fuel and biogas as the primary fuel. Combustion, performance and emission characteristics were studied in respect to compression ratio, injection timing, EGR ratios and biogas flow rate.

#### **3.2 Experimental Design**

The experiments were carried out on a compression ignition engine modified to operate as a dual fuel engine by introducing biogas with air as the main charge. The modification included adding a mixing unit to the air inlet system for the air to mix homogeneously with biogas before being introduced into the combustion chamber. The mixing unit was also used to homogeneously mix the exhaust gases with biogas and air during the EGR operation. The pictorial view of the experiment is demonstrated in Fig.3.1.

During this experimental study, a 3.5 kW single cylinder, water cooled, four stroke, multifuel, variable compression ratio research engine was modified to operate as a dual fuel engine as described in the schematic illustration in the Fig.3.2.

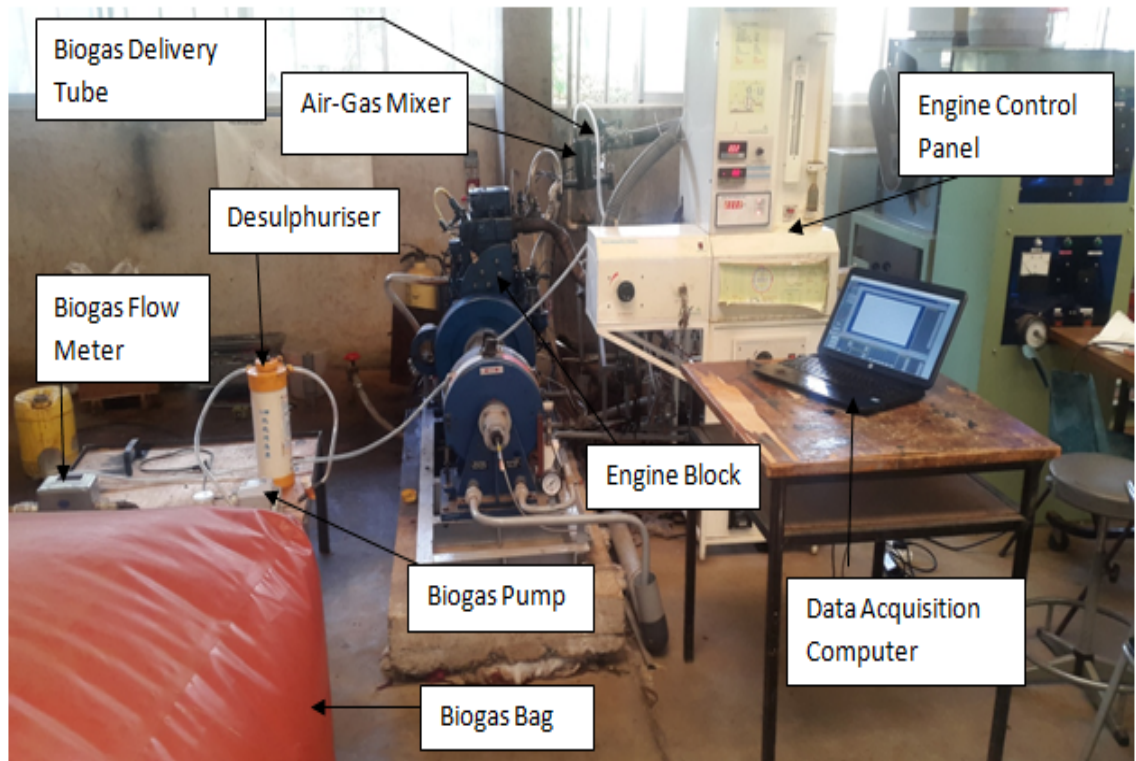
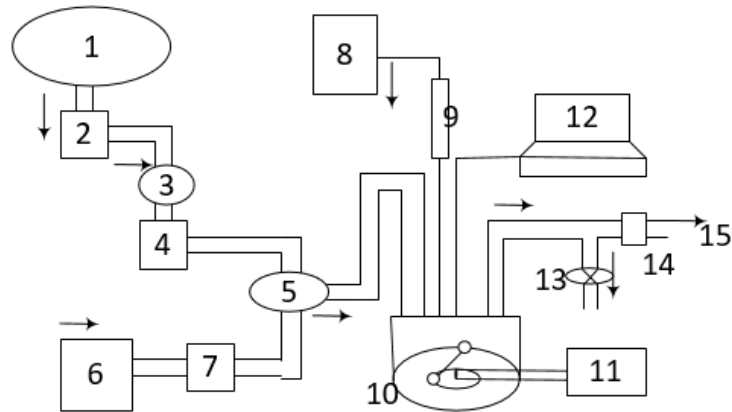


Figure 3.1: The Experimental Pictorial View

### 3.2.1 Research Diesel Engine Setup

The engine setup that was used in this research was a variable compression, Multi-fuel, single cylinder, four stroke engine from Apex Innovations Pvt. Ltd [62] with the parameters as shown in the Table.3.1. The engine is connected to an eddy current type dynamometer for loading as shown in Fig. 3.3. The operation mode of the engine can be changed from diesel to petrol engine control unit (ECU) or from petrol ECU to diesel mode.



1. Biogas bag, 2. Desulphuriser, 3. Pump, 4. Gas flow meter, 5. Gas-air mixer, 6. Air box, 7. Air flow meter, 8. Diesel tank, 9. Burette, 10. Engine, 11. Dynamometer, 12. Computer, 13. EGR, 14. Gas analyser, 15. Exhaust

Figure 3.2: The schematic experimental setup

### 3.2.2 Components of the Research Engine

The engine has several components and sensors for efficient operation, measurement and data collection. These components include dynamometer, control panel, air box and fuel tank.

#### 3.2.2.1 Dynamometer

Determining the brake power of the engine involves the measurement of its torque and angular speed of its output shaft. Engine torque is normally measured by a device known as a dynamometer. The type of the dynamometer that was used in this experiment is an eddy current dynamometer model AG10 with maximum pressure of 160kPa, torque of 11.5Nm and weight of 130kg [63].

An eddy current dynamometer consists of a stator on which are fitted a number of electromagnets and a rotor disc and coupled to the output shaft of the engine. When

Table 3.1: Research Engine Specification

Parameter	Value
Displacement(cm <sup>3</sup> )	661
Number of Cylinders	1
Number of Strokes	4
Power(kW)	3.5
Compression Ratio	VCR(18-12)
Torque(Nm)	11.5

the rotor rotates, eddy currents are produced in the stator due to magnetic flux set up by the passage of field current in the electromagnets. These eddy currents oppose the rotor motion, thus loading the engine and a moment arm measures the torque.

A strain gauge load cell is attached onto the dynamometer. It is incorporated in the restraining linkage between the casing and dynamometer bed plate and is used to measure dynamometer loading due to the rotational torque exerted on the casing. A rotary encoder is fitted on the dynamometer shaft to measure the engine crank angle.

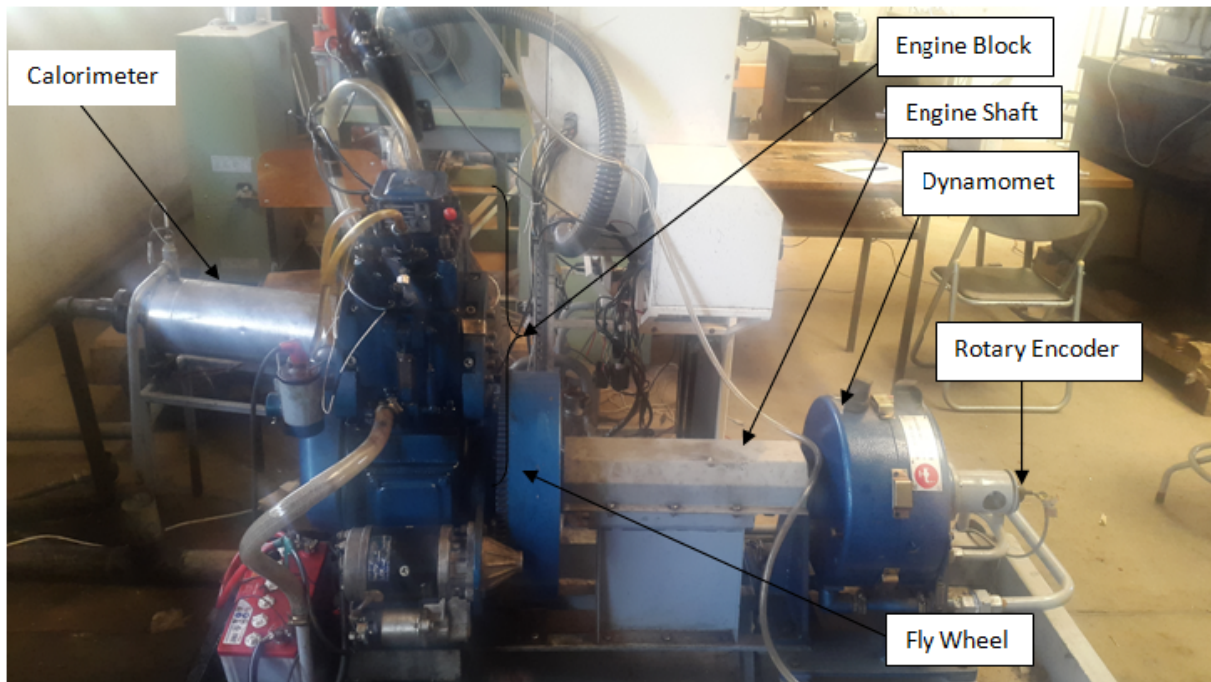


Figure 3.3: The research engine used in this experiment

### 3.2.2.2 Engine Control Panel

The research engine consists of a control panel with a piezo powering unit, voltmeter, load indicator, dash board panel and the diesel fuel barrette as shown in Fig.3.5.

The piezo sensor and the crank angle sensor were connected to a piezo powering unit model AX-409. The signals from the sensors were transferred to the piezo powering unit through cables. The dash board holds the control knobs for speed and the engine loading. It also has the ignition coil for starting the engine.

### 3.2.2.3 Fuel Tank

The engine used in this experiment was a multi-fuel engine. A 15 liter capacity fuel tank was partitioned into two sections for diesel and petrol fuel. For petrol fuel, the tank

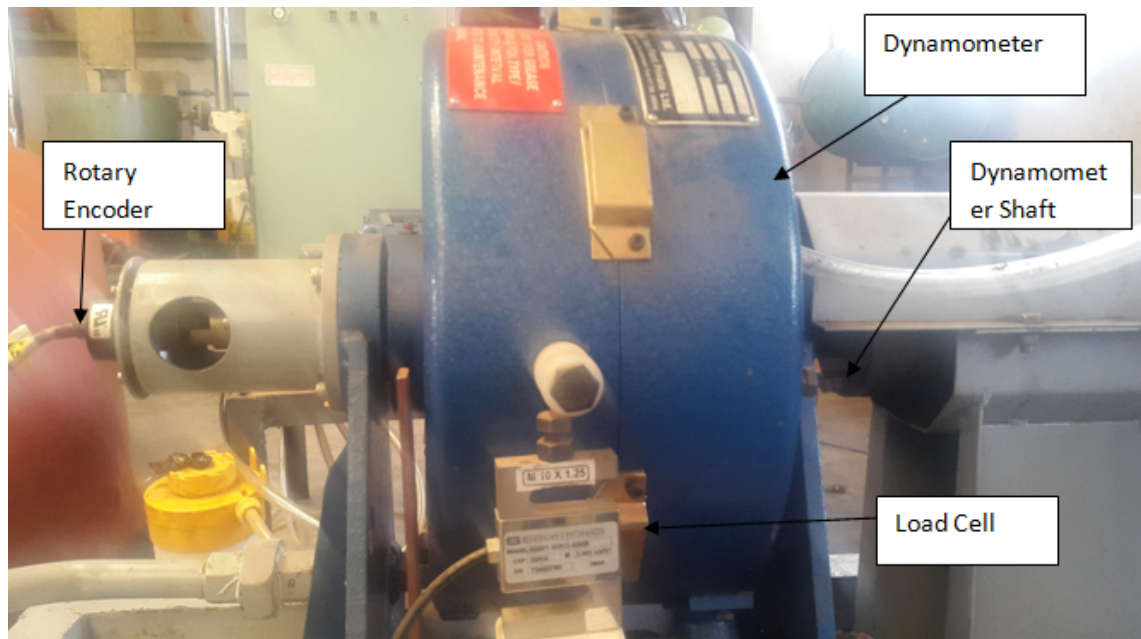


Figure 3.4: Eddy current dynamometer was equipped with fuel pump and fuel over flow pipe to regulate fuel over flow.

#### 3.2.2.4 Air Box

The engine has one air box fixed just under the fuel tank. Air from the air box is taken to the engine air inlet manifold through an air hose pipe.

The purpose of an air box is to dampen out the pulsations in the air as it flows to the engine. It is equipped with the orifice to enable air consumption measurement. It also has a manometer and a pressure transmitter to measure the differential pressure across the orifice.

### 3.3 Engine Modification

The diesel engine used in this experimental study was modified to a dual fuel engine. The modification included addition of a biogas intake system and and exhaust recircu-



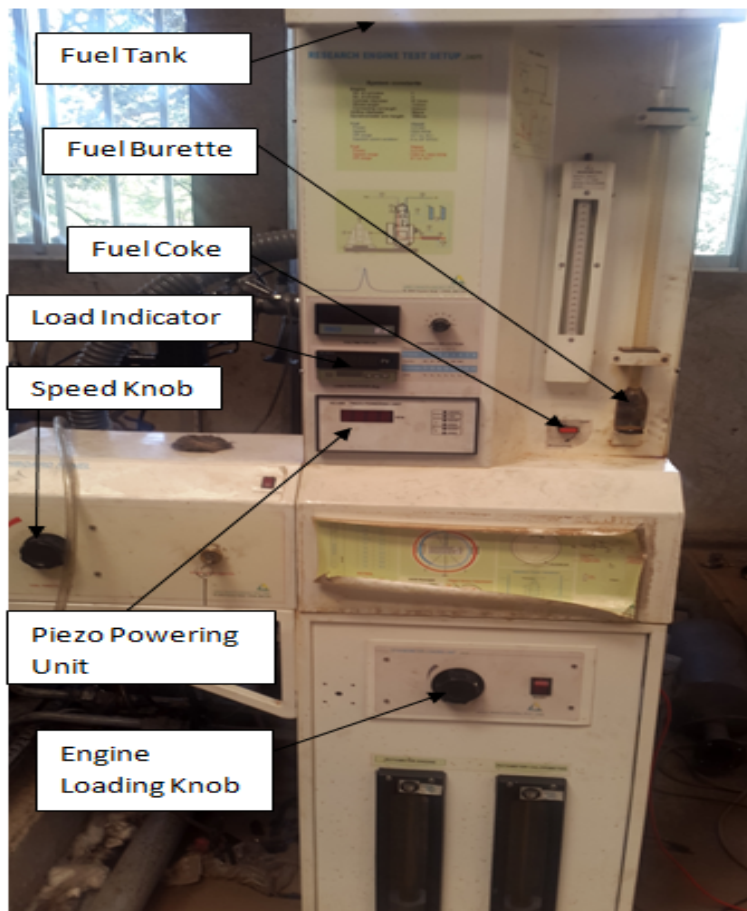


Figure 3.5: Engine Control Panel

lation system.

### 3.3.1 Biogas Supply

Biogas that was used in the experiment was produced through the process anaerobic digestion from a well rationed mixture of water hyacinth and cow dung by the Institute of Energy and Environmental Technology (IEET) at Jomo Kenyatta University of Agriculture and Technology. The properties of the biogas used are as shown in Table.3.2

The gas was collected in a 4kg gas bag and was treated to remove excess water va-

Table 3.2: Composition of Biogas

Component	Quantity
Density(kg/m <sup>3</sup> )	1.22
Methane (%)	49-53
CO <sub>2</sub> (%)	21-29
N <sub>2</sub> (%)	17-19
Calorific Value(kJ/kg)	19100

por and hydrogen sulphide before it was introduced into the engine. Treatment was mainly to improve the combustibility of biogas and avoid corrosion of engine parts by hydrogen sulphide.

### 3.3.1.1 Dehydrator

During biogas production, water vapor is one of the products of anaerobic digestion. Biogas from the gas bag was passed through a dehydrator to remove water vapor as shown in Fig.3.6. A dehydrator allows gas to expand during the flow which allows the moisture in the gas to condense and settles in the dehydrator as the dry biogas continues to flow into the engine [64].

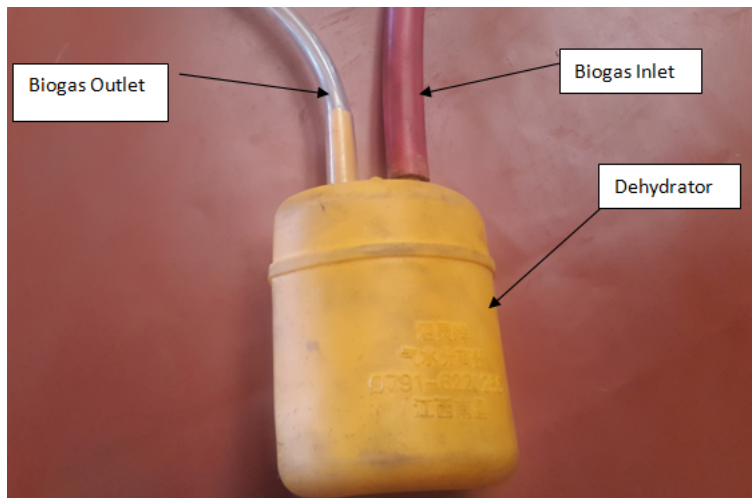


Figure 3.6: Dehydrator

### 3.3.1.2 Desulphuriser

Biogas from anaerobic digestion contains the principle component methane, carbon-dioxide and hydrogen sulphide among other components. Among other things, the hydrogen sulphide concentration in the biogas is dependent on the substrates used [65].

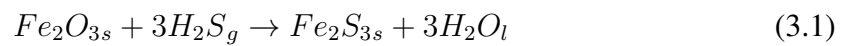
Hydrogen sulphide is an extremely toxic gas to humans when inhaled in high concentrations. In biogas application, hydrogen sulphide component is oxidized during combustion, leading to the formation of acidic sulfur dioxide ( $\text{SO}_2$ ) that is very corrosive and leads to quick wear of engine parts.

It was important to reduce the concentration of hydrogen sulphide before being introduced into the combustion chamber. In this experiment, hydrogen sulphide was removed by chemical reaction method. Biogas from the dehydrator was allowed to enter the desulphuriser as shown in Fig.3.7 that contains iron oxides ( $\text{Fe}_2\text{O}_3$ ) in the form of iron sponge (iron oxide-impregnated wood chips). Hydrogen sulphide was removed



Figure 3.7: Desulphuriser

by reacting it with iron oxide to form insoluble iron sulfides according to the Eqn.3.1 and then hydrogen sulphide free biogas was allowed to flow to the engine through the gas pump and the gas flow meter. [66, 67].



### 3.3.1.3 Biogas Pressure Pump

Biogas was passed through a 220 VAC + -10% power gas pump as shown in Fig 3.8. The pump had a capacity of raising the gas pressure to 22kpa and maximum flow rate of 36 l/min. The gas pump was used to increase the biogas flow rate beyond the

engine aspiration flow rate. This helped to study of the effect of biogas flow rate on the performance and emission of the engine.

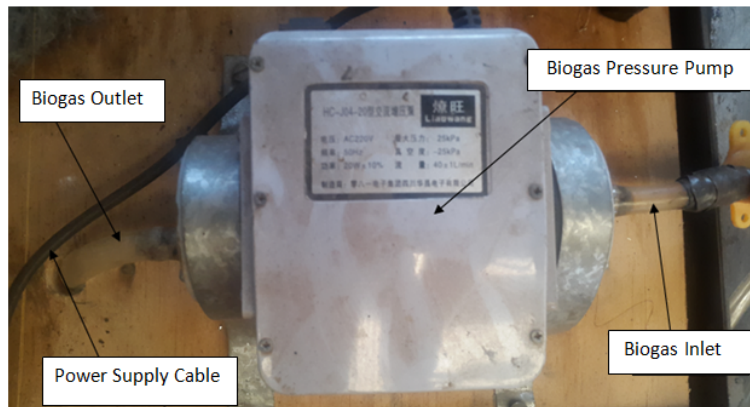


Figure 3.8: Biogas Pressure Pump

### 3.4 Fuel-Air Mixing Unit

The fuel air mixing unit was designed to allow proper mixing of biogas and air before the mixture was introduced into the combustion chamber as the main charge for combustion. The pictorial and the design model of the mixing unit are shown in Fig.3.9. Fig.3.9 A is the installed mixer and Fig.3.9 B is the 3D model of the mixer. The mixing unit was designed to ensure homogeneous mixing for air and biogas and allow into the engine sufficient air and biogas for optimum operation conditions.

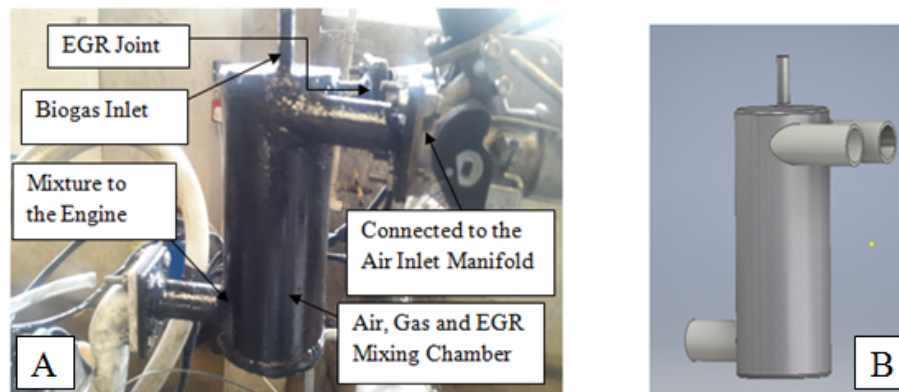
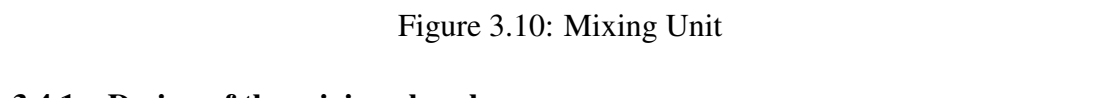


Figure 3.9: Air, Biogas and EGR Mixing Unit

The mixing unit was fabricated of steel material (mild steel) because of its low cost and ease of fabrication. It consisted of three inlet pipes, mixing chamber and one outlet pipe. The inlet pipes were for air, biogas and exhaust gas recirculation as shown in Fig.3.10. The biogas inlet pipe was designed so that its axis was parallel to the axis of the mixing chamber. Air inlet pipe was designed to be tangential to the mixing chamber and so that its axis was perpendicular to the axis of the biogas inlet pipe. This was aimed at creating swirling effect of air during inlet and turbulence for better mixing of air and biogas. Exhaust gas recirculation inlet pipe was also designed to be tangential



Performance of a dual fuel engine largely depends on the proper mixing of air and

the engine [68]. The volumetric capacity of the engine that was used in this research was 661cc so the volume of the mixing chamber was designed to be more than 661cc. Using a cylindrical steel pipe of an internal diameter of 86 mm and using the Eqn.3.2, the length that would give the volume of the mixing chamber greater than 661cc was any length greater than 113.8 mm. Considering sufficient resident time for homogeneous mixing and installation conditions to the modified engine, a length of 196 mm was selected for the design as shown in Fig.3.10.

$$V = \frac{\pi D^2 L}{4} \quad (3.2)$$

### 3.4.2 Design of Biogas Inlet Pipe

Dimensioning of the biogas inlet pipe plays a very important role in the performance of a dual fuel engine. It depends mainly on the fuel energy required by the engine operating at its maximum power and maximum speed and the calorific value of biogas used in the dual fuel operation [68]. Considering the engine that was used in this research, maximum power and speed of 3.5 kW and 1500rpm respectively, the biogas inlet pipe was designed using the following equations. The volumetric flow rate of air into the engine ( $V_a$ ) for a 4-stroke engine was calculated in Eqn.3.3 where  $V_c$ ,  $\eta_{vol}$  and N are engine volumetric capacity, volumetric efficiency and maximum speed respectively.

$$V_a = \frac{V_c N}{2 \times 60 \times 1000} \times \eta_{vol} \quad (3.3)$$

The engine was considered to have volumetric efficiency of 85% so that with the volumetric capacity of 661cc and maximum speed of 1500rpm, the volumetric flow rate



was calculated as  $V_a = 7.023 \times 10^{-3} \text{ m}^3/\text{s}$ . The air intake velocity  $C_{in}$  was calculated using Eqn. 3.4 where  $A$  is the cross-sectional area of the engine inlet manifold.

$$V_a = C_{in} \times A \quad (3.4)$$

Considering the engine's inlet manifold diameter, 20mm, then from equation 3.4, the calculated value of the air inlet velocity was 22.35m/s. At maximum rated power of the engine, the biogas fuel consumption was calculated from Eqn.3.5 where  $f_b$ , sfc and  $P$  are fuel consumption, engine specific fuel consumption and power output of the engine respectively [68].

$$f_b = \frac{sfc \times P}{3600} \quad (3.5)$$

The maximum replacement of diesel by biogas in this experimental study was up to 80% and for  $P = 3.5\text{kW}$ , the maximum biogas fuel consumption was calculated using the Eqn. 3.6 where  $f_{bc}$  is the biogas fuel consumption.

$$f_{bc} = 0.8f_b \quad (3.6)$$

The diameter of the biogas inlet pipe was then calculated from Eqn.3.7 where  $A_b$  is the cross sectional area of the biogas pipe as shown in Eqn. 3.8 where  $d_b$  is the diameter of the biogas inlet pipe.

$$f_{bc} = A_b \times C_{in} \quad (3.7)$$

$$d_b = \sqrt{\frac{4 \times f_{bc}}{\pi \times C_{in}}} \quad (3.8)$$

The diameter required for the biogas inlet pipe was calculated to be 5.9mm, considering factor of safety, the diameter of the biogas inlet should not be less than 0.5 times the diameter of the engine air inlet manifold and 10mm was considered to be the diameter in design for this experimental study.

### 3.4.3 Exhaust Gas Recirculation Unit

Modifications that were done on the research engine during this experiment included addition of EGR system. Exhaust gases from combustion process are always at high temperatures and may contain corroding compounds. In designing the exhaust recirculation system, mild steel pipes were used to take care of those factors as shown in Fig.3.11A. The pipes were connected to the gas mixing unit as shown in Fig.3.11B to allow proper mixing of air, biogas and the recirculated exhaust gases to mix before being introduced into the combustion chamber.

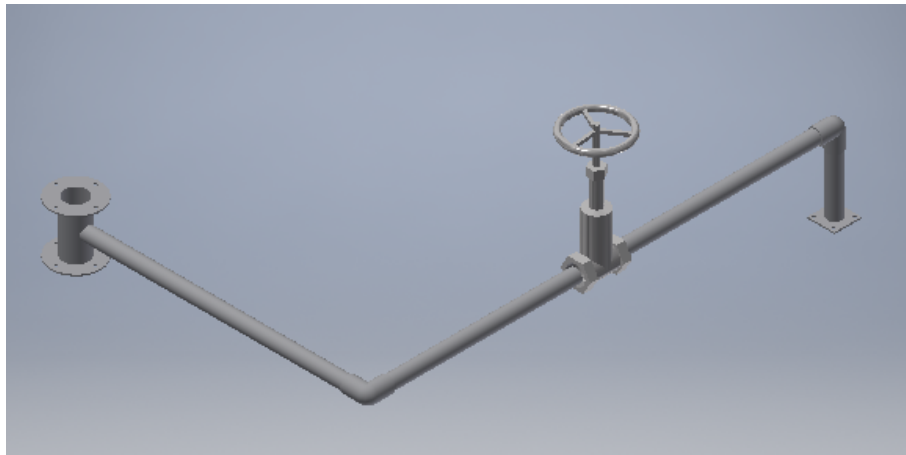


Figure 3.11: EGR connection from the exhaust pipe to the mixer

The EGR system was designed so that a percentage of the exhaust from the combustion chamber was channeled from the exhaust pipe of the engine and mixed with the inlet air and fuel gas in the gas mixer and then induced back into the combustion chamber.

The system was fitted with a control valve to control the percentage of the exhaust gas recirculated during the experiment. The piping was fabricated from a 25mm diameter steel cylindrical pipes. The dimensioning of the pipe was based on the size of the engine exhaust pipe. The maximum percentage of the exhaust recirculated was 40% so the diameter of the pipe was made 50% of the engine exhaust pipe [53].

### 3.5 Measurement Devices and Parameters

During this experimental study, engine power output, performance and emission parameters were measured. The engine performance was analysed using parameters such as; engine brake power, engine brake thermal efficiency, fuel consumption, biogas flow rate, brake specific fuel consumption and emissions.

The in-cylinder pressure variation was measured by a pressure transducer (piezo sensor) and the signal sent to the computer data acquisition system. The rate of heat release for each cycle was calculated using the Enginesoft software using Eqn.3.9, where  $Q$ ,  $\theta$ ,  $P$ ,  $V$  and  $\gamma$  is the heat release, crank angle, cylinder pressure, cylinder volume and specific heat ratio respectively.

$$\frac{dQ}{d\theta} = \frac{\gamma}{\gamma - 1} P \frac{dV}{d\theta} + \frac{1}{\gamma - 1} V \frac{dP}{d\theta} \quad (3.9)$$

### 3.5.1 Engine Brake Power

Brake power is the actual engine power output at the output shaft. Measurement of engine brake power was done by determining the torque and angular speed of the engine output shaft. Engine torque and its angular speed are used to calculate brake power as shown in Eqn.3.10.

The engine torque was measured by an eddy current dynamometer. An eddy current dynamometer uses the eddy currents that oppose the rotor motion, thus loading the engine and a moment arm measures the torque as it is explained in Section 3.2.2.1. A rotary encoder is fitted on the engine shaft for crank angle signal as shown in Fig.3.12. A rotary encoder is an electro-mechanical device that measures the angular position or motion of a shaft which is typically further processed elsewhere into the digital code that represents engine speed.

$$\text{Brake Power} = \frac{2\pi NT}{60} \quad (3.10)$$

where T is torque

$$T = WR$$

$$W = 9.81 \times \text{Net mass applied in kg.}$$

R is the radius and N is speed in revolutions per minute (rpm)

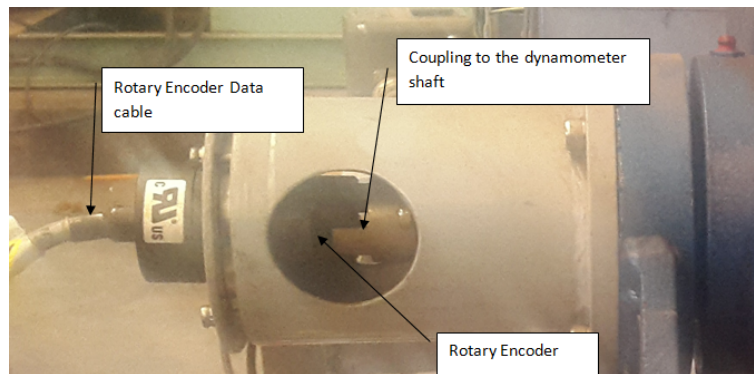


Figure 3.12: Rotary encoder fitted on the engine shaft

### 3.5.2 Indicated Power

Indicated power is the rate of work transfer from the fuel within the cylinder to the piston. It is the total power developed by combustion of fuel in the combustion chamber. It is more than the engine brake power and the difference is called friction power. Friction power is the power absorbed in overcoming engine friction, and driving engine accessories [69, 70].

A dynamic pressure sensor (piezo sensor) is fitted in the cylinder head to sense combustion pressure. A rotary encoder is fitted on the engine shaft for crank angle signal. Both signals are simultaneously scanned by an engine indicator (electronic unit) and communicated to computer. The software in the computer draws pressure crank-angle and pressure volume plots and computes indicated power of the engine.

### 3.5.3 Fuel Consumption

In this dual fuel engine experiment, measurement of fuel consumption involved measuring the biogas fuel consumption and diesel fuel consumption separately. Their flow

rates were measured using biogas flow meter and glass burette respectively under different engine operating conditions and the consumption calculated using their different densities.

### 3.5.3.1 Biogas Fuel Consumption

During the experiments, the amount of biogas consumed was measured using a gas flow meter as shown in Fig.3.13. The flow meter was connected between the engine and the gas pump to measure the flow rate as the biogas was introduced to the engine through the gas mixer.

The flow meter was calibrated to measure the volume of fuel that flows through

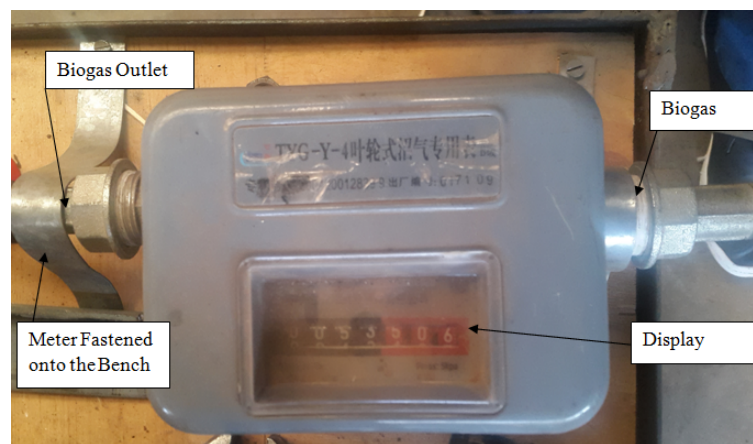


Figure 3.13: Biogas Flow Meter

in a particular period of time in  $\text{m}^3$  up to  $1000 \text{ m}^3$  with accuracy of  $0.001 \text{ m}^3$ . During the experiment, the initial reading of the flow meter was recorded and the engine was operated for a particular load under different test conditions for one minute and the final flow meter reading was recorded after the experiment. The difference between the final and the initial meter reading in one minute was recorded as the volume of biogas

consumed per minute.

Biogas fuel consumption in kg/hour was calculated using the density of biogas (1.22 kg/m<sup>3</sup>) and converting the volume per minute flow rate to volume per hour. Multiplying the density of biogas with the flow rate in volume per hour for each test results gave the biogas fuel consumption.

Using the biogas mass flow rate, biogas energy share was calculated. Biogas energy share is the ratio of energy supplied by the primary fuel (biogas), to the sum of the energy supplied by the biogas and the pilot fuel diesel. Biogas energy share is important in analysing the premixed lean combustion stage. Biogas energy share was calculated using Eqn.3.12 where  $\dot{m}f_b$ ,  $\dot{m}f_d$ ,  $CV_b.\dot{m}f_b$  and  $CV_d.\dot{m}f_d$  is the biogas mass flow rate, diesel mass flow rate, energy supplied by biogas and diesel respectively.

$$\text{Biogas energy share} = \frac{\text{Energy supply by biogas}}{\text{Total energy supplied by (biogas + diesel)}} \quad (3.11)$$

$$\text{Biogas energy share} = \frac{CV_b.\dot{m}f_b}{CV_b.\dot{m}f_b + CV_d.\dot{m}f_d} \quad (3.12)$$

### 3.5.3.2 Diesel Fuel Consumption

In dual fuel engine, engine power is obtained from the combustion of two fuels. Each fuel contributes a percentage to the total fuel energy. The contribution of diesel in this experiment was computed by measuring the diesel fuel flow into the engine during different engine tests.

The diesel fuel consumed by an engine was measured by determining the volume flow of the fuel in a given time interval during each test. The volume flow was measured using a glass burette having graduations in milliliters (ml) as shown in Fig. 3.14. During each test, the volume flow was measured for a particular time, (one minute for each engine loading) and then using the diesel density ( $873 \text{ kg/m}^3$ ), fuel consumption in (kg/hour) was calculated by multiplying the volume flow rate with the diesel density.

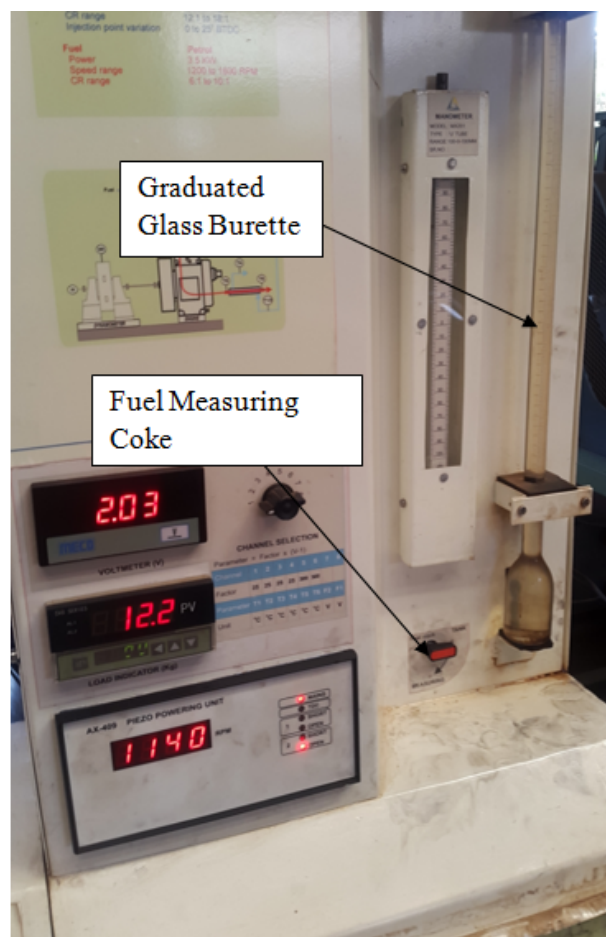


Figure 3.14: Glass Burette for Measuring Diesel Flow



### 3.5.4 Thermal Efficiency

Thermal efficiency of an engine is the ratio of its output power to the power supplied by the fuel as shown in Eqn.3.13. It is the dimensionless measure of the performance of an engine. It is the engine's fuel conversion efficiency.

$$\eta_t = \frac{\dot{W}}{\dot{m}_f CV} \quad (3.13)$$

Where  $\dot{W}$ ,  $\dot{m}_f$  and CV is the engine power output, fuel flow rate to the engine and fuel calorific value respectively.

Thermal efficiency of the dual fuel engine was obtained from the ratio of the engine power output to the power supplied by both diesel fuel and biogas. Fuel power contribution of each fuel was obtained by multiplying calorific values of each with their respective mass flow rates as shown in the Fig.3.14. Thermal efficiency for an engine can be defined as either brake thermal efficiency or indicated thermal efficiency.

$$\eta_{ther} = \frac{\dot{W}}{\dot{m}_{fb} CV_b + \dot{m}_{fd} CV_d} \quad (3.14)$$

Where  $\eta_{ther}$ ,  $\dot{W}$ ,  $\dot{m}_{fb}$ ,  $CV_b$ ,  $\dot{m}_{fd}$ ,  $CV_d$  is the thermal efficiency, power output, biogas fuel flow rate, biogas calorific value, diesel fuel flow rate and calorific value of diesel respectively.

#### 3.5.4.1 Brake Thermal Efficiency

The brake thermal efficiency of the dual fuel engine is the ratio of its brake power to the power supplied by the two fuels in the combustion chamber. Brake thermal efficiency

was for various test was calculated as shown in Eqn.3.15.

$$\eta_{bt} = \frac{\dot{W}_b}{\dot{m}_{fb}CV_b + \dot{m}_{fd}CV_d} \quad (3.15)$$

Where  $\eta_{bt}$ ,  $\dot{W}_b$ ,  $\dot{m}_{fb}$ ,  $CV_b$ ,  $\dot{m}_{fd}$ ,  $CV_d$  is the brake thermal efficiency, brake power, biogas fuel flow rate, biogas calorific value, diesel fuel flow rate and calorific value of diesel respectively.

#### 3.5.4.2 Indicated Thermal Efficiency

Indicated thermal efficiency was calculated in almost the same way as brake thermal efficiency but using indicated power as obtained in Section 3.5.2. Indicated thermal efficiency was calculated as shown in Eqn.3.16.

$$\eta_{it} = \frac{\dot{W}_i}{\dot{m}_{fb}CV_b + \dot{m}_{fd}CV_d} \quad (3.16)$$

Where  $\eta_{it}$ ,  $\dot{W}_i$ ,  $\dot{m}_{fb}$ ,  $CV_b$ ,  $\dot{m}_{fd}$ ,  $CV_d$  is the indicated thermal efficiency, engine indicated power, biogas fuel flow rate, biogas calorific value, diesel fuel flow rate and calorific value of diesel respectively.

#### 3.5.5 Measurement of Emissions

During the experiments, exhaust gases were measured using a Testo 350-S flue gas analyser which comprised of a control unit and a testo 350-S/-XL flue gas analyser as shown in Fig.3.15.

The analyser measures Oxygen (0 to 25%), carbon-monoxide (0 to 10,000 ppm), nitric oxide (0 to 3,000 ppm), nitrogen-dioxide (0 to 500 ppm), sulfur dioxide (0 to

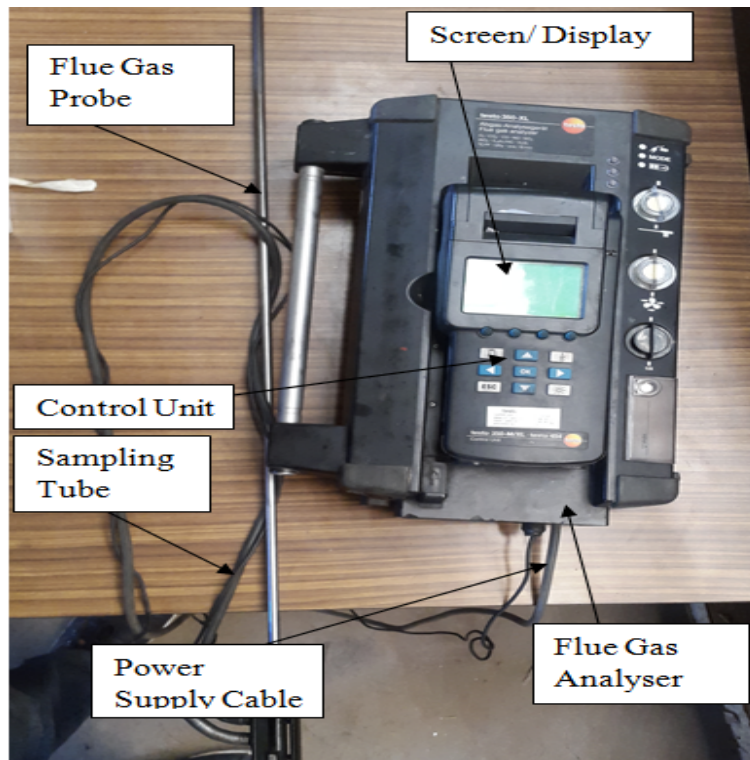


Figure 3.15: Testo 350-S Gas Analyser

5,000 ppm), hydrocarbons (HC) (0 to maximum volume of HC), gas temperature (-40 to 600 F) and measures carbon-dioxide (0 to maximum volume of CO<sub>2</sub>) and equipment efficiency (0 to 100%) [71].

#### 3.5.5.1 Emission Measuring Procedure

An opening was created in the exhaust pipe to allow the insertion of the flue gas analyser probe. The probe and the sampling tube were connected to the gas analyser. The analyser was powered on to start measuring the emission concentrations. At the start of each test, the probe was inserted into the opening created on the exhaust pipe. The sample was then taken in by the gas analyser through the sampling tube and measuring would start by pressing the start on the control unit.

The content of the exhaust gas was displayed on the gas analyser control unit display. The readings of HC, NO<sub>x</sub>, SO<sub>x</sub>, CO<sub>2</sub>, O<sub>2</sub>, for each test were allowed to stabilize for 2 minutes and then the results were printed out by pressing the print button on the gas analyser control unit.

### **3.6 Experimental Procedure**

In this section, the procedures followed to achieve the objectives of this experiment are discussed. Steps followed to carry out the experiments at varying compression ratios and varying injection timing are explained in details here. Methods for varying the flow rates of biogas and EGR into the engine are also discussed in this section.

#### **3.6.1 Varying the Compression Ratio**

The research engine that was used in this experiment was a variable compression ratio engine. It used the tilting block mechanism to vary the compression ratio without changing the geometry of the combustion chamber. The mechanism works by varying the TDC position of the piston [72, 73].

To study the effect of compression ratio on combustion, performance and emission characteristics of the dual fuel engine, the compression ratio was varied between 18 and 14. Performance, combustion and emission experimental data was collected for compression ratio 14, 16 and 18.

### 3.6.1.1 Procedure

The mechanism is provided with the compression ratio indicator as shown in Fig. 3.16 which indicates the compression ratio marks of 12, 14, 16 and 18. To change the com-

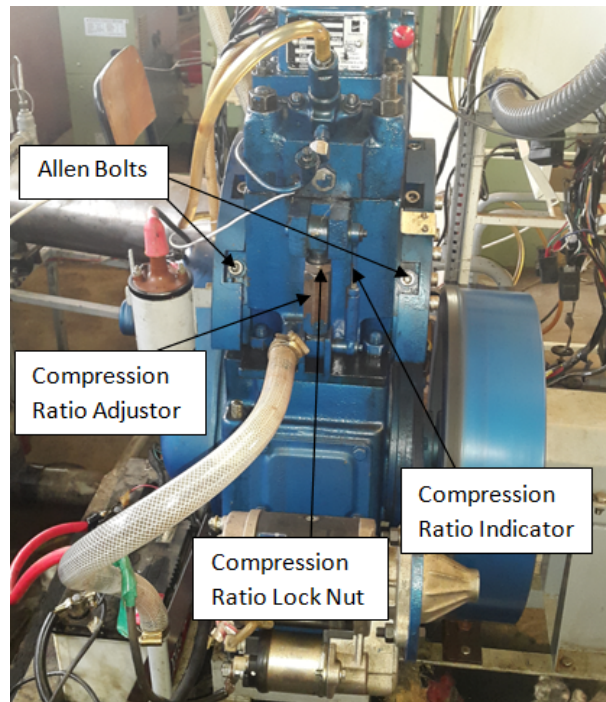


Figure 3.16: Compression Ratio Adjustment Mechanism

pression ratio, the allen bolts on both sides of the block were loosened, the compression ratio lock nut was also loosened to enable the compression ratio adjustor to rotate and move to a specific compression ratio mark on the CR indicator. After adjusting to the required CR, the lock nut was then tightened and all the allen bolts tightened. The new compression ratio was then configured in the software and the tests carried out.

### 3.6.2 Varying the Injection Timing

Fuel injection system is mainly designed to deliver fuel into the combustion chamber, however, how the fuel is delivered makes the difference in engine performance,

emissions, and noise characteristics. Varying the injection timing of the engine allows for the optimum point where the engine performance and emission characteristics are optimum.

### 3.6.2.1 Procedure

The engine injection point was set at  $23^\circ$  bTDC and was marked point "F" on the flywheel which was eight teeth from TDC mark as shown in Fig.3.17. To adjust the injection timing, the high pressure fuel pipe from the fuel pump was removed and the decompression lever raised to a vertical position to free the flywheel for hand operation.

The flywheel was then rotated in either direction(clockwise or anti-clockwise) and

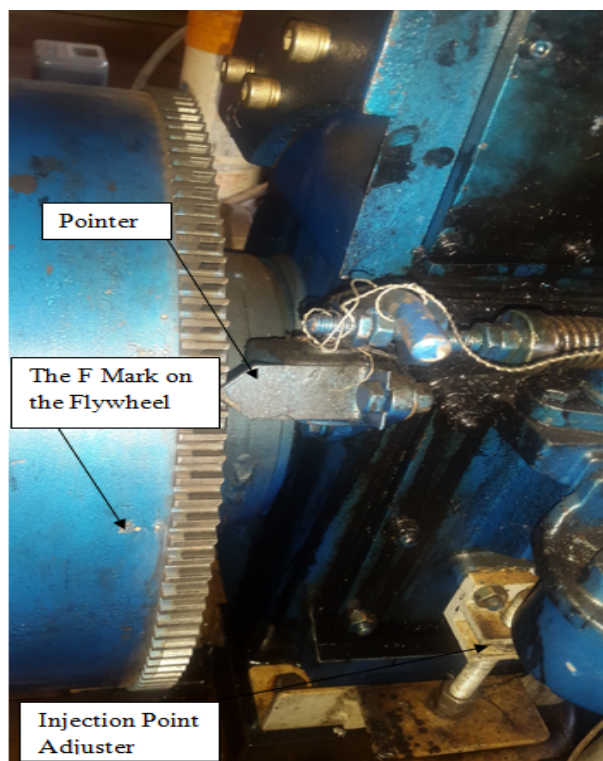


Figure 3.17: Injection Point Adjustment System

the point at which fuel spilled was noted and the difference between that point and

the preset point noted so that the teeth in between are used to give the injection timing. Each two teeth from the "F" mark on the flywheel represent crank angle of  $2.2^\circ$ . Therefore, from the standard set injection timing  $23^\circ$ , addition of two teeth advanced injection timing to  $25.2^\circ$  bTDC. Investigation was done for the injection timings of  $20.8^\circ$ ,  $23.0^\circ$ ,  $25.2^\circ$ ,  $27.4^\circ$  and  $29.5^\circ$  bTDC

### 3.6.3 Variation in Biogas and EGR Flow Rates

To investigate the effect of biogas flow rate on combustion, performance and emission characteristics of a dual fuel engine, biogas flow was regulated by a flow control valve. The flow was adjusted by turning the valve by 1/4, 1/2 and full valve opening. Tests were carried out for each valve opening/flow rate. The 1/4 valve opening represented 20% biogas and 80% diesel, 1/2 valve opening represented 40% biogas and 60% diesel and full valve opening represented 80% biogas and 20% diesel fuel into the engine.

The effect of EGR rates of 10%, 20%, 30% and 40% were considered in this study and the  $\text{NO}_x$  variation was recorded using an exhaust gas analyzer. Using the flow rate of EGR, the EGR ratios were calculated using Eqn.3.17 where  $\text{EGR}(\%)$ ,  $\dot{m}_{egr}$ ,  $\dot{m}_a$  and  $\dot{m}_b$  is the EGR percentage, EGR mass flow rate, air mass flow rate and biogas mass flow respectively. EGR mass flow rate was controlled by an EGR control valve that was designed on the EGR system.

$$\text{EGR}(\%) = \frac{\text{mass of EGR recirculated}}{\text{Total charge into the combustion chamber}}$$

$$\text{EGR}(\%) = \frac{\dot{m}_{egr}}{\dot{m}_a + \dot{m}_{egr} + \dot{m}_b} \quad (3.17)$$

## **CHAPTER FOUR**

### **4.0 RESULTS AND DISCUSSION**

#### **4.1 Introduction**

Results of the experiments on the effect of compression ratio, injection timing and biogas flow rate on the combustion, performance and emission of dual fuel engine are presented in this chapter. Also the results from the experiment on effect of EGR on  $\text{NO}_x$  emission in the dual fuel engine are presented in this section. The variations and trends of the results are also discussed in this chapter. This chapter is divided into four sections to explain the effect of compression ratio, injection timing, biogas flow rate and EGR in details.

#### **4.2 Simulation of the Gas Mixing Unit**

Modeling and simulation has become a very important tool in engineering when designing systems because it helps in avoiding the unnecessary costs, time and other challenges that come up during designing and testing. The mixing unit was simulated to show the performance and homogeneity in mixing of the gases. The simulation was done using ANSYS CFD cfx version R17.0 and results of the animation are shown in Fig. 4.1 and 4.2.

#### **4.3 Effect of Compression Ratio on Combustion, Performance and Emission**

To study the effect of compression ratio, the engine was operated at a constant speed of 1500rpm and a constant injection timing of  $23^\circ$  bTDC. Engine load was varied from



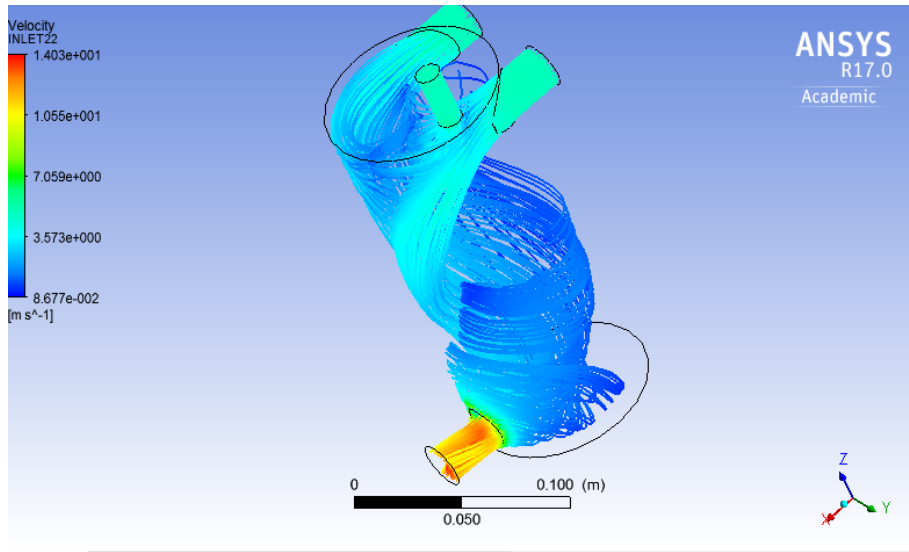


Figure 4.1: Velocity distribution in the gas mixer

3kg to 12 kg for compression ratio of 14:1, 16:1 and 18:1 and the performance and emission characteristics of the engine were analysed. This section therefore presents the results and discussion of performance characteristics of brake thermal efficiency, brake specific fuel consumption and mechanical efficiency and also the emission characteristics of  $\text{NO}_x$ , carbon dioxide, hydrocarbons and carbon monoxide.

### 4.3.1 Combustion Characteristics Analysis

#### 4.3.1.1 Cylinder Pressure

Fig. 4.3 shows the cylinder pressure variation with the crank angle for different compression ratios 18:1, 16:1 and 14:1. It can be observed from the figure that as the compression ratio increased, the peak pressure increased. Porpatham *et al.*, [18] reported similar results in the experiment to find out the effect of compression ratio on the performance and combustion of a biogas fueled spark ignition engine. This trend was attributed to faster combustion at high compression ratios [74]. It can also be seen

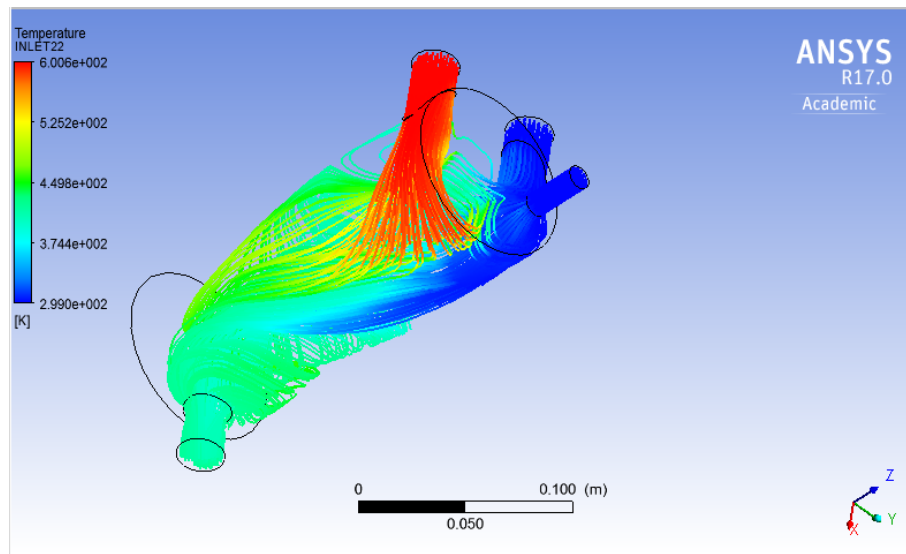


Figure 4.2: Temperature distribution in the mixer

that as the compression ratio reduced, the peak cylinder pressure shifted more to the power stroke (after TDC). The peak cylinder pressure at CR of 18:1, 16:1 and 14:1 was at 11°, 12° and 19° aTDC respectively. This is due to late combustion at low compression ratios caused by increased ignition delay.

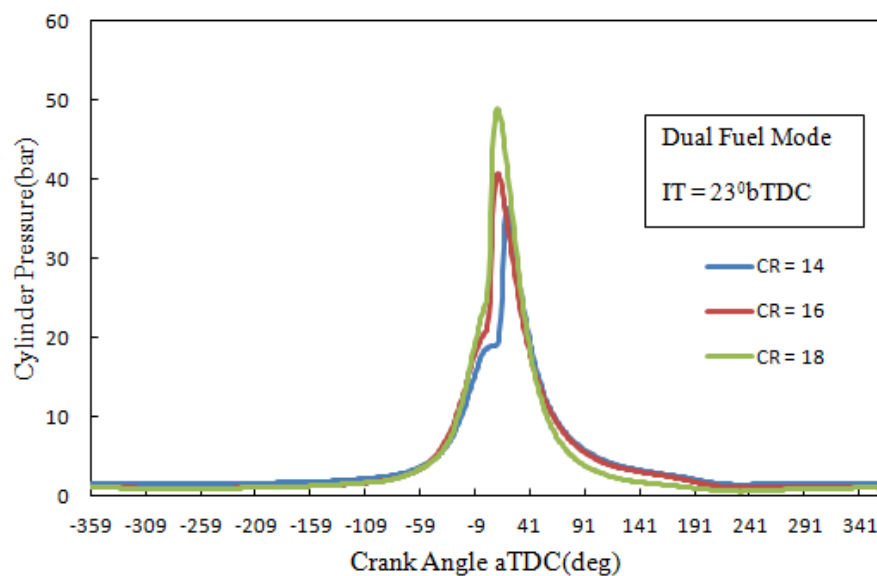


Figure 4.3: Variation of cylinder pressure with crank angle at different CR

#### **4.3.1.2 Net Heat Release**

Net heat release history of the engine defines the combustion efficiency of fuel that in turn affects the engine performance and HC, NO<sub>x</sub>, CO and other engine exhaust emissions. It depicts the ignition delay and the smoothness of the combustion process at different compression ratios for the dual fuel engine.

Fig.4.4 shows the variation in the net heat release of the engine with the crank angle at different compression ratios. The maximum net heat release of 54.1 J/deg was observed at the compression ratio of 18:1. As the compression ratio reduced from 18:1 to 14:1, net heat release rate reduced by 4% on average. The average reduction in the peak net heat release rate for the reduction in compression ratio from 18:1 to 14:1 was 14.83 J/deg. The increase in net heat release at high compression ratio was attributed to a better pilot fuel atomization that led to better and fast combustion and higher air temperature [75]. The negative heat release was caused by the transfer of heat into the cylinder surfaces [48, 76]

### **4.3.2 Performance Characteristics Analysis**

#### **4.3.2.1 Brake Thermal Efficiency**

Fig.4.5 shows the variation of brake thermal efficiency with the engine load at different compression ratios. Brake thermal efficiency increases as the load increases for all the compression ratios and for both dual fuel operation and diesel fuel operation. The increase in thermal efficiency with increase in the load is attributed to the higher power

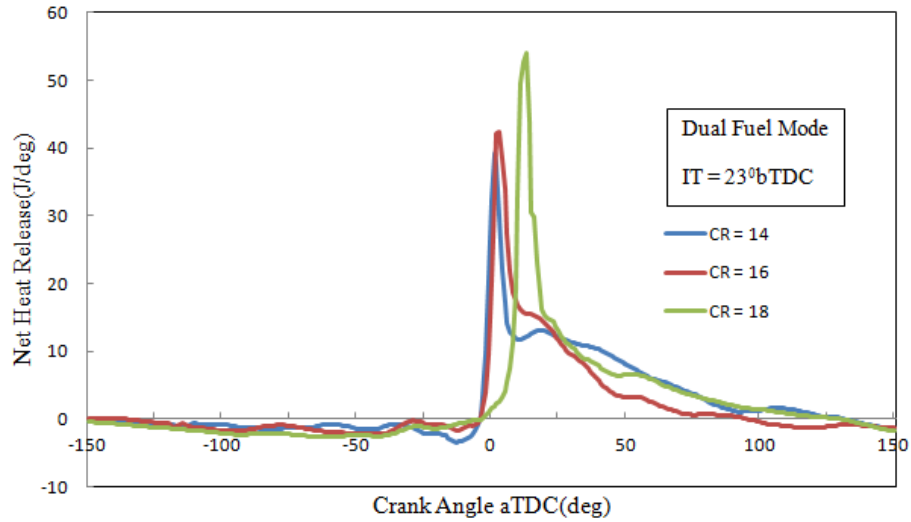


Figure 4.4: Variation of net heat release with crank angle at different CR produced at higher loads. There is a 19% increase in the thermal efficiency when the compression ratio was increased from 16 to 18. Hariram *et al.*, [48] in the study of the influence of compression ratio on the combustion and performance characteristics of a direct injection compression engine obtain similar results.

The increase in thermal efficiency with compression ratio is attributed to the rise in temperature and pressure in the combustion chamber that increases with the increase in compression ratio [38,77]. The increase in temperature and pressure in turn leads to increased combustion of biogas in the combustion chamber. It is also observed from the figure that the thermal efficiency of the dual fuel engine at all loads under dual fuel operation is lower than that of the diesel engine. By average, the thermal efficiency dropped by 17% between the diesel operation and dual fuel operation at CR 18. The drop in the thermal efficiency under dual fuel is caused by the fact that biogas contains carbon-dioxide which replaces oxygen in the combustion chamber thus causing

incomplete combustion in dual fuel engine [78].

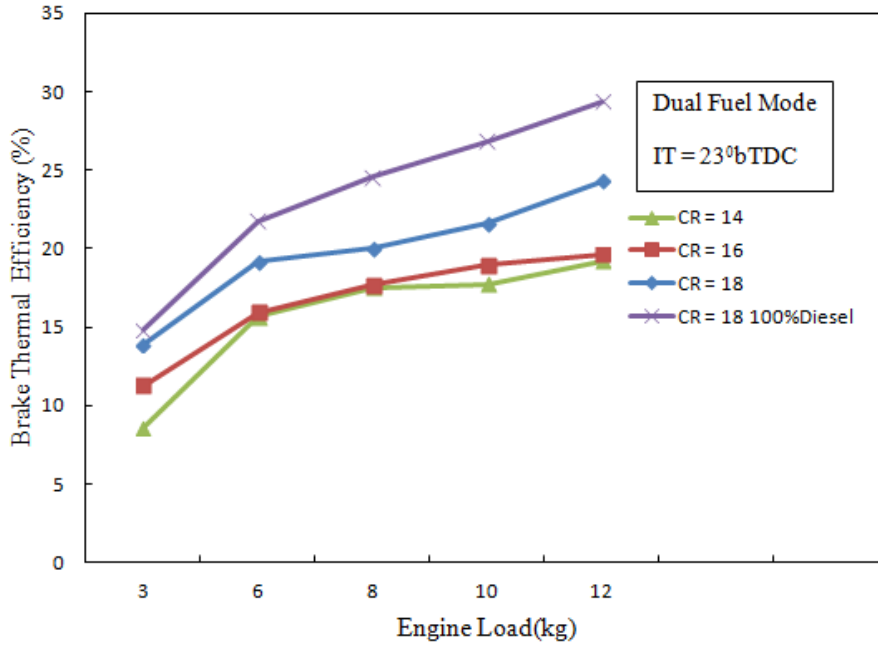


Figure 4.5: Brake thermal efficiency variation with engine load at different CR

#### 4.3.2.2 Brake Specific Fuel Consumption (BSFC)

Brake specific fuel consumption variation is shown in Fig.4.6. It can be observed that the brake specific fuel consumption of dual fuel engine is higher than under diesel fuel operation. The increase in brake specific fuel consumption of a dual fuel engine is caused by lower heating value (calorific value) of biogas [43]. Another reason for the increased brake specific fuel consumption under dual fuel operation is the presence of  $\text{CO}_2$  in biogas that leads to low fuel conversion efficiency [78]. The figure also shows the reduction in BSCF for both diesel and dual fuel operations with increase in the engine loading. This is attributed to the incomplete combustion and slow burning that lead to low fuel conversion efficiency at low loads [79].

It can also be observed from the figure that the BSFC lowers with increasing compression ratio. There is about 26% drop at a load of 3kg for the increase of compression ratio from 14 to 18. This trend is attributed to the better combustion at higher compression ratios [30]. Similar results were also observed by V. Hariram *et al.*, [48] in their research to study the influence of compression ratio on combustion and performance characteristics of direct injection compression ignition engine.

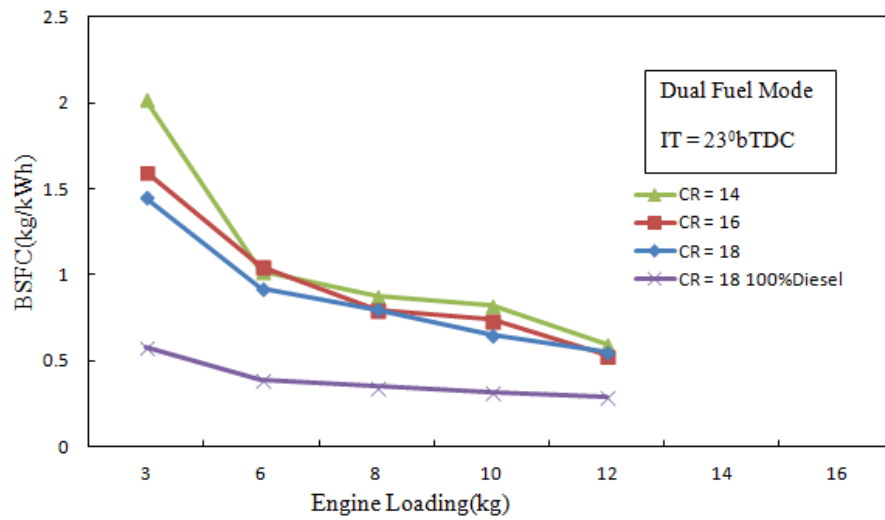


Figure 4.6: Variation in brake specific fuel consumption with load at different CR

#### 4.3.2.3 Mechanical Efficiency

Variations in mechanical efficiency of the dual fuel engine with compression ratio and engine loading is shown in Fig.4.7. For the dual fuel engine, the mechanical efficiency is lower than that of a purely diesel operated engine by 63% on average. However its also observed that for both the dual fuel engine at all compression ratios and diesel engine, the mechanical efficiency increases with the increase in the engine loading. The mechanical efficiency trend does not increase regularly with the increase in the

compression ratio. This trend can mainly be described by the increase of frictional power at high compression ratio [51].

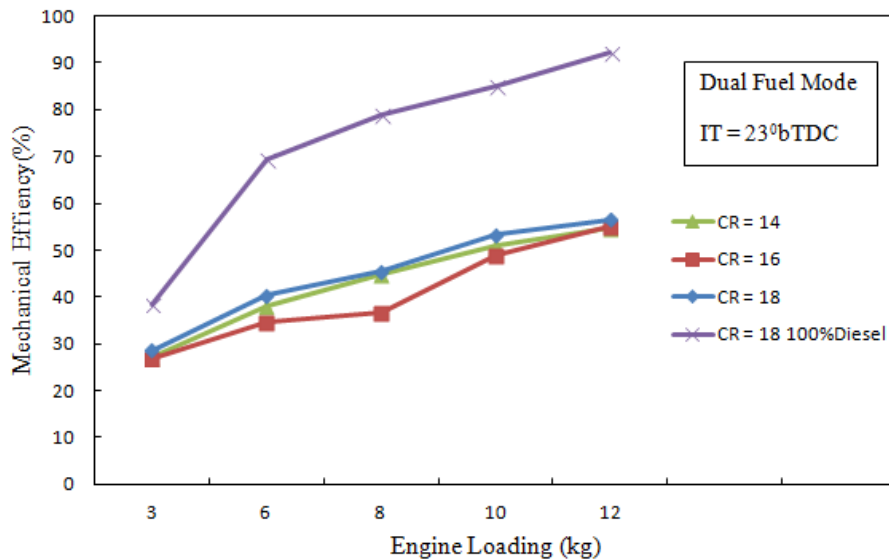


Figure 4.7: Variation in mechanical efficiency with load at different CR

### 4.3.3 Emission Analysis

#### 4.3.3.1 Carbon-dioxide Emission

Fig.4.8 shows the variation in the carbon-dioxide emission with the engine loading at different compression ratios. It can be observed that at high compression ratios, CO<sub>2</sub> emission in the exhaust increases. The reason for an increase in CO<sub>2</sub> with increase in compression ratio is that at high compression ratio, the clearance volume of the combustion chamber reduces which leads to increase in temperatures of combustion and thus better combustion. Better combustion leads to high CO<sub>2</sub> in the combustion exhaust. Similar results were obtained by Bora *et al.*, [35] in the experiment to optimize the injection timing and compression ratio of a raw biogas powered dual fuel engine.

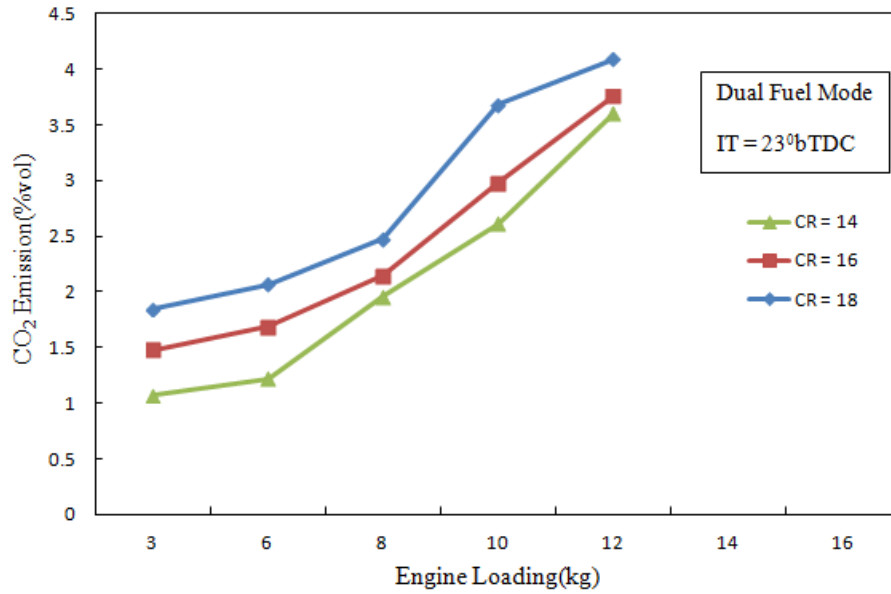


Figure 4.8: Variation in CO<sub>2</sub> emission with load at different CR

#### 4.3.3.2 NO<sub>x</sub> Emission

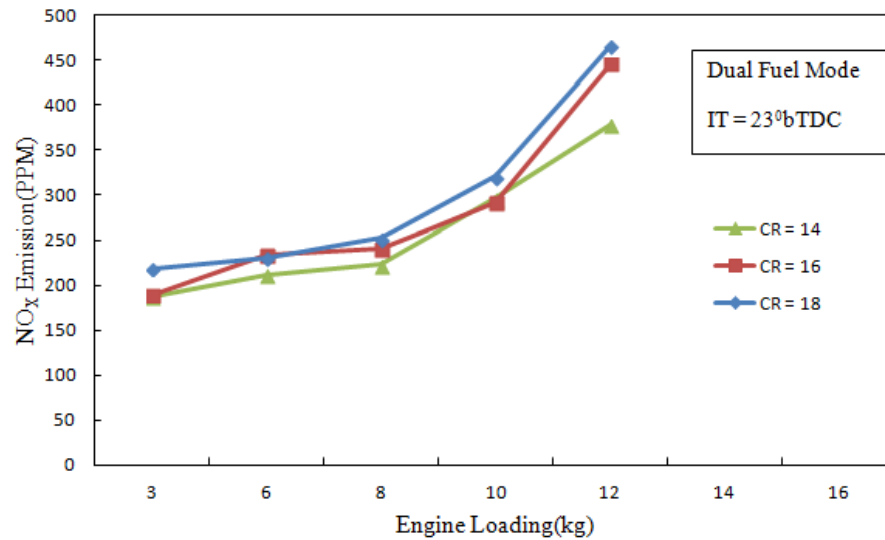


Figure 4.9: Variation in NO<sub>x</sub> emission with load at different CR

In Fig.4.9 the variation of the NO<sub>x</sub> emission with the engine load for different compression ratios is illustrated. It can be seen from the figure that NO<sub>x</sub> emission increase as the compression ratio increases. There is a 20% increase on average in NO<sub>x</sub> for the compression ratio increase from 14 to 18. The rise in NO<sub>x</sub> with compression ratio is



attributed to the increase in cylinder temperature.

At high compression ratios, the clearance volume reduces and thus the combustion temperatures increase leading to oxidation of nitrogen gas and high  $\text{NO}_x$  emission. It can also be observed from the figure that for all the compression ratios, the  $\text{NO}_x$  emission increases with increase in the engine load. One reason for this is that at high load, there is increased combustion temperature and pressure at high engine loads [18, 79].

#### **4.3.3.3 Carbon monoxide Emission**

The effect of compression ratio on carbon-monoxide emission is illustrated in the Fig.4.10. It can be observed in the figure that high compression ratios have low CO emissions. The existence of high CO emissions at low compression ratio describes the incomplete combustion of the biogas-air mixture in the combustion chamber. This is caused by low combustion temperatures that limit flame propagation [19].

The figure also shows that at low loads, the emission of CO is high for all the compression ratios and reduces as the load increases. This is attributed to the dilution of the charge with  $\text{CO}_2$  in biogas that leads to low temperatures in the combustion chamber that subsequently reduces the oxidation of CO and increases CO emission at low loads. Increasing load also causes increase in temperatures thus increasing combustion and reducing CO emission [34].

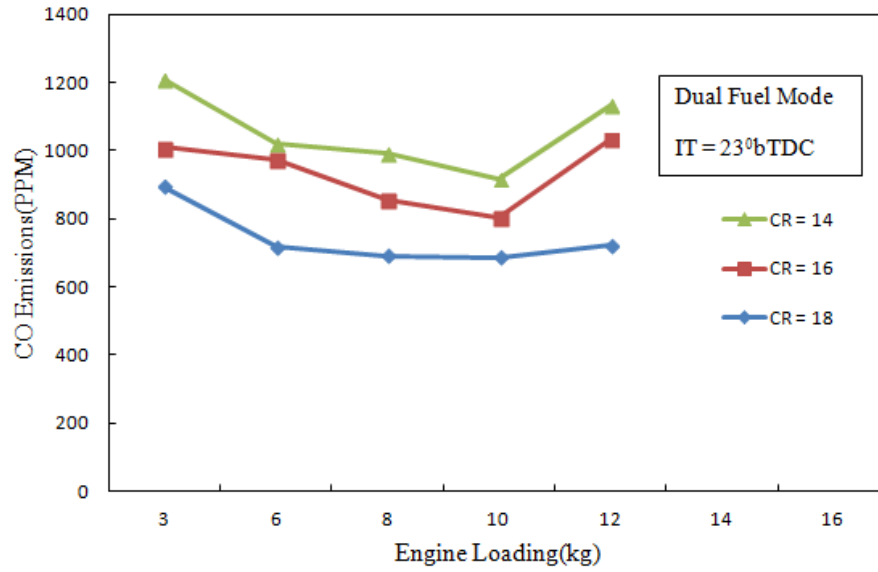


Figure 4.10: Variation in CO with load at different CR

#### 4.3.3.4 Unburnt Hydrocarbons

The unburnt hydrocarbon is the product of incomplete combustion of fuel. Fig.4.11 illustrates that HC emission reduced with the increase in the compression ratio. In this study, on average the HC emission decreased by 60% with the increase in CR from 16 to 18. The reason behind this trend is that at high compression ratio, cylinder temperature increases and thus facilitates proper flame propagation and complete fuel combustion [35, 77]. It can also be observed from the figure that HC emission also reduces as the engine load increases. This is also attributed to the rise in cylinder temperature at high loads that facilitates complete combustion.

#### 4.4 Effect of Injection Timing on Combustion, Performance and Emission

Injection timing is one of the most important parameters in the combustion, performance and emission of a dual fuel engine. It influences the ignition delay, cylinder

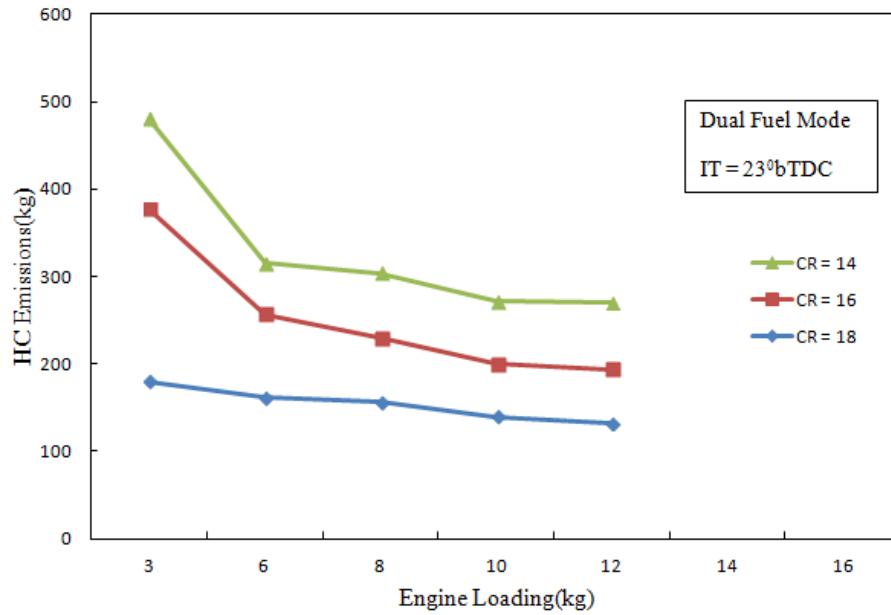


Figure 4.11: Variation in HC with load at different CR temperature and cylinder pressure that in turn affect the rate of fuel combustion.

This section explains the results from the experimental study of the effects of injection timing on the combustion, performance and emission of a dual fuel engine. The experiments were carried out with the engine at a compression ratio of 18:1 that showed superior performance and emission characteristics in the previous experiments as shown in Section 4.3. The variations in combustion, performance and emission characteristics with injection timing are discussed in this section.

#### 4.4.1 Combustion Characteristics Analysis

##### 4.4.1.1 Cylinder Pressure

Dual fuel combustion process takes place in three stages; premixed combustion of pilot fuel (diesel) and a portion of air-biogas mixture, combustion of gaseous fuel and diffu-

sion combustion where residual pilot fuel and gaseous fuel burn [80]. The in-cylinder pressure variation with crank angle depicts the effect of injection timing on the fuel ignition and combustion behavior.

Fig.4.12 shows the variation in the in-cylinder pressure with crank angle for different pilot fuel injection points. The figure indicates that advanced injection of the pilot diesel fuel increased the peak cylinder pressure of the dual fuel engine. The highest peak pressure of 49 bar was obtained at the injection timing of  $29.5^\circ$  bTDC. Retarding the injection timing to  $20.8^\circ$  bTDC reduced the peak pressure to 28 bar from the standard 42 bar at  $23.0^\circ$  bTDC. This trend in pressure variation is due to the fact that advanced injection timing introduces pilot diesel fuel into the combustion chamber earlier in the first stage of combustion meaning that there is earlier diesel fuel ignition thus more energy is released during the compression stroke that leads to the rise in cylinder pressure [81–83].

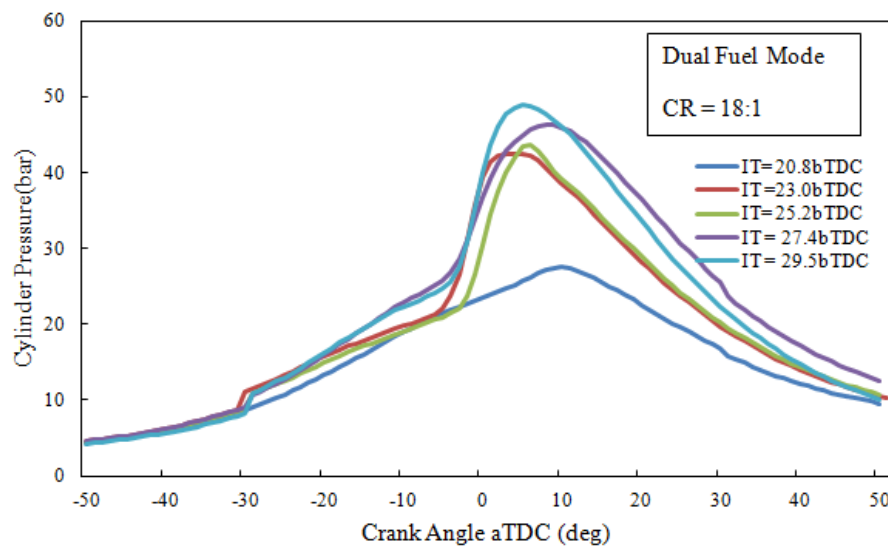


Figure 4.12: Variation in cylinder pressure with crank angle at different IT

#### 4.4.1.2 Net Heat Release

Fig.4.13 shows the variation of the net heat release of the biogas dual fuel engine with crank angle for different diesel fuel injection timings. The figure depicts that as the injection timing was advanced, the net heat release increased. Retarding the injection timing reduced the net heat release of the engine. The peak heat release rate was 60 J/deg at injection timing of  $29.5^{\circ}$  bTDC. The increase in the peak net heat release rate with advancing pilot fuel injection is due to the fact that with advanced injection, biogas-air mixture and the injected pilot diesel fuel have sufficient time for homogeneous mixing [47]. This leads to a better flame propagation and thus increasing the rate of heat release.

It can be seen from the Fig.4.13 that as the injection timing was advanced to  $29.5^{\circ}$  bTDC, the peak net heat release occurred at  $5^{\circ}$  before TDC. This is because the charge premixed combustion phase started earlier. Retarding the injection timing from  $23^{\circ}$  bTDC to  $20.8^{\circ}$  bTDC led to the reduction in the peak net heat release. This was attributed to the unavailability of sufficient time for the fuel to mix homogeneously and a large portion of fuel burning slowly in the diffusion phase of the combustion process [81, 82].

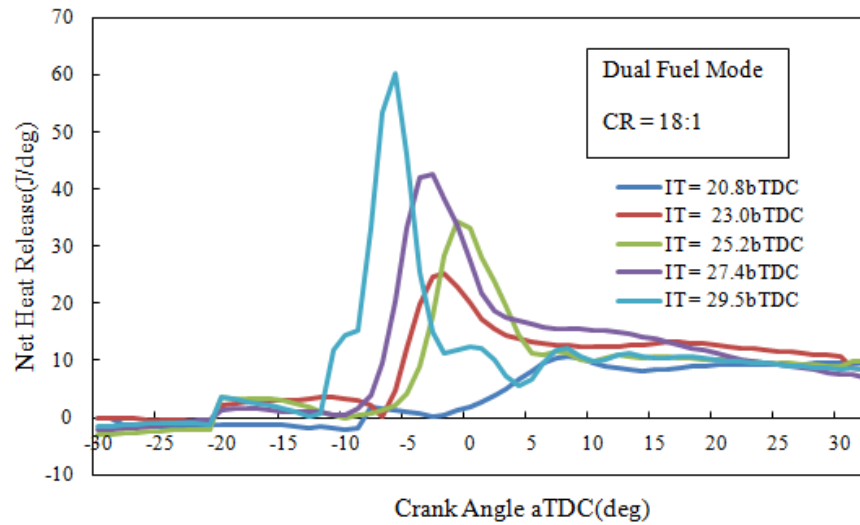


Figure 4.13: Variation of NHR with crank angle at different IT

#### 4.4.2 Performance Characteristics Analysis

##### 4.4.2.1 Brake Thermal Efficiency

The results from the experiments in Fig.4.14 show the variation in brake thermal efficiency of a dual fuel engine operating at a compression ratio of 18:1, speed of 1500rpm and varying the load from 3kg to 12kg. It can be observed from the figure that retarding the injection timing from 23.0° bTDC to 20.8° bTDC, the brake thermal efficiency reduced by 31% on average. The brake thermal efficiency of the engine at full load for 23.0°, 25.2°, 27.4° and 29.5° was 24.3%, 24.6%, 25.1% and 25.7% respectively. Similar results were obtained by Debabrata Barik *et al.*, [34]. The reason for the increase in thermal efficiency with increased advanced injection timing is that it allows more evaporated pilot fuel to accumulate in the combustion chamber than in standard injection timing and allows time for the pilot fuel to homogeneously mix with the air and biogas which leads to high combustion efficiency [35, 84].

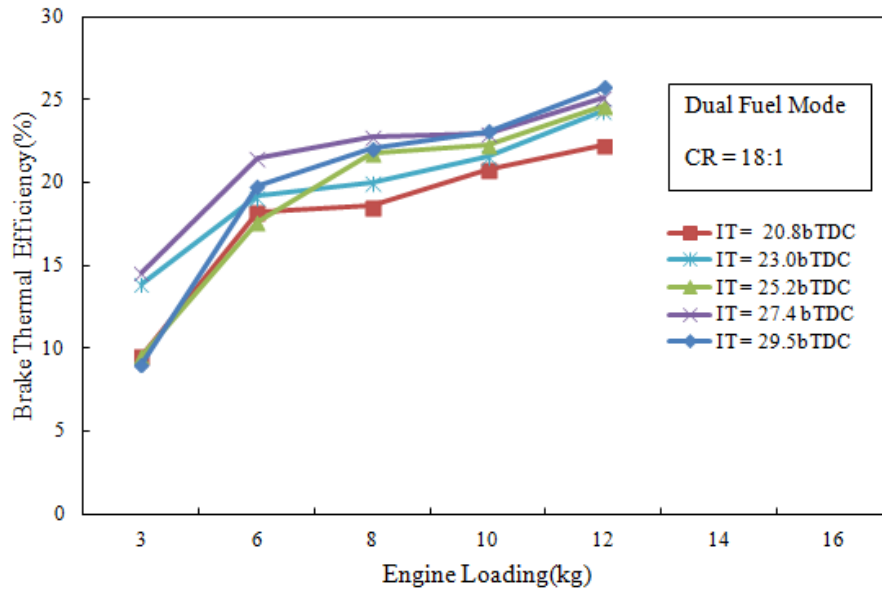


Figure 4.14: Variation in brake thermal efficiency with load at different IT

#### 4.4.2.2 Brake Specific Fuel Consumption

Fig.4.15 shows the variation of brake specific fuel consumption (BSFC) with the load at different injection timing (IT). It can be observed that when the injection timing was retarded to 20.8° bTDC from the standard 23.0° bTDC, BSFC increased by an average of 44%. Advancing the injection timing by 4.4° to 27.4° bTDC reduced the BSFC by an average of 16%. Fig.4.15 also indicates that there is a decrease in the BSFC for all the injection timings as the engine load was increased. Debabrata Barik *et al.*, [34] in the experimental investigation on the behavior of a DI diesel engine fueled with raw biogas-diesel dual fuel at different injection timing obtained similar results.

The reason for this trend in the BSFC with injection timing is that for advanced injection timing, there is an earlier start of combustion before TDC which leads to the rise in temperature causing high fuel energy conversion efficiency. This leads to an

improvement in BSFC at advanced injection timing [52, 85, 86].

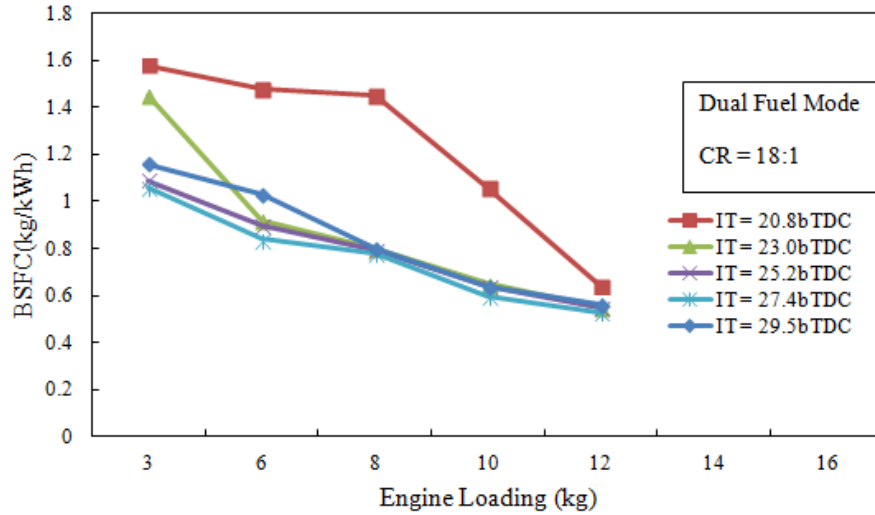


Figure 4.15: Variation of injection timing with load at different IT

#### 4.4.2.3 Mechanical Efficiency

Variation of mechanical efficiency with load at different injection timings were plotted as shown in Fig.4.16. According to the figure, mechanical efficiency of the dual fuel engine reduced as the injection timing was advanced. There was no significant change in mechanical efficiency as the injection timing was retarded from 23.0° bTDC to 20.8° bTDC. The reason for the reduction in mechanical efficiency with advancing injection timing is that there is an increase in frictional power at advanced injection timing due to increased in-cylinder temperature.

Fig.4.16 also shows that mechanical efficiency increased with increasing engine load for all the injection timings. This is attributed to the increase in temperature and in-cylinder pressure at high loads that lead to efficient fuel combustion and higher brake



power. [87].

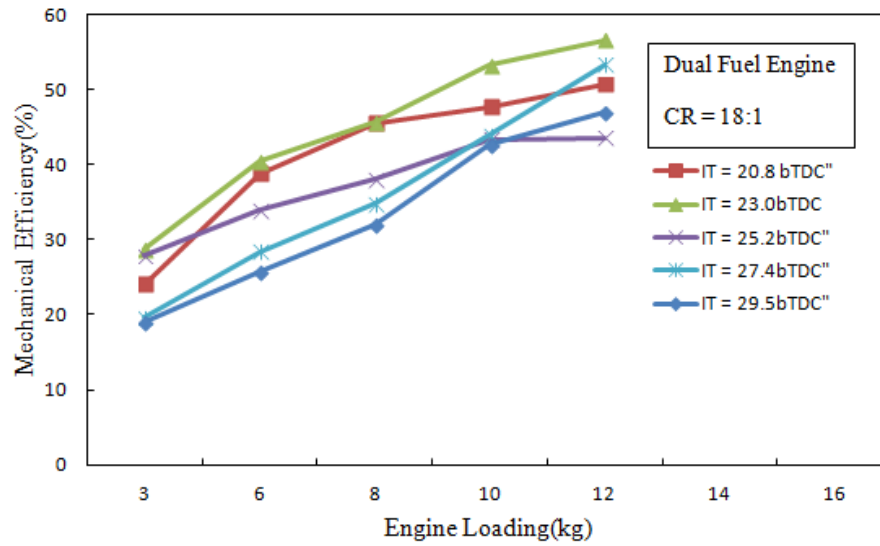


Figure 4.16: Variation of mechanical efficiency with load at different IT

### **4.4.3 Emission Analysis**

#### **4.4.3.1 Unburned Hydrocarbons**

Unburned hydrocarbons emission in the exhaust of an engine is mainly due the partial or incomplete combustion. Fig.4.17 shows how HC emission varied with the load at different injection timings of the pilot fuel. It can be seen from the figure that HC emission reduced with the increase in the load for all the injection timings. This is because at low engine loads, there is a lean air fuel mixture and low temperatures which leads to poor combustion thus increased unburned HC emission. At higher engine loads, high temperatures emphasize proper fuel combustion and reduce the HC emission.

Advancing the injection timing from the standard IT of  $23.0^{\circ}$  bTDC to  $29.5^{\circ}$  bTDC reduced HC emission by an average of 11% while retarding the injection timing to  $20.8^{\circ}$  bTDC increased HC emission by 25%. Similar results were obtained in a previous research [32, 35]. The trend of HC emission with the advancing and retarding of injection timing is due to the fact that at advanced injection timing, there is earlier start of combustion relative to TDC and thus an increase in in-cylinder temperature that leads to complete combustion of the charge and thus a reduced HC emission [16].

#### **4.4.3.2 Carbon monoxide Emission**

As shown in Fig.4.18, CO emission reduced with advanced timing. Advancing the injection timing from  $23^{\circ}$  bTDC by  $2.2^{\circ}$ ,  $4.4^{\circ}$  and  $6.5^{\circ}$  reduced the CO emissions by

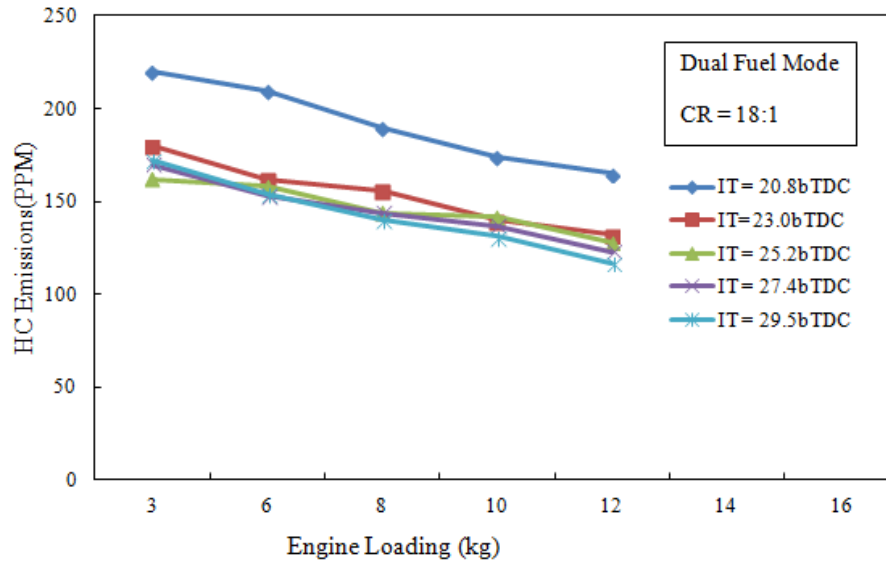


Figure 4.17: Variation in HC with load at different IT

14.5%, 15% and 28% on average respectively. Retarding the injection timing from the standard injection timing of 23.0° bTDC to 20.8° bTDC led to the increased CO emissions with the maximum at 893ppm. This variation in the CO with injection timing is caused by the fact that with advanced injection timing, there is an increased oxidation process between carbon and oxygen molecules due to an increased in-cylinder temperature and increased time interval of combustion [35].

#### 4.4.3.3 NO<sub>x</sub> Emission

NO<sub>x</sub> emissions from combustion engine are mainly in form of NO. These NO<sub>x</sub> compounds are formed from nitrogen ionization with oxygen at high temperatures [88].

Fig.4.19 shows the variation NO<sub>x</sub> emission with load for different injection timings (IT).

NO<sub>x</sub> emission increased with the increase in engine load for all the pilot fuel injection

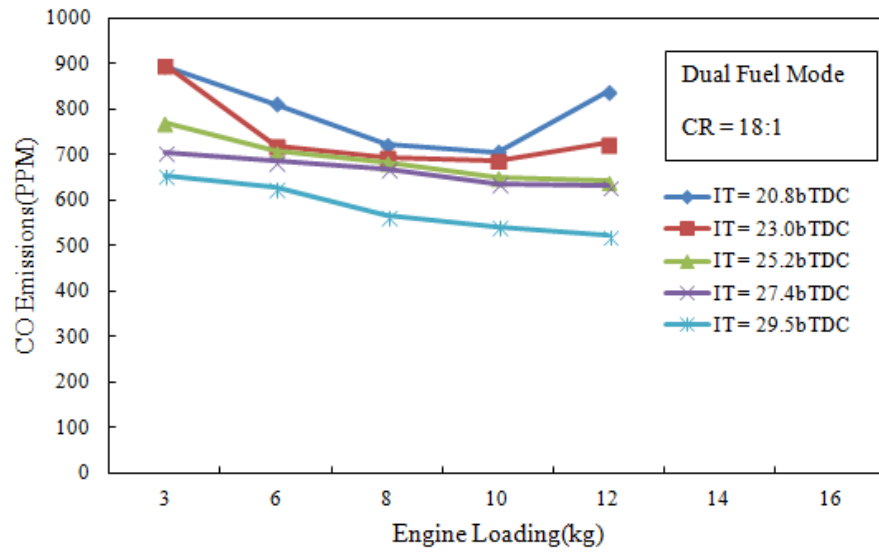


Figure 4.18: Variation of CO with load at different IT timings. This is due to gradual increase in the in-cylinder temperature with the load. Advancing injection timing led to increased  $\text{NO}_x$  emission and retarding the injection

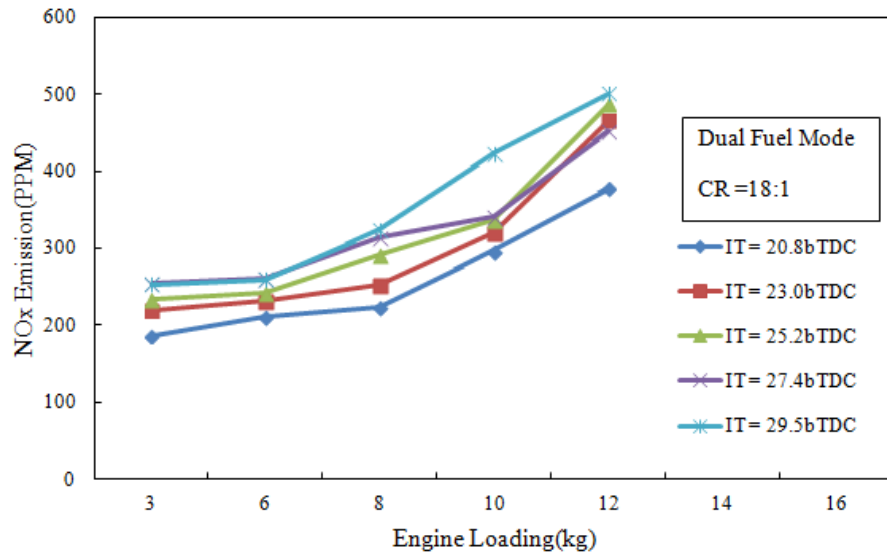


Figure 4.19: Variation of  $\text{NO}_x$  with load at different IT timing caused a reduction in  $\text{NO}_x$  emission as shown in Fig.4.19. As the injection timing was advanced from  $23.0^\circ$  to  $29.5^\circ$ , the  $\text{NO}_x$  emission was on average increased by 32%. Similar results are depicted in other research for dual fuel engines [16, 29].

The rise in  $\text{NO}_x$  emission with advancing injection timing was so significant at high loads (full load). The rise in the  $\text{NO}_x$  emission with advancing in injection timing is due to high temperature and pressure buildup in the combustion chamber due to an earlier start of combustion before TDC [16, 32, 85, 89, 90].

#### **4.4.3.4 Carbon-dioxide Emission**

Injection timing (IT) influences the combustion of the fuel in dual fuel engine. Its influence on combustion can be depicted with the variation of  $\text{CO}_2$  emission at different pilot fuel injection timings. Fig.4.20 shows the variation of  $\text{CO}_2$  with load for different IT. It is observed from the figure that retarding the injection timing reduced the  $\text{CO}_2$  emission and advancing the injection timing increased the  $\text{CO}_2$  emission. Retarding the injection timing by  $2.2^\circ$  reduced the  $\text{CO}_2$  and advancing the injection timing by  $2.2^\circ$ ,  $4.4^\circ$  and  $6.5^\circ$  increased the  $\text{CO}_2$  emission by 10%, 31% and 38% on average respectively.

The increase in  $\text{CO}_2$  emission at advanced injection timing is attributed to complete combustion of the charge due to earlier start of combustion before TDC [91].

#### **4.5 Effect of EGR on the Performance and Emission**

$\text{NO}_x$  formation in internal combustion engines is predominant when the combustion temperatures are high. High temperatures in the combustion chamber facilitate the reaction between oxygen and nitrogen forming  $\text{NO}_x$  [92]. Exhaust gas recirculation (EGR) influences the combustion temperatures in internal combustion engine thus af-

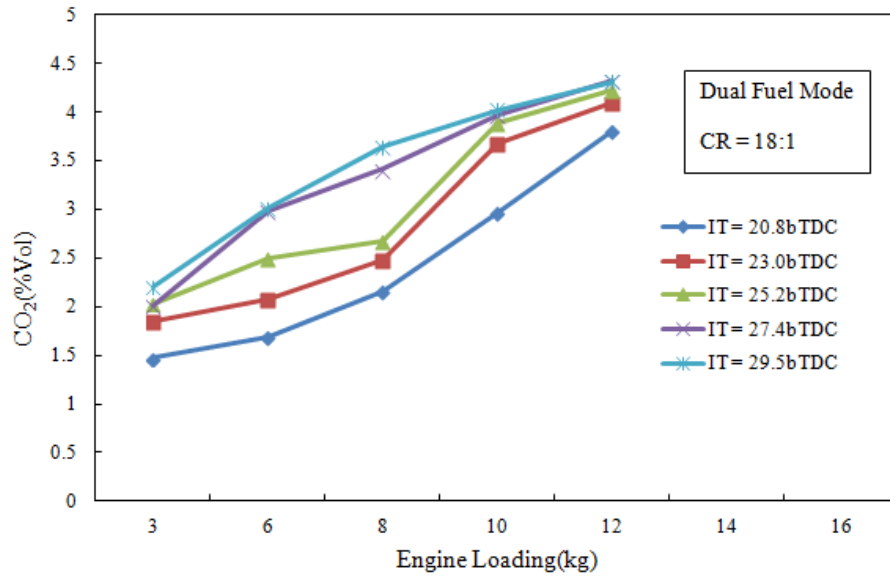


Figure 4.20: Variation of CO<sub>2</sub> emission with load at different IT  
fecting the formation of NO<sub>x</sub> as discussed in Section 2.4.3.

#### 4.5.1 Performance Characteristics Analysis

##### 4.5.1.1 Brake Thermal Efficiency

Fig.4.21 shows the relationship between EGR percentages and thermal efficiency of a dual fuel engine.

It can be observed from the figure that as the EGR percentage increased, the thermal efficiency of the engine reduced. The variation in the thermal efficiency is minimum for low loads. At full load, the difference in thermal efficiency is significant, 20% reduction in thermal efficiency for the increase in EGR from 0% to 40%. The reason for reduction in thermal efficiency is that at high loads, burnt gases replace air that is required for complete combustion leading to a reduction in thermal efficiency [53,54].

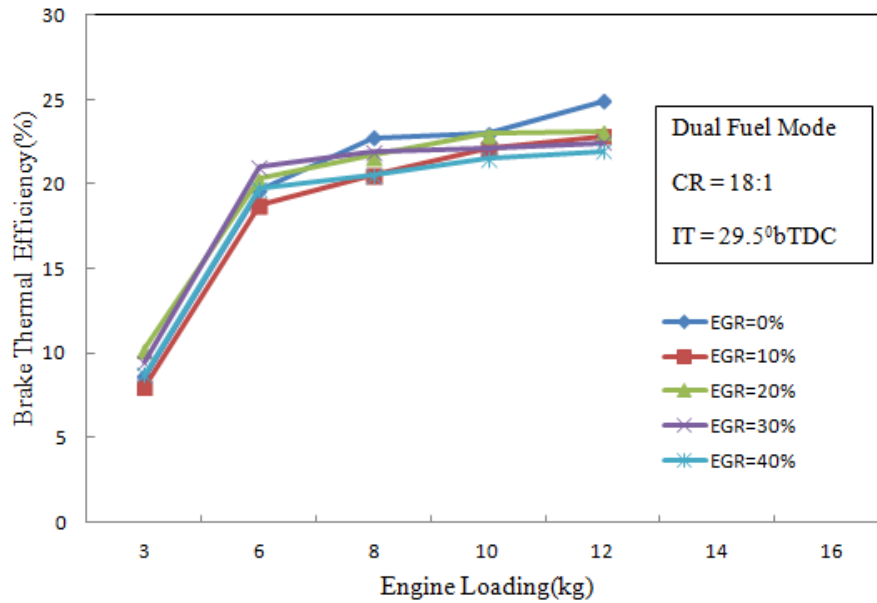


Figure 4.21: Variation of BTE with load

#### 4.5.1.2 Brake Specific Fuel Consumption

Fig. 4.22 shows the variation in brake specific fuel consumption with the load at different EGR rates. The figure points out that there is a reduction in brake specific fuel consumption with increasing EGR rates. One reason for this trend maybe the burning of the unburned HC that was recirculated in the exhaust gases [53]. Another reason is that exhaust gas recirculation increases the inlet temperatures of the charge which facilitates combustion thus improving the brake specific fuel consumption of the engine.

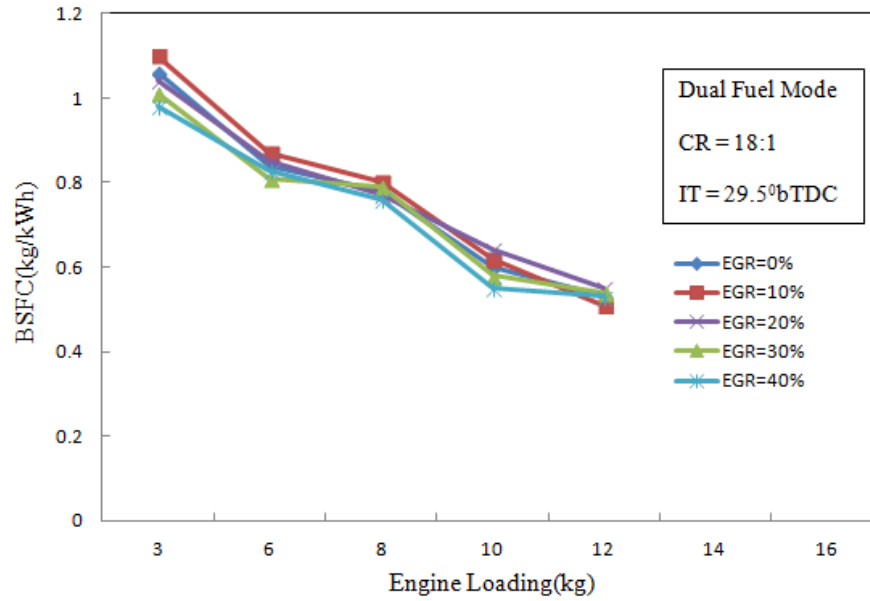


Figure 4.22: Variation of BSFC with load

## 4.5.2 Emission Analysis

### 4.5.2.1 $\text{NO}_x$ Emission

From Fig.4.23, the variation of  $\text{NO}_x$  emission with the load for different EGR flow rates can be depicted. It can be observed from the figure that as the EGR flow rate increased, the  $\text{NO}_x$  emission reduced. The emissions also increased as the engine load increased for EGR all flow rates.

The  $\text{NO}_x$  emission reduced by 38% on average for the increase in EGR percentage from 0% to 40%. The reason for the reduction in the  $\text{NO}_x$  is that, increasing the EGR rate, the exhaust gases displaced air in the combustion chamber thus reducing oxygen available for combustion leading to a reduction in the in-cylinder temperature. Reducing the combustion temperature reduces the formation of  $\text{NO}_x$  in the combustion



chamber and subsequently in the engine emissions [53,93].

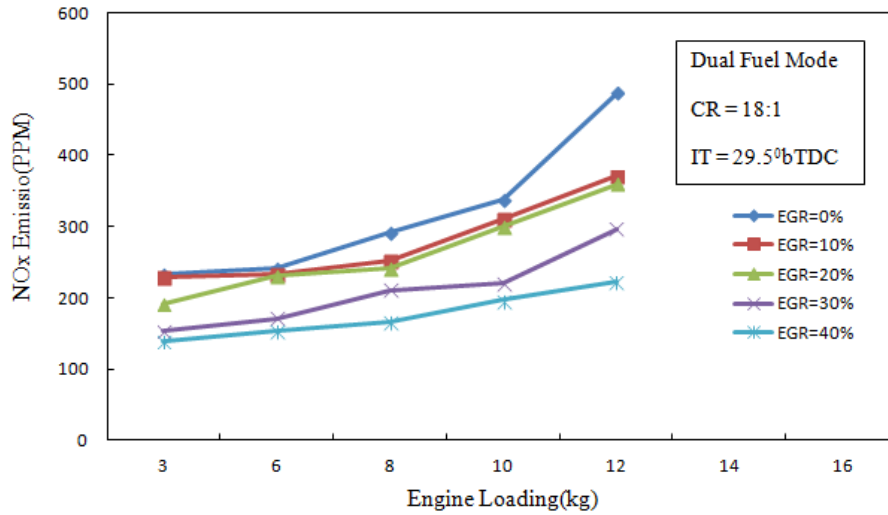


Figure 4.23: Variation in NO<sub>x</sub> with load

#### 4.5.2.2 HC Emission

Variation of HC emission with load at different EGR flow rates is shown in Fig.4.24. From the figure, it can be seen that as the EGR increased, HC emission reduced. From 0% to 10%, 20%, 30% and 40% of EGR, there was a decrease of 4%, 6%, 12%, and 18% on average respectively in the emission of HC. A reduction in the HC emission was attributed to the burning of a portion the recirculated unburned HC. As the exhaust gas was recirculated, a portion of the previously unburned HC at an elevated temperature from the previous cycle was burnt reducing the HC emission in the exhaust gas [50,94]

#### 4.5.2.3 CO Emission

In Fig.4.25, the variations of CO emission with the load at different EGR ratios are illustrated. It can be observed that at low EGR ratios, there was no prominent effect on

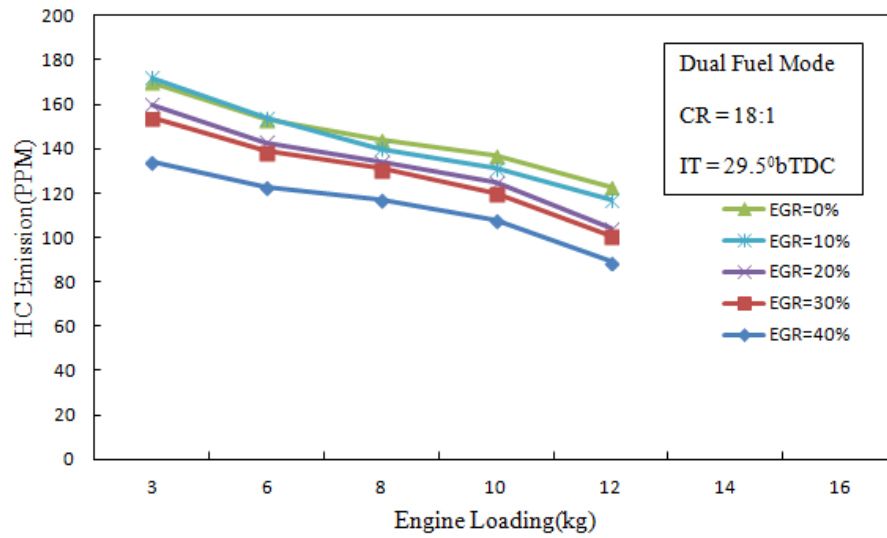


Figure 4.24: Variation of HC with load

CO emissions. As the EGR ratios increased to 30% and 40%, CO emissions increased by 5% and 8% respectively. The rise is significant at higher loads. The increase in CO emission at high EGR rates was due to the incomplete combustion due to temperature reduction and oxygen deficiency caused by the introduction of EGR [50,54,93].

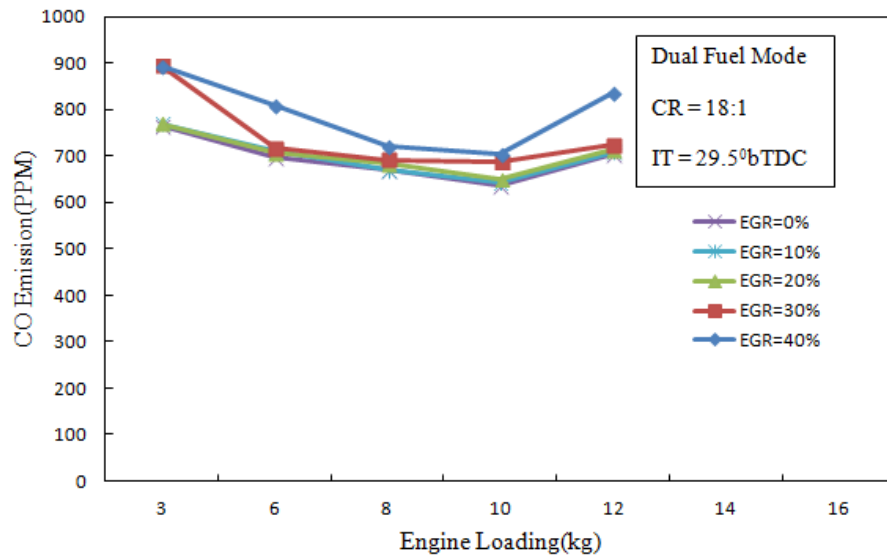


Figure 4.25: Variation of CO emission with load

#### 4.5.2.4 CO<sub>2</sub> Emission

The effect of EGR on emission of CO<sub>2</sub> is shown in Fig.4.26. The figure shows how CO<sub>2</sub> emission varied at different engine loads with different EGR ratios. From the figure, it can be seen that EGR ratios did not have a great effect on CO<sub>2</sub> emission. There was a slight reduction in CO<sub>2</sub> emission at low EGR ratios and as the ratios increased more, CO<sub>2</sub> emission increased again. The reduction in CO<sub>2</sub> at low EGR ratios of 10% and 20% was due to incomplete combustion due to biogas introduction. The rise in CO<sub>2</sub> at high EGR ratios of 30% and 40% was attributed to the addition of CO<sub>2</sub> from biogas and recirculated exhaust gases that increased the CO<sub>2</sub> emission [52].

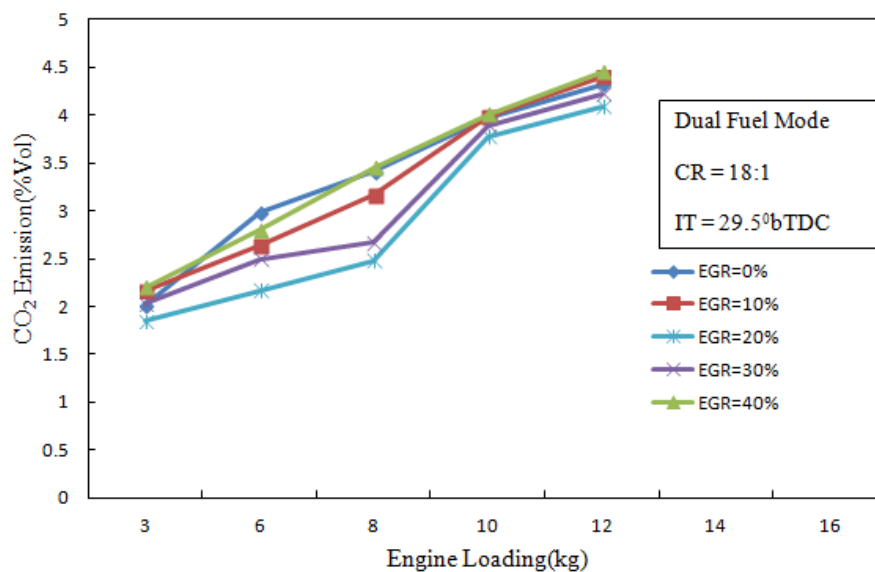


Figure 4.26: Variation of CO<sub>2</sub> with load

## **4.6 Effect of Biogas Ratio on Performance and Emission**

The flow rate of the primary fuel is very vital to the performance and emission characteristics of the dual fuel engine. It influences the combustion temperature thus affecting rate of combustion and the exhaust emissions.

### **4.6.1 Performance Characteristics Analysis**

#### **4.6.1.1 Brake Thermal Efficiency**

Fig.4.27 shows the variation in brake thermal efficiency with load for different biogas flow rates. The flow rates were determined by the flow rate control valve. The figure shows that the highest brake thermal efficiency was obtained at the load of 12kg when the flow control valve was half open. At 80% biogas rate, it is seen that the thermal efficiency reduced. This trend was caused by the presence of CO<sub>2</sub> in biogas and low calorific value of biogas. High flow rates of biogas replaced more of air causing a deficiency of oxygen leading to incomplete burning thus a reduction in thermal efficiency [78,95].

#### **4.6.1.2 Brake Specific Fuel Consumption**

As shown in Fig.4.28, the brake specific fuel consumption (BSFC) reduced with the reduction in the biogas ratio. BSFC increased as the control valve was opened more to increase the biogas ratio. This was because at low biogas ratio, the diesel fuel intake increases and diesel has higher calorific value than biogas which improves the engine fuel consumption at low flow rates [95,96].

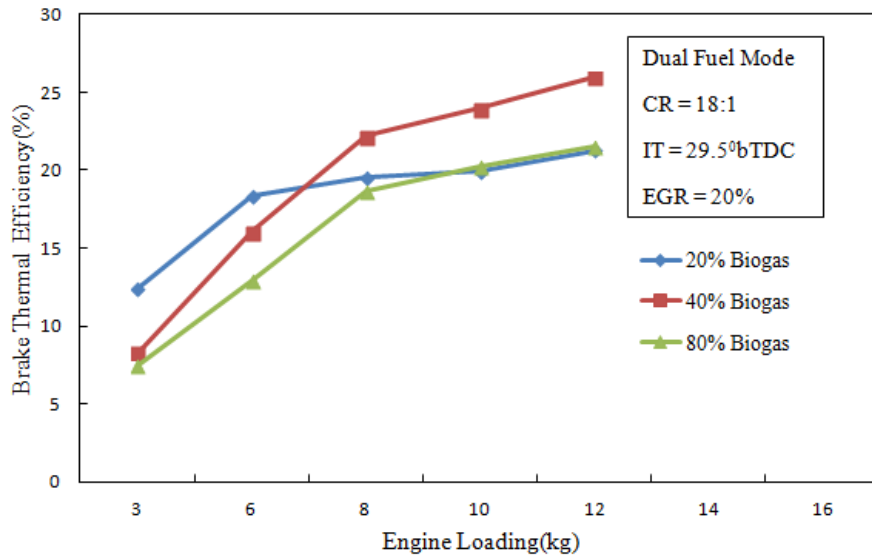


Figure 4.27: Variation of BTE with load at different biogas ratios

There was an improvement of 61% on average in brake specific fuel consumption improved for the reduction in the flow rate from 80% biogas to 20% biogas flow. Similar results were obtained by Hawi *et al.*, [27] in an experiment to investigate engine performance and emission of a diesel piloted engine .

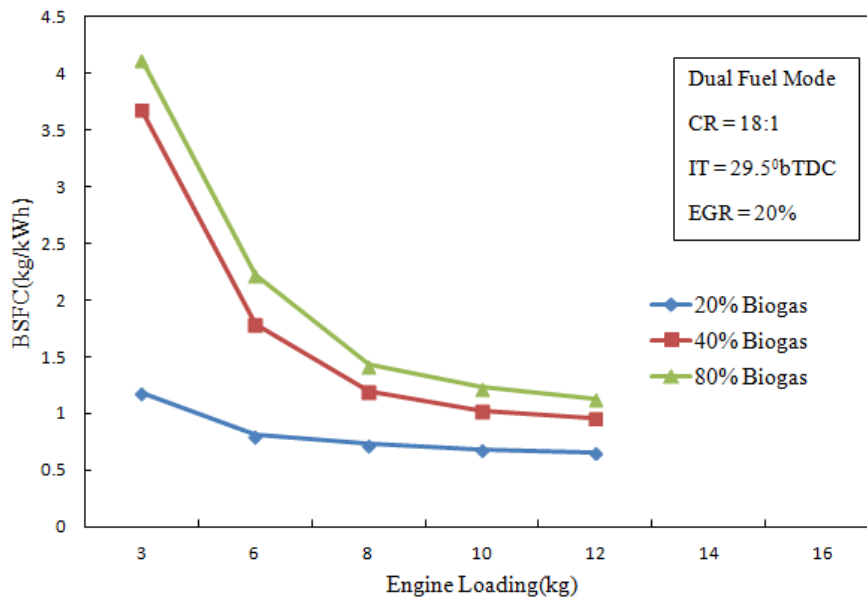


Figure 4.28: Variation of BSFC with load at different biogas ratios

## 4.6.2 Emission Characteristics Analysis

### 4.6.2.1 NO<sub>x</sub> Emission

NO<sub>x</sub> emission formation is mainly dependent on the in-cylinder temperatures, availability of oxygen and the retention time for the reaction for during combustion. The availability of oxygen is dependent on the air-biogas mixture ratios.

Fig.4.29 illustrates the variation of NO<sub>x</sub> emission with the load for different biogas ratios. It can be observed from the figure that with increased biogas ratio, (valve fully open) the NO<sub>x</sub> emission reduced by about 40% at full load. The NO<sub>x</sub> emission variation for 40% and 20% biogas flow rate shows that there was no significant difference. Debabrata Barik *et al.*, [43] obtained similar results for different biogas ratios. The reduction in the NO<sub>x</sub> emission at 80% biogas ratio was caused by low cylinder temperatures due to presence of CO<sub>2</sub> in biogas.

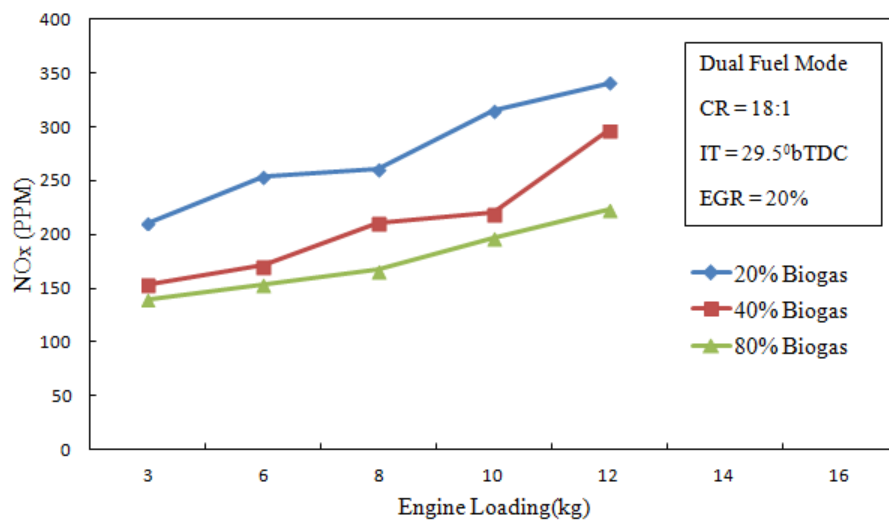


Figure 4.29: Variation in NO<sub>x</sub> emission with load at different ratios

#### 4.6.2.2 HC Emission

The unburned hydrocarbon variation with load at different biogas ratios is depicted in Fig. 4.30. The figure shows that the HC emissions increased with the increase in biogas ratios. The figure points out that at the full flow control valve opening, HC emission was maximum. The reason for this trend is that with high biogas ratios, portion of air-biogas mixture leaves the combustion chamber through exhaust manifold unburned due to incomplete combustion [43].

For all the biogas ratios, the HC emissions reduced with the increasing load. This is due to the high temperatures at high loads that facilitate complete combustion. HC emission reduced by 33% on average as the flow rate was reduced from 80% biogas to 20% biogas ratio.

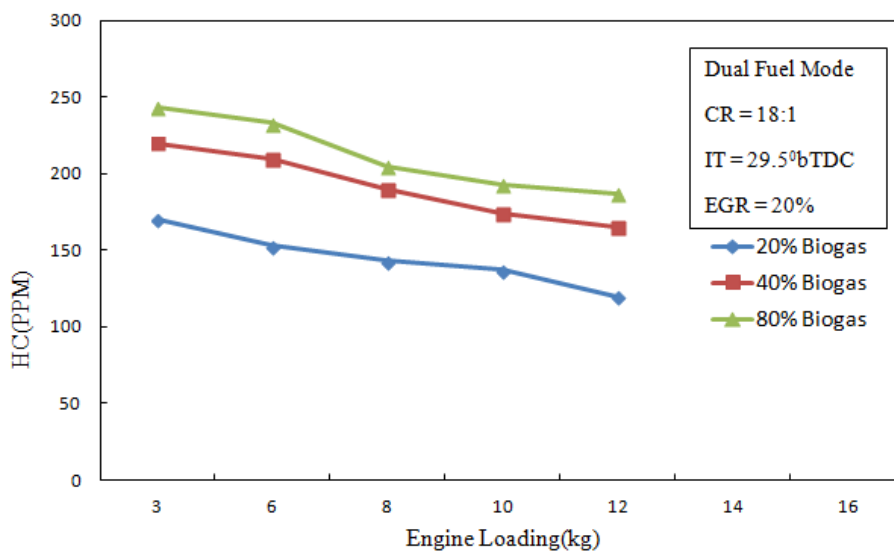


Figure 4.30: Variation of HC with load at different biogas ratios

#### 4.6.2.3 CO Emission

Emission of carbon monoxide at different biogas flow rates is shown in Fig.4.31. It is observed that biogas ratio of 80% biogas produced the highest CO emission. The flow rates at 40% biogas and 20% biogas had no significant difference on their effect on CO emission. The reason for high CO emissions at high biogas ratio was the introduction of  $\text{CO}_2$  into the combustion chamber that led to incomplete combustion causing a rise in CO emission.

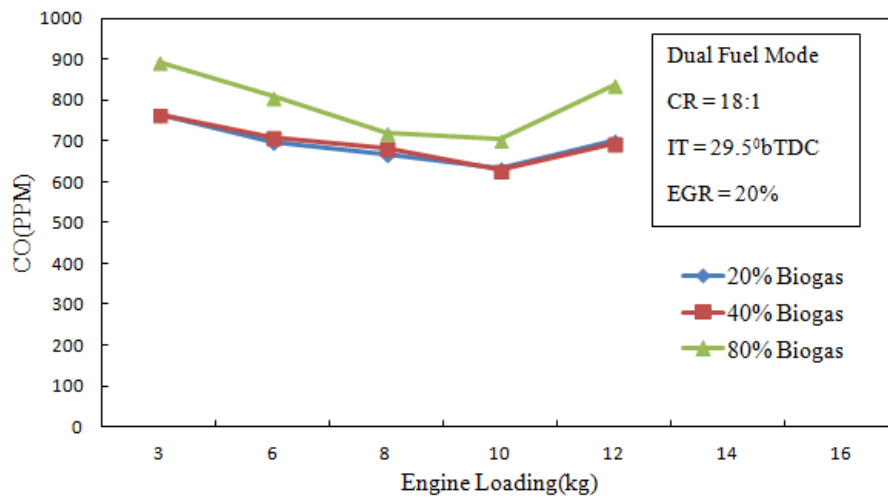


Figure 4.31: Variation of CO with load at different biogas ratios



#### 4.6.2.4 CO<sub>2</sub> Emission

CO<sub>2</sub> is the product of fuel combustion. CO<sub>2</sub> emission from combustion indicates the degree of fuel combustion. For complete combustion, CO<sub>2</sub> emission is higher than for incomplete fuel combustion. Fig.4.32 illustrates the variations in the CO<sub>2</sub> emission with load at different biogas flow rates.

It can be seen from the figure that CO<sub>2</sub> emission is lowest at full load. However the variations in CO<sub>2</sub> emission is not very different for all the flow rates. CO<sub>2</sub> emission increased as the load increased for all the flow rates. This is because there is complete combustion at full load due to high in-cylinder temperatures.

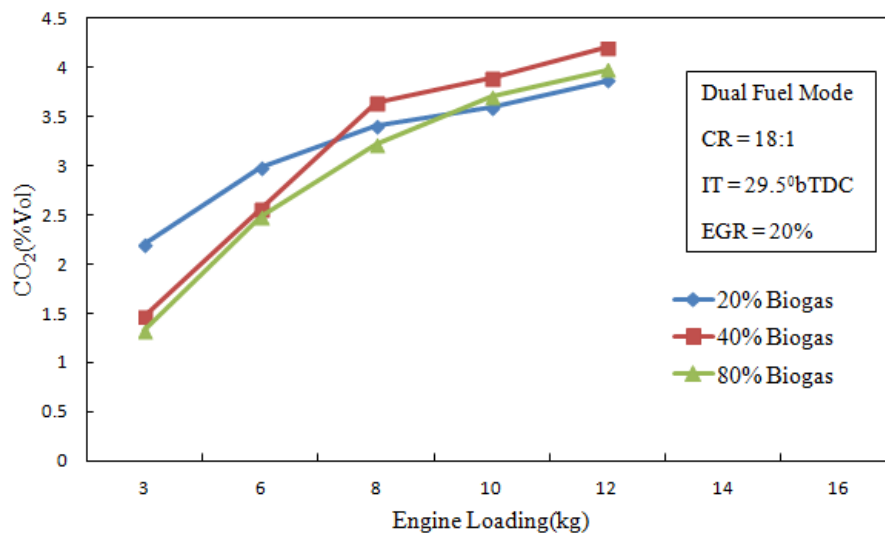


Figure 4.32: Variation of CO<sub>2</sub> with load at different biogas ratios

## **CHAPTER FIVE**

### **5.0 CONCLUSIONS AND RECOMMENDATIONS**

#### **5.1 Concluding Remarks**

This chapter concludes the thesis with a summary of the findings from the effects of combustion parameters on the performance and emission characteristics of a dual fuel engine using biogas. Possible continuation and expansion of this research is also recommended in this chapter.

Experimental study was done on the effects of combustion parameters on performance and emission characteristics of a dual fuel engine running on biogas. The experiments were conducted in a single cylinder, DI, water cooled VCR diesel engine. Investigations carried out included; study of the effect of compression ratio, injection timing and biogas flow rate on combustion, performance and emission characteristics of a dual fuel engine and the effect of EGR on  $\text{NO}_x$  emission. The CR investigation was carried out for CR of 14:1, 16:1 and 18:1 at standard IT  $23.0^\circ\text{bTDC}$ . The study of effect of injection timing was done at a constant CR of 18:1 for  $20.8^\circ\text{bTDC}$ ,  $23.0^\circ\text{bTDC}$ ,  $25.2^\circ\text{bTDC}$ ,  $27.4^\circ\text{bTDC}$  and  $29.5^\circ\text{bTDC}$ . Biogas flow rate and EGR experiments were carried out at a CR of 18:1 and injection timing of  $29.5^\circ\text{bTDC}$ . The following conclusions were deduced from the results that were obtained from the experiments.

1. Dual fuel engine showed lower brake thermal efficiency, higher specific fuel consumption, and lower mechanical efficiency compared to single fuel diesel engine

operation. Therefore, dual fuel operation reduces the mechanical efficiency of the engine.

2. Brake thermal efficiency of 24.9%, peak cylinder pressure of 49bar, peak heat release rate of 54.1J/deg were obtained at the highest compression ratio of 18:1. Specific fuel consumption of the dual fuel engine also improved to 0.55 kg/kWh at compression ratio of 18:1. Thermal efficiency, cylinder pressure and net heat release rate of the dual fuel engine increase with the increase in the engine's compression ratio. Low levels of HC and CO of 117 ppm, and 521 ppm respectively were observed at CR of 18:1. Proportional amount of  $\text{NO}_x$  and  $\text{CO}_2$  emission were obtained at compression ratio of 16:1 with engine load of 10kg. therefore increasing compression ratio reduced the emission of HC and CO.
3. Advancing the injection timing improved brake thermal efficiency, brake specific fuel consumption and increased the in-cylinder pressure and net heat release rate of the dual fuel engine. Advancing the injection timing to  $29.5^\circ$  bTDC reduced HC and CO by 11% and 14% respectively.
4. Increasing the EGR ratio to 40% reduced the thermal efficiency by 20%. The  $\text{NO}_x$  and HC emission reduced by 38% and 18% on average respectively for the increase in EGR percentage from 0% to 40%. EGR ratio did not significantly affect CO and  $\text{CO}_2$  emission. Exhaust gas recirculation (EGR) reduced the thermal efficiency of the dual fuel engine.
5. Variation in biogas flow rate showed that increasing the flow rate reduced brake

thermal efficiency of the engine. Brake specific fuel consumption increased with higher increase in biogas flow rate.  $\text{NO}_x$  emission reduced with increase in biogas flow rate.

6. From the analysis of results, it can be concluded that a 3.5 kW single cylinder, water cooled, four stroke diesel engine modified into a dual fuel engine fueled with both biogas and diesel has optimum combustion, performance and emission characteristics at compression ratio of 18:1, injection timing of  $29.5^\circ\text{bTDC}$ , EGR ratio of 20%, 40% biogas, at full load and engine speed of 1500 rpm.

## **5.2 Recommendations**

For the application of biogas in dual fuel engine, the research presented in this thesis can be extended in two ways; biogas production and application and performance of the dual fuel engine.

1. **Biogas production and application.** Biogas production process also leads to production of substances that hinder combustion for example  $\text{CO}_2$ . There is a need to study more about processing the gas so as to increase the percentage of the combustible components of biogas, hydrogen and methane. Biogas has a very low density which makes it occupy a very large space. This means that its small mass occupies a very big volume and makes it not practical to be applied in mobile automotive engines. Biogas also reduces thermal efficiency of the engine. A study of compressing biogas to have more mass to volume ratio for easy application mobile automotive engines is required. This will also improve

the volumetric efficiency of the dual fuel engine.

2. **Performance.** With the investigations to increase the compression ratio, advance injection timing, vary the biogas flow rate and vary the EGR ratios in dual fuel engine operation, the thermal efficiency of the dual fuel engine remained lower than that of the diesel engine, brake specific fuel consumption remained higher than that of diesel fuel and the mechanical efficiency remained lower than that of the diesel fueled engine. In order to improve thermal efficiency, a study should be done using biogas under high compression ratio, advanced injection timing, homogeneous charge compression ignition (HCCI) and using a turbocharger.

## REFERENCES

- [1] World Energy Council, “World Energy Resources,” *World Energy Council Report*, p. 468, 2013.
- [2] International Energy Agency, “Energy and climate change,” tech. rep., 2015.
- [3] United Nations, “Kyoto Protocol to the United Nations Framework Convention on Climate Change,” 1998.
- [4] I. E. Agency, “Carbondioxide Emissions From Fuel Combustion,” tech. rep., 2014.
- [5] J. Olivier, M. Muntean, and J. Peters, “Trends in global CO<sub>2</sub> emissions: 2015 report,” *PBL Netherlands Environmental Assessment Agency & European Commission’s Joint Research Centre (JRC)*, pp. 1–78, 2015.
- [6] International Energy Agency, “CO<sub>2</sub> Emissions From Fuel Combustion Highlights,” Tech. Rep. IEA - STATISTICS, 2015.
- [7] REN21, “Renewable Energy Policy Network for the 21st Century,” tech. rep., Ren1, 2014.
- [8] V. Makareviciene, E. Sendzikiene, S. Pukalskas, A. Rimkus, and R. Vegneris, “Performance and emission characteristics of biogas used in diesel engine operation,” *Energy Conversion and Management*, vol. 75, pp. 224–233, nov 2013.
- [9] P. M. Duc and K. Wattanavichien, “Study on biogas premixed charge diesel dual fuelled engine,” *Energy Conversion and Management*, vol. 48, pp. 2286–2308,

aug 2007.

- [10] N. R. Banapurmath, V. S. Yaliwal, S. Kambalimath, A. M. Hunashyal, and P. G. Tewari, "Effect of Wood Type and Carburetor on the Performance of Producer Gas-Biodiesel Operated Dual Fuel Engines," *Waste and Biomass Valorization*, vol. 2, pp. 403–413, jul 2011.
- [11] A. Boretti, "Dual Fuel H<sub>2</sub>-Diesel Heavy Duty Truck Engines with Optimum Speed Power Turbine,"
- [12] C. B. Braga. S. L, J.C. Egusquiza, "Performance and Gaseous Emissions Characteristics of a Natural Gas / Diesel Dual Fuel Turbocharged and Aftercooled Engine," vol. 31, no. 2, pp. 142–150, 2009.
- [13] D. K. Das, S. P. Dash, and M. K. Ghosal, "Performance evaluation of a diesel engine by using producer gas from some under-utilized biomass on dual-fuel mode of diesel cum producer gas," pp. 1583–1589, 2012.
- [14] D. Kozarac, D. Vuilleumier, S. Saxena, and R. W. Dibble, "Analysis of benefits of using internal exhaust gas recirculation in biogas-fueled HCCI engines," *Energy Conversion and Management*, vol. 87, no. 10, pp. 1186–1194, 2014.
- [15] V. R. A. M Ravi, K C K Vijayakuramar, A Murugesan, D Sivachalapathi, "Effect of Electronic Flow on Performance and Emission Characteristics of Dual Fuel Diesel Engine Run on Biogas," *International Journal of Advanced Engineering Technology*, vol. 7, no. 1, pp. 177–181, 2016.

- [16] S. Murugan, "Effects of Varying Injection Timing on Performance and Emission Characteristics of Dual Fuel Engine Fueled with Biogas," *International Journal of Scientific & Engineering Research*, vol. 4, no. 12, pp. 97–103, 2013.
- [17] C. Park, S. Park, Y. Lee, C. Kim, S. Lee, and Y. Moriyoshi, "Performance and emission characteristics of a SI engine fueled by low calorific biogas blended with hydrogen," *International Journal of Hydrogen Energy*, vol. 36, pp. 10080–10088, aug 2011.
- [18] E. Porpatham, A. Ramesh, and B. Nagalingam, "Effect of compression ratio on the performance and combustion of a biogas fuelled spark ignition engine," *Fuel*, vol. 95, pp. 247–256, may 2012.
- [19] N. H. S. Ray, M. Mohanty, and R. Mohanty, "A Study on Application of Biogas as fuel in Compression Ignition Engines," *International Journal of Innovations in Engineering and Technology*, vol. 3, no. 1, pp. 239–245, 2013.
- [20] D. Barik, S. Sah, and S. Murugan, "Biogas Production and Storage for Fuelling in Internal Combustion Engines," *International Journal of Emerging Technology and Advanced Engineering*, vol. 3, no. 3, pp. 193–202, 2013.
- [21] P. Njogu, R. Kinyua, P. Muthoni, and Y. Nemoto, "Biogas Production Using Water Hyacinth ( *Eichhornia crassipes* ) for Electricity Generation in Kenya," *Energy and Power Engineering*, no. May, pp. 209–216, 2015.
- [22] Ashington Ngigi, "Kenya National Domestic Biogas Programme," Tech. Rep.



November 2009, 2009.

- [23] T. Schmidt, “Agro-Industrial Biogas in Kenya,” tech. rep., 2010.
- [24] P. Frost and S. Gilkinson, “Interim Technical Report First 18 Month Performance Summary For Anaerobic Digestion Of Dairy Cow Slurry At AFBI Hillsborough,” Tech. Rep. August, 2010.
- [25] D. Ludington, “Calculating the Heating Value of Biogas,”
- [26] S. Swami Nathan, J. Mallikarjuna, and A. Ramesh, “An experimental study of the biogas-diesel HCCI mode of engine operation,” *Energy Conversion and Management*, vol. 51, pp. 1347–1353, jul 2010.
- [27] Hawi. M, Kiplimo.R, and Ndiritu.H, “An Experimental Investigation on Engine Performance and Emission of a Dual-piloted Biogas Engine,” *Journal of Sustainable Research in Engineering*, vol. 1, no. 4, pp. 41–47, 2014.
- [28] N. E. Stratagy, “Fossil Fuels: Envionmental Effects,” 1995.
- [29] K. Murthy, N. Madhwesh, and B. R. Shrinivasarao, “Influence of Injection Timing on the Performance of Dual Fuel Compression Ignition Engine with Exhaust Gas Recirculation,” *International Journal of Engineering Research and Development*, vol. 1, no. 11, pp. 36–42, 2012.
- [30] Y. B. Mathur, M. P. Poonia, a. S. Jethoo, and R. Singh, “Optimization of Compression Ratio of Diesel Fuelled Variable Compression Ratio Engine,” vol. 2, no. 3, pp. 99–101, 2012.

- [31] M. Y. Selim, "Sensitivity of dual fuel engine combustion and knocking limits to gaseous fuel composition," *Energy Conversion and Management*, vol. 45, pp. 411–425, feb 2004.
- [32] G. H. A. Alla, H. A. Soliman, O. A. Badr, and M. F. A. Rabbo, "Effect of injection timing on the performance of a dual fuel engine," *Energy Conversion and Management*, vol. 43, pp. 269–277, 2002.
- [33] A. Henham and M. K. Makkar, "Combustion of Simulated Biogas in a Dual-fuel Diesel Engine," *Energy Conversion and Management*, vol. 39, no. 16, pp. 2001–2009, 1998.
- [34] D. Barik and S. Murugan, "Experimental investigation on the behavior of a DI diesel engine fueled with raw biogas - diesel dual fuel at different injection timing," *Journal of the Energy Institute*, vol. 30, pp. 1–16, 2015.
- [35] B. J. Bora and U. K. Saha, "Optimisation of injection timing and compression ratio of a raw biogas powered dual fuel diesel engine," *Applied Thermal Engineering*, vol. 92, pp. 111–121, 2016.
- [36] F. José, A. Gilson, and B. D. Lima, "Dual-Fuel ( Natural Gas / Biodiesel ) Engines : Fundamentals , Performance and Environmental Impact," *Alternative Energies*, vol. 34, pp. 47–68, 2013.
- [37] M. Deb, G. R. K. Sastry, R. S. Panua, R. Banerjee, and P. K. Bose, "Effect of Hydrogen-Diesel Dual Fuel Combustion on the Performance and Emission

- Characteristics of a Four Stroke-Single Cylinder Diesel Engine,” *International Journal of Mechanical, Aerospace, Mechanical and Manufacturing Engineering*, vol. 9, no. 6, pp. 848–854, 2015.
- [38] R. S. Hosmath, N. R. Banapurmath, S. V. Khandal, V. N. Gaitonde, Y. H. Basavarajappa, and V. S. Yaliwal, “Effect of compression ratio , CNG fl ow rate and injection timing on the performance of dual fuel engine operated on honge oil methyl ester ( HOME ) and compressed natural gas ( CNG ),” *Renewable Energy*, vol. 93, pp. 579–590, 2016.
- [39] A. S. M. S. Shafeez and R. M. Z. A. Majid, “Performance of Diesel-Compressed Natural Gas ( CNG ) Dual Fuel ( DDF ) Engine via CNG-Air Venturi Mixjector Application,” *Mechanical Engineering*, vol. 39, pp. 7335–7344, 2014.
- [40] G. S. Jatana, M. Himabindu, H. S. Thakur, and R. V. Ravikrishna, “Strategies for high efficiency and stability in biogas-fuelled small engines,” *Experimental Thermal and Fluid Science*, vol. 54, pp. 189–195, 2014.
- [41] E. Rajasekar and S. Selvi, “Review of combustion characteristics of CI engines fueled with biodiesel,” *Renewable and Sustainable Energy Reviews*, vol. 35, no. 10, pp. 390–399, 2014.
- [42] M. M. Ibrahim, J. V. Narasimhan, and A. Ramesh, “Comparison of the predominantly premixed charge compression ignition and the dual fuel modes of operation with biogas and diesel as fuels,” *Energy*, vol. 89, pp. 990–1000, 2015.

- [43] D. Barik and S. Murugan, "Investigation on combustion performance and emission characteristics of a DI (direct injection) diesel engine fueled with biogas-diesel in dual fuel mode," *Energy*, vol. 72, pp. 760–771, aug 2014.
- [44] I. D. Bedoya, A. A. Arrieta, and F. J. Cadavid, "Effects of mixing system and pilot fuel quality on diesel – biogas dual fuel engine performance," *Bioresource Technology*, vol. 100, pp. 6624–6629, 2009.
- [45] International Fund for Agricultural Development, "Flexi Biogas systems : inexpensive , renewable energy for developing countries." 2012.
- [46] O. M. I. Nwafor, "Effect of advanced injection timing on the performance of natural gas in diesel engines," vol. 25, no. 1, pp. 11–20, 2000.
- [47] B. Yang, L. Wang, L. Ning, and K. Zeng, "Effects of pilot injection timing on the combustion noise and particle emissions of a diesel/natural gas dual-fuel engine at low load," *Applied Thermal Engineering*, vol. 102, no. May, pp. 822–828, 2016.
- [48] V. Hariram and R. V. Shangar, "Influence of compression ratio on combustion and performance characteristics of direct injection compression ignition engine," *Alexandria Engineering Journal*, vol. 54, no. 4, pp. 807–814, 2015.
- [49] S. Reifarth, *EGR-Systems for Diesel Engines*. PhD thesis, 2010.
- [50] S. K. Mahla, L. M. Das, and M. K. G. Babu, "Effect of EGR on Performance and Emission Characteristics of Natural Gas Fueled Diesel Engine," *Jordan Journal*

- of Mechanical and Industrial Engineering*, vol. 4, no. 4, pp. 523–530, 2010.
- [51] N. R. Kumar, Y. M. C. Sekhar, and S. Adinarayana, “Effects of Compression Ratio and EGR on Performance , Combustion and Emissions of Di Injection Diesel Engine,” *International Journal of Applied Science and Engineering*, vol. 11, no. 1, pp. 41–49, 2013.
- [52] J. C. Ge, M. S. Kim, S. K. Yoon, and N. J. Choi, “Effects of pilot Injection Timing and EGR on Combustion, Performance and Exhaust Emissions in a Common Rail Diesel Engine Fueled with a Canola Oil Biodiesel-Diesel Blend,” *Energies*, vol. 8, no. 7, pp. 7312–7325, 2015.
- [53] K. Venkateswarlu, B. Sree, and S. Chandra, Rama V. Venkata, “The Effect of Exhaust Gas Recirculation and Di-Tertiary Butyl Peroxide on Diesel-Biodiesel Blends for Performance and Emission Studies,” *International Journal of Advanced Science and Technology*, vol. 54, no. 10, pp. 49–60, 2013.
- [54] M. Hawi, R. Kiplimo, and H. Ndiritu, “Effect of Exhaust Gas Recirculation on Performance and Emission Characteristics of a Diesel-Piloted Biogas Engine,” *Smart Grid and Renewable energy*, no. 6, pp. 49–58, 2015.
- [55] A. Paykani and R. K. Saray, “Effect of exhaust gas recirculation and intake pre-heating on performance and emission characteristics of dual fuel engines at part loads,” vol. 19, pp. 1346–1352, 2012.
- [56] R. S. Kumar, M. Loganathan, and E. J. Gunasekaran, “Performance , emission

- and combustion characteristics of CI engine fuelled with diesel and hydrogen,” *Front Energy*, pp. 1–9, 2015.
- [57] D. F. Maki and P. Prabhakaran, “An Experimental Investigation on Performance and Emissions of a Multi Cylinder Diesel Engine Fueled with Hydrogen-Diesel Blends,” *World Renewable Congress*, pp. 3557–3564, 2011.
- [58] N. Zhang, Z. Huang, X. Wang, and B. Zheng, “Combustion and emission characteristics of a turbo-charged common rail diesel engine fuelled with diesel-biodiesel-DEE blends,” *Front Energy*, vol. 5, no. 1, pp. 104–114, 2011.
- [59] N. Vinayagam and G. Nagarajan, “Experimental Study of Performance and Emission Characteristics of DEE-Assisted Minimally Processed Ethanol Fueled HCCI Engine,” *International Journal Of Automotive Technology*, vol. 15, no. 4, pp. 517–523, 2014.
- [60] Y. A. O. Chunde, Z. Zhihui, C. Chenshun, and X. U. Guanglan, “Experimental study on the effect of gaseous and particulate emission from an ethanol fumigated diesel engine,” *Technological Sciences*, vol. 53, no. 12, pp. 3294–3301, 2010.
- [61] E. Commision, “The 2015 international Climate Change Agreement: Shaping international climate policy beyond 2020,” Tech. Rep. 2013, 2015.
- [62] Apex Innovations, “Research Engibe Test Set Up,” tech. rep.
- [63] H. Gitano, “Dynamometer Basics,” *University Science Malaysia*, 2007.

- [64] R. B. Nallamothu, A. Teferra, and P. B. V. A. Rao, “Biogas Purification , Compression and Bottling,” vol. 2, no. 6, pp. 34–38, 2013.
- [65] Kronos International, “Hydrogen sulfide elimination from biogas Hydrogen sulfide elimination from biogas,” *Technical Information*, pp. 1–4.
- [66] A. Siefers, N. Wang, A. Sindt, J. Dunn, J. McElvogue, E. Evans, and T. Ellis, “A Novel and Cost-Effective Hydrogen Sulfide Removal Technology Using Tire Derived Rubber Particles,” *Proceedings of the Water Environment Federation*, vol. 2010, no. 12, pp. 4597–4622, 2010.
- [67] International Process Plant, “Hydrogen Plant Operation Manual.”
- [68] M. Klaus, von, *A Handbook of Engine for Biogas; Theory, Modification, Economic Operation*. 1988.
- [69] W. W. Pulkrabek, *Engineering Fundamentals of the Internal Combustion Engine* .
- [70] J. Heywood, B, *Internal Combustion Engine Fundamentals*. 1988.
- [71] Test AG, “Testo 350-S Control Unit in Combination With 350-S/-XL Flue Gas Analyser.”
- [72] S. Jiang, M. H. Smith, and M. Takekoshi, “A Study of a Variable Compression Ratio and Displacement Mechanism Using Design of Experiments Methodology,” pp. 355–371.

- [73] S. Tomar, R. Mishra, S. Bisht, S. Kumar, A. Balyan, and G. Saxena, "Optimisation of Connecting Rod Design to Achieve VCR," *International Journal of Engineering Research and Applications*, vol. 3, no. 6, pp. 281–286, 2013.
- [74] V. V. Bora, Bhaskor J, Ujjwal K. Saha, Soumya Chatterjee, "Effect of compression ratio on performance , combustion and emission characteristics of a dual fuel diesel engine run on raw biogas," *Energy Conversion and Management*, no. November 2014, 2014.
- [75] S. K. Nayak, S. K. Nayak, P. C. Mishra, and S. Tripathy, "Influence of compression ratio on combustion characteristics of a VCR engine using Calophyllum inophyllum biodiesel and diesel blends," *Journal of Mechanical Science and Technology*, vol. 29, no. 9, pp. 4047–4052, 2015.
- [76] S. Patil, "Investigation on Effect of Variation in Compression Ratio on Performance and Combustion Characteristics of C.I Engine Fuelled With Palm Oil Methyl Ester (POME) and Its Blends By Simulation," *Global Journal of Researches in Engineering Auutomotive Engineering*, vol. 12, no. 3, 2012.
- [77] B. J. Bora, U. K. Saha, S. Chatterjee, and V. Veer, "Effect of compression ratio on performance , combustion and emission characteristics of a dual fuel diesel engine run on raw biogas," *Energy Conversion and Management*, vol. 87, pp. 1000–1009, 2014.
- [78] D. Barik and S. Murugan, "Investigation on combustion performance and emission characteristics of a DI ( direct injection ) diesel engine fueled with biogas e



- diesel in dual fuel mode,” *Energy*, vol. 72, pp. 760–771, 2014.
- [79] A. Anbarasu and A. Karthikeyan, “Performance and Emission Characteristics of Direct Injection Diesel Engine Running On Canola Oil / Diesel Fuel Blend,” *International Journal of Engineering Trends and Technology*, vol. 15, no. 08, pp. 82–93, 2014.
- [80] K. Wannatong, N. Akarapanyavit, S. Siengsanorh, and S. Chanchaona, “Combustion and Knock Characteristics of Natural Gas Diesel Dual Fuel Engine,” *SAE Technical Paper*, vol. 01, pp. 1894–1899, 2007.
- [81] R. Sathiyamoorthi and G. Sankaranarayanan, “Combustion characteristics of DIC engine on various injection parameters using neat lemongrass oil-diesel blends,” *Journal of Chemical and Pharmaceutical Sciences*, no. 9, pp. 103–108, 2015.
- [82] A. Turkcan and M. Canakci, “Combustion Characteristics of an Indirect Injection (IDI) Diesel Engine Fueled with Ethanol/Diesel and Methanol/Diesel Blends at Different Injection Timings,” *Sustainable Transport*, pp. 3565–3572, 2011.
- [83] L. Sun, Y. Liu, K. Zeng, R. Yang, and Z. Hang, “Combustion performance and stability of a dual-fuel diesel-natural-gas engine,” *Proceedings of the Institution of Mechanical Engineers, Part D: Journal of Automobile Engineering*, vol. 229, no. 2, pp. 235–246, 2014.
- [84] H. Chotai, “Review on Effect of Varying Injection Pressure and Injection Timing

- on Performance and Emissions of Diesel Engine operating on Diesel / Biodiesel,” *International Conference on Multidisciplinary Research and Practice*, vol. I, no. 7, pp. 310–312.
- [85] R. G. Papagiannakis, D. T. Hountalas, and C. D. Rakopoulos, “Theoretical study of the effects of pilot fuel quantity and its injection timing on the performance and emissions of a dual fuel diesel engine,” *Energy Conversion and Management*, vol. 48, no. 11, pp. 2951–2961, 2007.
- [86] K. K. Khatri, D. Sharma, S. L. Soni, S. Kumar, and D. Tanwar, “Injection CI Engine Operated on Preheated Karanj-Diesel Blend,” *Jordan Journal of Mechanical and Industrial Engineering*, vol. 4, no. 5, pp. 629–640, 2010.
- [87] B. G. S. Rostami, M. K. D. Kiani, and Shahrekord, “Effect of the Injection Timing on the Performance of a Diesel Engine Using Diesel-Biodiesel Blends,” *International Journal of Automotive and Mechanical Engineering (IJAME)*, vol. 10, no. December, pp. 1945–1958, 2014.
- [88] Environmental Protection Agency (EPA), “Nitrogen Oxides ( NO<sub>x</sub> ), Why and How They Are Controlled,” Tech. Rep. November, 1999.
- [89] C. Y. Junheng Liu, Anren Yao, “Effects of injection timing on performance and emissions of a HD diesel engine with DMCC,” *Fuel*, vol. 134, pp. 107–113, 2014.
- [90] M. Pandian, S. P. Sivapirakasam, and M. Udayakumar, “Influence of Injection Timing on Performance and Emission Characteristics of Naturally Aspirated

- Twin Cylinder CIDI Engine Using Bio-diesel Blend as Fuel,” *International Journal of Recent Trends in Engineering*, vol. 1, no. 5, pp. 113–117, 2009.
- [91] M. C. Cenk Sayin, “Effects of Injection Timing on the Engine Performance and Exhaust Emissions of a Dual- Fuel Diesel Engine,” *Energy Conversion and Management*, vol. 50, pp. 203–213, 2009.
- [92] C. Baukal, “Everything you need to know about NO<sub>x</sub>,” *Metal Finishing*, vol. 103, no. 11, pp. 18–24, 2005.
- [93] H. Dangar and G. P. Rathod, “Combine Effect of Exhaust Gas Recirculation ( EGR ) and Varying Inlet Air Pressure on Performance and Emission of Diesel Engine,” *Journal of Mechanical and Civil Engineering*, vol. 6, no. 5, pp. 26–33, 2013.
- [94] V. Pirouzpanah and R. Sarai, “Reduction of emissions in an automotive direct injection diesel engine dual-fuelled with natural gas by using variable exhaust gas recirculation,” *Automotive Engineering*, vol. 217, no. 8, pp. 719–725, 2003.
- [95] K. Senthilkumar, S. Vivekanandan, A. Nagar, T. Nadu, A. Nagar, and T. Nadu, “Investigating the Biogas as Secondary Fuel for Ci Engine,” *International Journal of Applied Environmental Sciences*, vol. 11, no. 1, pp. 155–163, 2016.
- [96] S. Bari, “Effect of Carbon Dioxide on the Performance of Biogas/Diesel Duel-Fuel Engine,” *World Renewable Energy Conference*, no. Goodger 1980, pp. 1007–1010, 1996.

- [97] D. R. Tobergte and S. Curtis, "Effect of Compressed Natural Gas Mixing on the Engine Performance and Emissions," *Journal of Chemical Information and Modeling*, vol. 53, no. 9, pp. 1689–1699, 2013.
- [98] B. B. Sahoo, *Clean development mechanism potential of compression ignition diesel engines using gaseous fuels in dual fuel mode*. PhD thesis, 2010.
- [99] B. J. Bora, B. K. Debnath, N. Gupta, U. K. Saha, and N. Sahoo, "Investigation on the Flow Behaviour of a Venturi Type Gas Mixer Designed for Dual Fuel Diesel Engines," vol. 3, no. 3, pp. 202–209, 2013.

## **Appendix ONE**

### **Air-Gas Mixing Unit**

Air-gas mixing unit is an important tool in CI engine conversion to a dual fuel engine. It is the modification that determines the introduction of the gaseous fuel into the combustion chamber.

#### **A.1 Types of Air-Gas Mixers**

The gas mixer is very important in dual-fuel engine, as it provides a combustible mixture of fuel gas and air in the required quantity and quality for efficient operation of the engine under all conditions.

T. Yusaf *et al.*, [97] designed a venturi mixer to mix CNG with air in a dual fuel engine test. In their study, they investigated the mixing efficiency of venturi mixers and found that the 8-hole venturi mixer gives better mixing performance than the 4-hole mixer. Sahoo [98] used a T-junction gas mixer in an experiment to use syngas in a dual fuel engine. Bhaskor J. Bora *et al.*, [99] in the investigation on the flow behavior of a venturi type gas mixer designed for dual fuel engines designed a channel having a T-junction with two gas inlets and an outlet for air-gas mixture.

#### **A.2 Considered Designs for the Mixer**

Different designs were generated for the homogeneous gas mixing depending on various equations and calculations. Different designs that were considered are shown in

Fig.A.2, Fig.A.3 and Fig.3.10.

In the first design; Fig.A.2, the EGR inlet was directly opposite to the mixture outlet.

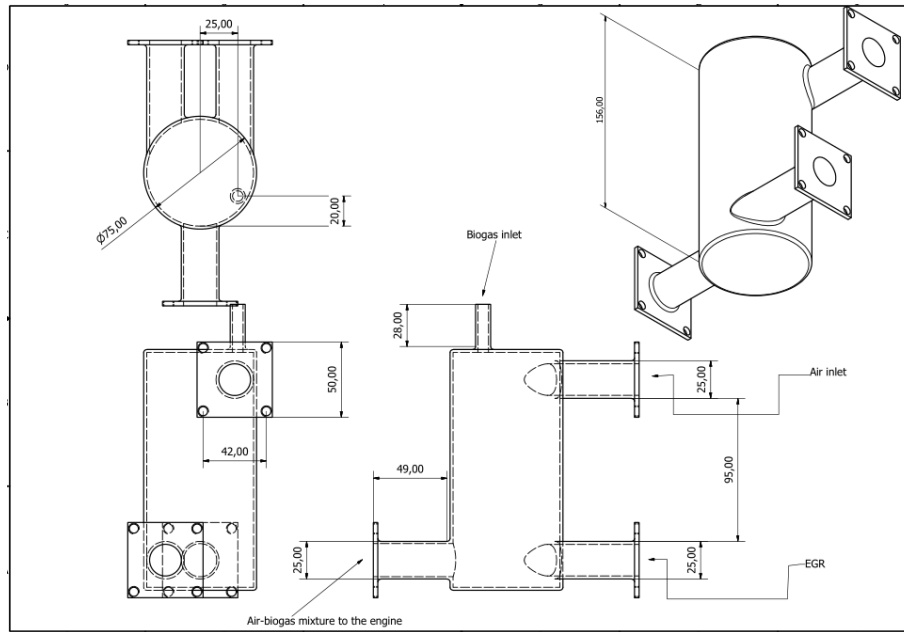


Figure A.1: First mixer design

Results of simulation indicated that for this design, there was no sufficient time for EGR to mix with air-gas mixture before entering into the combustion chamber. The second design in Fig.A.3 shows the EGR and air inlet pipes connected parallel to each other to the mixing chamber. The volume of the mixing chamber was 689 cc which was acceptable design because it was greater than the engine capacity. However, the height of the mixing chamber was short, thus residence time in the mixing chamber was not enough for homogeneous mixing.

The mixer design that was used in this research is the design shown in Fig.3.10. This design according to the simulation as shown in Fig.A.4, A.5, A.6 produced a ho-



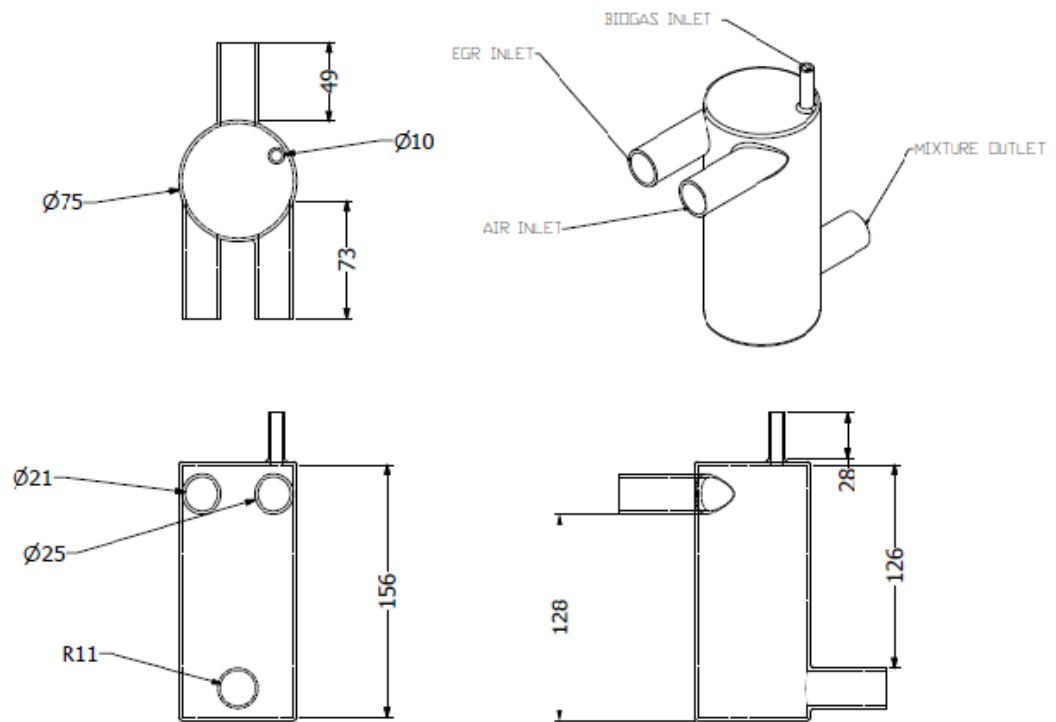


Figure A.3: Second design of the gas mixer

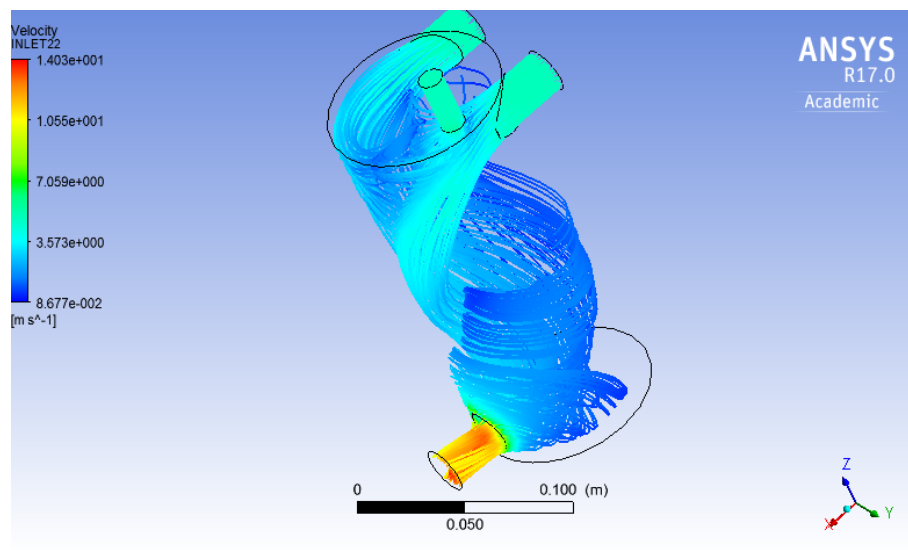


Figure A.4: Velocity distribution in the gas mixer



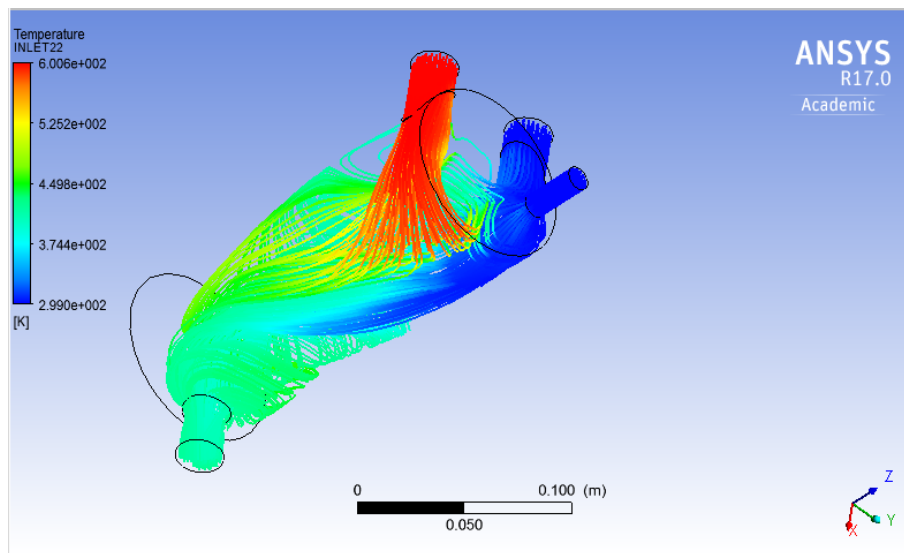


Figure A.5: Temperature distribution in the mixer

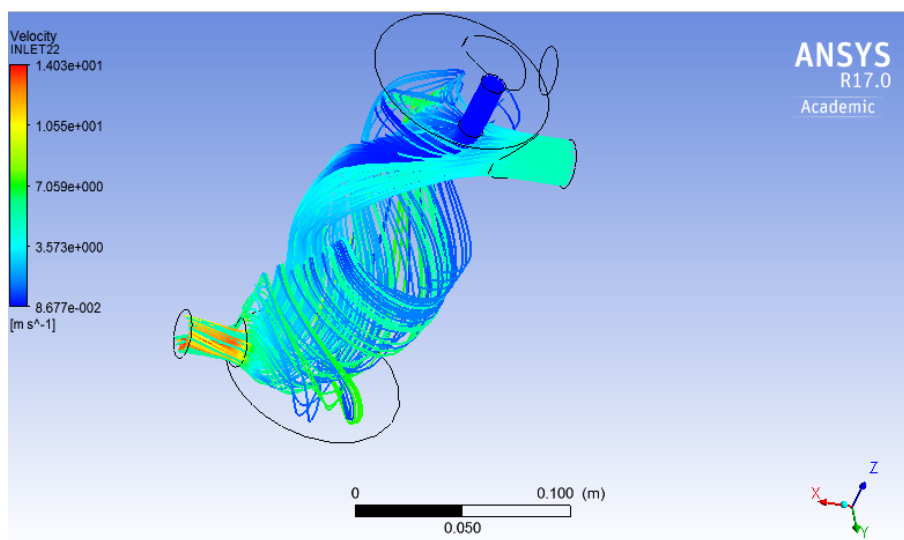


Figure A.6: Velocity distribution before EGR